4-1-2012

Dominant Upper Extremity Kinematics and Muscular Activity in Sonographers during Kidney Scanning

Jennifer Elizabeth Edwards
Grand Valley State University, jenn.e.edwards@gmail.com

Dominant Upper Extremity Kinematics and Muscular Activity in Sonographers during Kidney Scanning

Jennifer Elizabeth Edwards

A Thesis Submitted to the Graduate Faculty of

GRAND VALLEY STATE UNIVERSITY

In

Partial Fulfillment of the Requirements

For the Degree of

Master of Science in Engineering with an emphasis in Biomedical Engineering

Seymour and Esther Padnos College of Engineering and Computing

April 2012

Acknowledgements

I would like to acknowledge the following people for their help, guidance, and eagerness to participate in this study: committee members, volunteers, occupation therapy graduate students, Rick and Lynn Carlton, and my family. This project was funded under the National Science Foundation American Recovery and Reinvestment Act of 2009 (ARRA) (Public Law 111-5).

Abstract

Due to the prevalence of work-related musculoskeletal disorders in sonographers, this study evaluated upper extremity kinematics and determined if co-contraction was present during kidney scans. The results provided a greater understanding of joint range of motion and muscular activity, which could be helpful in assessing risk of injury. Four sonographers had reflective markers and surface electromyography electrodes placed on their dominant upper extremity. A Vicon MX motion capture system was used to record the marker positions and electromyography data while the sonographers were scanning a volunteer's kidneys. The shoulder joint center was determined using the instantaneous helical axis method. The wrist and elbow joint centers were determined by taking the difference between markers located medially and laterally about the joint. Three shoulder angles (flexion/extension, abduction/adduction, and interior/exterior rotation), one elbow angle (flexion/extension), and one wrist angle (flexion-extension) were determined by kinematics. The results indicated that the sonographers were scanning with the shoulder in flexion, abduction, and external rotation. The shoulder abduction was always greater than published acceptable limits. The range of elbow flexion angles during this study was 9.3 to 102.2 degrees. The wrist joint was always in extension except for portions of one scan. The wrist joint angles exceeded acceptable published limits during all scans. The electromyograms indicated that the agonistic muscles in the upper arm and forearm were activated simultaneously with the antagonistic muscles at

multiple instances throughout the scans, indicating co-contraction was regularly occurring.

Table of Contents

List of Tables

Appendices

List of Figures

Appendices

Definition of Terms

Directional human motion terms-

Medial: toward midline.

Lateral: away from midline.

Proximal: toward the head or trunk.

Distal: away from the head or trunk.

Superior: toward the head.

Inferior: toward the feet.

Anterior: front side of the body.

Posterior: back side of the body.

Joint motion terms-

Flexion: decrease in joint angle between body segments.

Extension: increase in joint angle between body segments.

Abduction: movement away from midline.

Adduction: movement toward midline.

Internal rotation: rotates the anterior surface toward midline.

External rotation: rotates the anterior surface away from midline.

1. Introduction

"Work-related musculoskeletal disorders are a group of syndromes characterized by soft tissue discomfort caused or aggravated by workplace exposures," which can affect the muscles, joints, tendons, ligaments, or nerves (Berkowitz, Pike, Russo, Lessoway, & Baker, 1997). Sonographers suffer from work-related musculoskeletal disorders as a result of ergonomic hazards and working conditions. Ergonomic hazards that are a risk for repetitive strain injury are repetitive motion, forceful motion, static muscle load, mechanical stress, and awkward posture (Yassi, 1997). Working conditions that contribute to work-related musculoskeletal disorders are scanning durations over 45 minutes, insufficient breaks between patients, and nonadjustable equipment (Yassi, 1997; Swinker & Randall, 2003; Roll, Baker, & Evans, 2009).

In 1997, 81% of sonographers reported scanning in pain; by 2009 the percentage had increased to 90% (Roll, Baker, & Evans, 2009). Advancements in ultrasound equipment have been attributed to an increase in sonographers reporting pain because ultrasound image processing time has decreased. This has resulted in shorter durations between patients and an increase in the number of patients scanned per day (Schoenfeld, Goverman, Weiss, & Meizner, 1999). The persistence of pain has resulted in 20% of sonographers prematurely retiring or leaving the profession (Brown & Baker, 2004). Current treatments for many musculoskeletal disorders are anti-inflammatory drugs, physical therapy, and occupational therapy (Roll, Baker, & Evans, 2009). Research on work-related musculoskeletal disorders in sonographers has consisted of qualitative and

quantitative studies. For this thesis, qualitative will refer to survey studies while quantitative will refer to kinematic studies. Quantitative studies have been localized to a small demographic area or had limited sample sizes (Roll, Baker, & Evans, 2009). The quantitative studies examined muscle activity and joint movements that were localized to the shoulder or observations of upper body movement (Village & Trask, 2007; Milkowski & Murphey, 2006).

An ultrasound is a diagnostic procedure that uses high frequency sound waves to produce visual images of organs, tissues, or blood flow. Ultrasounds are widely used because they are minimally invasive and, unlike x-ray, there is no exposure to radiation. An ultrasound examination is initiated by a sonographer placing gel on the patient in the area that is being studied. The gel enhances the conduction of sound waves. The sound waves are introduced by a handheld transducer which is moved across the area being scanned.

During an ultrasound examination, there are several factors that Jakes (2001) identified as contributing to injury or discomfort to muscles or joints. Minuscule movements of the transducer and gripping the transducer tightly may injure the muscle fibers to the fingers or tendons in the fingers, hand, and forearm. Twisting and bending of the wrist to the extremes of range of motion while applying pressure to the patient can increase strain in the wrist. Shoulder abduction while applying pressure to the patient for long durations can strain shoulder, neck, and back muscles. Performing an ultrasound in awkward positions can result in the sonographer continuously twisting his or her torso and neck to see the monitor. As a result of these movements, pain is primarily experienced in the shoulders, neck, wrist, back, and hands as identified by several authors

and is illustrated in Figure 1 (Jakes, 2001; Swinker & Randall, 2003; Murphy & Russo, 2000). The figure identifies the general area of discomfort rather than the specific muscles strained.

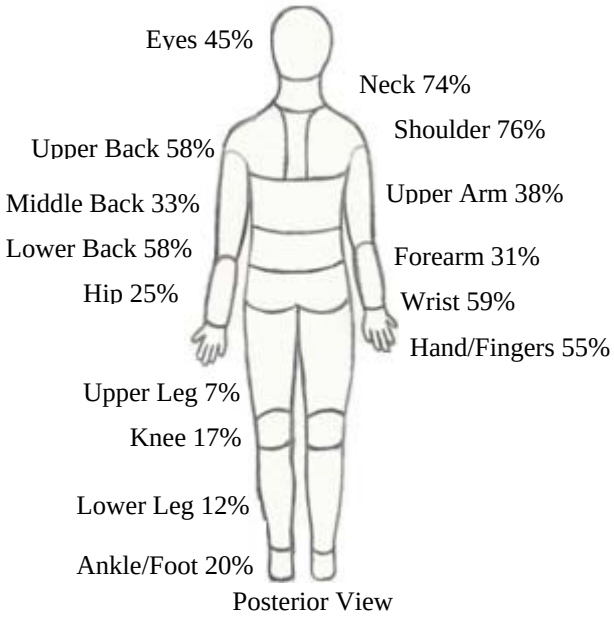

Figure 1: Anatomical locations of discomfort experienced by sonographers (Russo, Murphy, Lessoway, & Berkowitz, 2002)

1.1 Scope of the Study

Due to the prevalence of work-related musculoskeletal disorders in sonographers, this study evaluated upper extremity kinematics and determined if co-contraction was present in upper extremity muscle pairs during kidney scanning. There were three scanning factors used in this study: left and right kidney scans, two different ultrasound transducer designs, and two different scanning positions. Sonographers' upper extremity movements and muscular activity were recorded using a Vicon MX motion capture system. The kinematics investigated in this study were shoulder, elbow, and wrist joint angles. The results were compared: 1) for each joint angle to determine if there was a

trend present as a result of the scanning factors, 2) for shoulder abduction/adduction and wrist flexion/extension to acceptable published limits, and 3) to results published in a previous study by Burnett and Campbell-Kyureghyan (2010). Co-contraction of muscles pairs in the forearm and upper arm was investigated because it is a risk factor for repetitive strain injury (Malmivaara, van Tulder, & Koes, 2007).

This study was performed as a joint collaboration with occupational therapy graduate students at Grand Valley State University. In their thesis they analyzed the pressure exerted on the handle of the two different ultrasound transducer designs to determine if transducer design caused a significant change in the amount of pressure that was applied by the sonographers during scanning (Bullock, Conroy, & Vetter, 2011). Additionally, they used a questionnaire to quantify the amount of pain experienced after scanning. The Novel Pliance-X system was used to collect the pressure exerted by the hand on the pressure sensor mat wrapped around the transducer. This data was used to determine if there was a difference in the amount of pressure applied to the transducers. In their results they concluded that the smaller S5-1 transducer had increased average pressure and force exerted on it in comparison to the larger C5-1 transducer. The average pressure and force applied to the different transducers is shown in Table 1. Additional data from their study can be found in Appendix 10.3.

Table 1: Maximum and average pressure and force applied to the ultrasound transducers (Bullock, Conroy and Vetter 2011)

Transducer	Max Pressure (kPa)	Average Max Pressure (kPa)	Max Force (N)	Average Force (N)
C5-1	149.45	57.86	82.70	37.09
S5-1	125.84	64.58	88.86	54.33

2. Literature Review

The qualitative studies that have been performed have had larger sample sizes and a larger demographical area than the quantitative studies. The demographical area investigated was larger for qualitative studies because the majority involved surveys that were sent to sonographers throughout the United States of America. Data collected from qualitative studies has been analyzed using cross tabulation, meta-analysis, cross-sectional analysis, and statistical analysis. The quantitative studies have focused on muscle activity and arm position in reference to the shoulder. Roll et al. (2009) performed an extensive literature review on work-related musculoskeletal disorders in sonographers, which is summarized in Table 2.

Table 2: Assessment of researched publications on work-related musculoskeletal disorders experienced by sonographers and vascular technologists (Roll et al. 2009)

Sonography Studies	
Qualitative	Quantitative
Vanderpool et al. (1993)	Murphey and Milkowski (2006)
Necas (1996)	Village and Trask (2007)
Pike et al. (1997)	Bastian et al. (2009)
Smith et al. (1997)	Roll and Evans (2009)
Wihlidal and Shrawan (1997)	
Gregory (1998)	
Jakes (2001)	
McCulloch et al. (2002)	
Ransom (2002)	
Russo et al. (2002)	
Brown and Baker (2004)	
Muir et al. (2004)	
David (2005)	
Evans et al. (2009)	

2.1. Qualitative Studies

Targeted areas of interest for the qualitative studies were general health status, history of work-related injury, risk of injury, equipment utilized, overall work environment, demographic data, work experience, techniques for performing an ultrasound, and physical activity. The information collected from sonographers was used to determine factors that contribute to work-related musculoskeletal disorders, risks of work-related musculoskeletal disorders, modifications that are required for equipment utilized, consequences of work-related musculoskeletal disorders, and recommended workloads and procedures (Quanbury, Friesen, Friesen, & Arpin, 2006; Hutmire, Baker, Evans, & Roll, 2010; Berkowitz, Pike, Russo, Lessoway, & Baker, 1997; Vanderpool, Friis, Smith, & Harms, 1993). Factors that were determined to contribute to work-related musculoskeletal disorders were work experience, manipulating the transducer while maintaining pressure, shoulder abduction, twisting of the neck and trunk, inadequate recuperation time between patients, awkward posture, and scanning in a standing position (Hutmire, Baker, Evans, & Roll, 2010; Vanderpool, Friis, Smith, & Harms, 1993). Modifications suggested for current ultrasound equipment were enabling sonographers to maintain optimum joint angles, balanced posture, and allowing break durations similar to soft tissue recuperation time (Vanderpool, Friis, Smith, & Harms, 1993). The consequences of work-related musculoskeletal injuries were absenteeism from work, changing professions, or hospitals paying for additional compensation and rehabilitation (Wihlidal & Kumar, 1997; Brown & Baker, 2004). Working conditions that could decrease the severity of work-related musculoskeletal injuries have been suggested to be using an adjustable workstation, using a support cushion, alternating scanning with left

and right hand, performing various scans, wearing gloves that are textured to increase grip, and taking small breaks whenever possible (Jakes, 2001).

2.1.1. Qualitative Study Shortcomings

Understanding the shortcomings of previous investigations can be useful in developing future studies with fewer limitations. The shortcomings within the qualitative studies are ascertaining data from small demographical areas, small sample sizes, varying work environments, varying scanning techniques, varying scanning locations, and targeting the qualitative studies at sonographers that suffer from work-related musculoskeletal disorders. A small demographical area limits a qualitative study because it focuses on techniques, conditions, and methods that are dominant in one location and might not be a true representation of the sonography profession. The work environment for sonographers depends on the clinic that employs them, location of the clinic, number of sonographers employed, availability of adjustable equipment, and specialty of the clinic. Techniques that are used for scanning depend on the education that the sonographer received. Variations in education could be learning ergonomic techniques, ambidextrous techniques, or how to use equipment that aids in reducing muscle load. The location on the patient's body that sonographers scan determines scanning duration, posture, and joint movement. The size of the patient being scanned affects the grip pressure of the sonographer and the normal and lateral forces applied. The qualitative studies can generate bias by targeting sonographers that scan in pain or have experienced pain. This could result in an overestimation of sonographers that suffer from work-related musculoskeletal disorders.

2.2. Quantitative Studies

The purposes of the quantitative studies were evaluating muscle activity across the shoulders of sonographers using surface electromyography, quantifying posture during ultrasound scanning, and determining techniques to reduce muscle activity. In the quantitative study by Village and Trask (2007), surface electromyography was used to study activity in the following upper extremity muscles: supraspinatus, trapezius, infraspinatus, and flexor carpi ulnaris. Shoulder injuries have been suggested to occur during prolonged static contractions at as little as 3% maximum voluntary contraction. Muscle activity in all three shoulder muscles was above 3% maximum voluntary contraction for 90% of the scanning duration in this study. Posture assessment was determined using stop motion playback on recorded video where an observer categorized shoulder abduction and outward rotation into 15 degree increments from 0 to 90. Blood flow in the supraspinatus is significantly impeded if abduction is over 30 degrees. During 66% of the scan, the shoulder was greater than 30 degrees. The posture of a sonographer during scanning often can be described as awkward abduction and outward rotation of the shoulder. Gripping force was determined by generating a calibration equation from the maximum grip force with a hand-grip dynamometer and the electrical activity recorded by the electromyography electrodes on the flexor carpi ulnaris. The average gripping force over the duration of scanning time was 4 kilograms. The applied force to the transducer was 1 kilogram for 90% of the scanning time, which indicates that the hand had little resting time.

In the study performed by Milkowski and Murphy (2006), surface electromyography was used to study activity in the supraspinatus and trapezius muscles

for several different positions predetermined by the researchers. The positions were verified using a goniometer prior to data collection. Each position was maintained by the sonographer for 30 seconds. Muscle activity in the supraspinatus was reduced by 46% when shoulder abduction decreased from 75 to 30 degrees. When a sonographer used a support cushion under the forearm during scanning at 75 and 30 degrees of shoulder abduction muscle activity was further reduced by 32%. Muscle activity in the upper trapezius was reduced by 65% when forward shoulder flexion was reduced from 50 to 0 degrees. When both postures were compared for greatest and least shoulder abduction and flexion, muscle activity was reduced by 88%. These researchers suggest that the optimum posture for sonographers while using a support cushion under the forearm is 30 degrees or less shoulder abduction and zero degrees flexion.

In the study performed by Burnett and Campbell-Kyureghyan (2010), they determined joint angles for the scanning arm of seven sonographers using electrogoniometers for the following scans: thyroid, right abdominal, left abdominal, right deep venous thrombosis, and left deep venous thrombosis. The following joint angles were evaluated: wrist flexion and extension, wrist radial and ulnar deviation, elbow flexion and extension, forearm pronation and supination, and shoulder abduction. The results that they obtained for joint angles are shown in Table 3.

Table 3: Minimum, maximum, and average joint angles for five sonography scans (Burnett & Campbell-Kyureghyan, 2010)

Joint Angles		Scan				
		Thyroid	Right Abdominal	Left Abdominal	Right Deep Venous Thrombosis	Left Deep Venous Thrombosis
Wrist Extension(+)/Flexion(-) (Degrees)	Min	-64.3	-59.7	-51.3	-52.5	-60.4
	Max	15.2	31.7	21.5	50.4	21.8
	Average	-27.9	-20.9	-14.3	-8.9	-10.9
Wrist Radial(+)/Ulnar(-) Deviation (Degrees)	Min	-23.1	-26.6	-20.1	-25.2	-27.7
	Max	20.4	22.1	26.4	26.8	19.1
	Average	-1.8	-1.7	6.5	8.7	-5.2
Elbow Flexion (Degrees)	Min	--	--	--	--	--
	Max	84.1	98.1	85.6	78.1	82.7
	Average	26	31.7	31.4	45.1	27.3
Forearm Pronation(-)/ Supination(+) (Degrees)	Min	-34.2	-58.3	-43.8	-51.2	-60.1
	Max	70.5	67.4	71.9	76.6	67.5
	Average	9.3	-0.6	13.9	5.9	7.5
Shoulder Abduction (Degrees)	Min	56.5	39.6	36.8	52.5	29.2
	Max	104.5	99.1	99.2	107.7	93.6
	Average	74.8	72.8	71.9	78.9	68.9

2.2.1. Quantitative Study Shortcomings

Shortcomings of the quantitative studies were using a trained observer to determine joint angles from recorded video, maintaining a position to record muscle activity, using small test groups, and localizing the focus of the studies to muscle activity and joint movement in the shoulder. Determining shoulder abduction and outward rotation using a trained observer on stop motion playback affects the accuracy of the joint angles because the observer is using a 2D image to determine a 3D angle. This method of joint angle measurement could introduce a large angular error in the study. The study by Miklowski and Murphy (2006) focused on the muscle activity of a sonographer's position rather than that of an ultrasound examination. Measuring the muscle activity of

a sonographer holding a position may not accurately represent the activity experience during a scan. The study by Burnett and Campbell-Kyureghyan (2010) was unable to determine shoulder flexion/extension and shoulder internal/external rotation because electrogoniometers were used to determine the joint angles. The test groups of these studies were small, which caused large standard deviations due to the variety of techniques used by each sonographer. Localizing the muscle loads and joint movements to the shoulder only evaluates a portion of the movements that are occurring while a sonographer scans.

2.3. Acceptable Range of Motion Limits

McCulloch, Xie, and Adams (2002) define the acceptable limits for shoulder abduction between 0 and 20 degrees. When the shoulder is extended beyond the acceptable limits it can result in joint instability. Shoulder injuries can result from a reduction in blood flow to the supraspinatus and infraspinatus muscles. This can occur when the shoulder is abducted over 30 degrees which increases intramuscular pressure (Garg, Hegmann, & Kapellusch, 2006; Village & Trask, 2007).

Hedge (1998) defines the acceptable limits of wrist flexion/extension as 15 degrees flexion to 15 degrees extension. When the wrist is within these limits carpel tunnel pressure typically remains below 30 mmHg. A substantial increase in carpel tunnel pressure over 30 mmHg is undesired because it can cause detrimental affects to the median nerve. In animal studies increasing carpel tunnel pressure from 30 to 50 mmHg over short durations can disrupt blood flow along the side of the median nerve. Animal

and human studies have shown if carpel tunnel pressure ranges from 40 to 50 mmHg for 8 hours it can result in the complete blocking of nerve signals (Hedge, 1998).

2.4. Basis for Further Research

Areas of further research for studying work-related musculoskeletal disorders could be examining muscle activity, joint angles, and joint torques for the entire upper extremity, measuring how force is applied to the transducer, and using motion capture to determine the joint angles. The shoulder was the focus of previous investigations because most pain was experienced in the shoulder. Examining the muscle activity in the entire upper extremity could demonstrate how the sonographer coordinates all upper extremity muscles to perform an ultrasound scan. This could be used to establish the efficiency of the muscles by determining if excessive co-contraction of the muscles is occurring. Examining the joint angles in the upper extremity allows a baseline comparison of scanning techniques between sonographers. 3-D motion capture could be used to determine the joint angles in the upper extremity with more accuracy than stop motion playback of a 2-D video. Determining how force and pressure is applied to the transducer could establish if the sonographer is using a power grip or pinch grip. Additionally, it could determine the distribution of forces and pressures among individual fingers. The type of grip that the sonographer uses could affect the work-related musculoskeletal disorders in the hand. Examining the joint torques would establish a baseline for future transducer designs since there currently are no published studies that have examined joint torques. These further studies would build upon the qualitative studies by identifying factors that contribute to work-related musculoskeletal disorders,

potentially verifying the qualitative studies' conclusions. Further research could improve by joint angle observations and measurement techniques.

3. Background

3.1. Motion Capture

Motion capture is a process used to record and track the movements of a subject. The motion capture system used for this study was a Vicon MX motion capture system. This system records at a frame rate of 100 Hertz the three dimensional position of reflective markers placed on a subject in key landmark locations relevant to the research being performed. The positions of the markers are determined using the LED strobe lights on each camera. As the subject moves through the motion capture field the light from the strobes are reflected back into the camera lens by the markers. The lens collects the light and forms a focused image of the markers on the camera's sensor plane. The camera converts the pattern of light into data that represents the position and radius of each marker (Vicon MX Hardware System Reference, 2007). This is done by generating grayscale blobs that represent objects in the capture field then using centroid-fitting algorithms to determine which of the objects are likely to be markers (Go Further with Vicon MX T-Series, 2011).

3.2. Landmark Selection

Landmark locations for the reflective markers were selected based on the joint angles of interest and previous studies on the shoulder joint. Joint angles were determined for the wrist, elbow, and shoulder. The landmarks located medially and laterally from the elbow and wrist joint centers were selected to calculate the joint centers. The selected landmarks located medially and laterally from the elbow joint center are the epicondylus medialis humeri and epicondylus lateralis humeri. Radial and

ulnar styloid processes are located laterally and medially from the wrist joint center. In the different studies by Mesker et al. (1998), Veeger (2000), and Stokdijk et al. (2000), to determine the center of rotation for the shoulder joint, markers were placed in the following locations on the scapula: angulus acromialis, trigonum spinae scapulae, angulus inferior scapulae, most dorsal point of the acromioclavicular joint, and processus coracoideus. The five landmarks used by these researchers were selected as a result of multiple methods to determine the center of rotation for the shoulder joint. In each of these studies one of the following methods was used: linear regression (Mesker, van der Helm, Rozendaal, & Rozing, 1998), instantaneous helical axis method (Veeger, 2000), and sphere fit method (Stokdijk, Nagels, & Rozing, 2000). Three virtual markers were placed on both the forearm and the upper arm to determine the joint centers relative to a local coordinate system, anatomical reference frames, and joint angles. The hand marker locations were selected so that they could be used to calculate rotation about three axes at the wrist, if desired. The lower extremities had reflective markers placed on them for visualization purposes. The markers that were selected for the clavicle, scapula, humerus, and forearm matched the International Society of Biomechanics recommendations (Wu, et al., 2005). The processus xiphodeus and suprasternal notch markers recommended for the thorax were not used. The processus xiphodeus was not used because it is intrusive for female subjects and the attire worn by the sonographers could result in inaccurate representation of the location. The suprasternal notch was not used because of its proximity to the sternoclavicular joint. Additionally, the sternoclavicular joint could be used to determine the sternoclavicular and acromioclavicular joint angles, if desired. If there is not adequate space between two

reflective markers, the Vicon MX motion capture system will merge the markers into one or one marker could obscure the location of another marker. The entire landmark marker set is shown in Table 4.

Table 4: Reflective marker set to determine upper extremity joint angles

Extremity Location	Anatomical Location	Landmarks
Upper	Torso	Sternoclavicular joint
		C7
		T8
	Shoulder	Angulus acromialis
		Trigonum spinae scapulae
		Angulus inferior scapulae
		Acromioclavicular
		Processus coracoideus
	Elbow	Epicondylus lateralis humeri
		Epicondylus medialis humeri
	Wrist	Ulnar styloid process
		Radial styloid process
	Hand	2nd metacarpal base
		2nd metacarpal head
		2nd distal phalange head
		4th metacarpal base
		1st distal phalange base
	Humerus	Virtual marker 1
		Virtual marker 2
		Virtual marker 3
	Forearm	Virtual marker 1
		Virtual marker 2
		Virtual marker 3
Lower	Hip	Posterior superior iliac spine
		Anterior superior iliac spine
		Greater trochanter femoral
	Shank	Lateral tibial plateau
		Lateral malleolus tibial
	Foot	Calcaneus
		5th metatarsal head

3.3. Kinematics

Kinematics is the study of motion independent of forces. It focuses on the details of movement. Kinematic variables used to describe movement are linear and angular displacement, velocity, and acceleration. A complete and accurate quantitative description of a simple movement requires a large amount of data and a large number of calculations. The complete kinematics of a single body segment requires 18 data variables: center of mass position in three directions, center of mass linear velocity in three directions, center of mass linear acceleration in three directions, angle of the segment about three axes, angular velocity of the segment about three axes, and angular acceleration of the segment about three axes (Winter, 2009). Kinematics was used to determine the joint centers and angles for the shoulder, elbow, and wrist. The methods used to determine the joint centers are discussed in the following section, 3.3.1. Joint Center Calculation Methods. The process used to determine the joint angles is discussed in section 4.6. Motion Capture Data Analysis.

3.3.1. Joint Center Calculation Methods

Reflective markers for motion capture cannot be placed at joint centers for in-vivo subject studies because joint centers are located below the skin surface. As a result, joint centers were calculated based on the position of landmarks surrounding the joints. The instantaneous helical axis method was used to determine the shoulder joint center because it was modeled as a ball and socket joint. The half-distance between medial and lateral landmarks was used to determine the elbow and wrist joint centers because they were modeled as hinge joints.

3.3.1.1. Instantaneous Helical Axis Method

The instantaneous helical axis method was recommended by the International Society of Biomechanics to determine the shoulder joint center (Wu, et al., 2005). The instantaneous helical axis of a rigid body is a line in space that represents both the axis of rotation and the line along which translation occurs. The position and direction of the instantaneous helical axis is uniquely defined if the angular velocities of the landmarks are not equal to zero (Winter, 2009). The location of a point on the instantaneous helical axis when the angular velocities of the landmarks are not equal to zero was determined using the following equation:

$$\bar{p} = \overline{x}_o + \frac{\overline{\overline{\omega}}\,\overline{v}_o}{\omega^2} \quad (1)$$

where $\bar{p}$ is the location of a point on the instantaneous helical axis, $\overline{x}_o$ is the global position of the centroid of landmarks, $\overline{\overline{\omega}}$ is the skew-symmetric angular velocity matrix, $\overline{v}_o$ is the mean velocity of the landmarks, and ω is the magnitude of angular velocity. In the special case of pure translation $\bar{p} = \overline{x}_o$.

The variables to determine the instantaneous helical axis are defined in the following equations. The global position of the centroid of landmarks ($\overline{x}_o$) was determined using the following equation:

$$\overline{x}_o = \frac{1}{n}\sum_{i=1}^{n} \overline{x}_i \quad (2)$$

where n is the number of landmarks, i is the capture frame, and $\overline{x}_i$ is the global position of landmark i. The global positions of landmarks were determined by the Vicon MX motion capture system. Mean velocity of the landmarks ($\overline{v}_o$) was determined using the following equation:

$$\overline{v}_o = \frac{1}{n}\sum_{i=1}^{n} \overline{v}_i \tag{3}$$

where $\overline{v}_i$ is the velocity of landmark i. The velocity of each landmark was determined using a central difference formula:

$$\overline{v}_i = \frac{\overline{x}_{i+1} - \overline{x}_{i-1}}{2\Delta t} \tag{4}$$

where $\overline{x}_{i+1}$ is the global position of landmark i in the next frame of data collection, $\overline{x}_{i-1}$ is the global position of landmark i in the previous frame of data collection, and Δt is the change in time between data collection frames. The skew-symmetric angular velocity matrix ($\overline{\overline{\omega}}$) is:

$$\overline{\overline{\omega}} = \begin{bmatrix} 0 & -\omega_z & \omega_y \\ \omega_z & 0 & -\omega_x \\ -\omega_y & \omega_x & 0 \end{bmatrix} \tag{5}$$

where ω_x is the angular velocity about the x axis, ω_y is the angular velocity about the y axis, and ω_z is the angular velocity about the z axis (Woltring, 1990). The angular velocity vector ($\overline{\omega}$) was determined using the calculation provided by Sommer III (1992)

in *Determination of First and Second Order Instant Screw Parameters from Landmark Trajectories*:

$$\overline{\omega} = \begin{bmatrix} \omega_x \\ \omega_y \\ \omega_z \end{bmatrix} = \begin{bmatrix} \bar{\bar{X}}_{22} + \bar{\bar{X}}_{33} & -\bar{\bar{X}}_{12} & -\bar{\bar{X}}_{13} \\ -\bar{\bar{X}}_{21} & \bar{\bar{X}}_{11} + \bar{\bar{X}}_{33} & -\bar{\bar{X}}_{23} \\ -\bar{\bar{X}}_{31} & \bar{\bar{X}}_{32} & \bar{\bar{X}}_{11} + \bar{\bar{X}}_{22} \end{bmatrix}^{-1} \begin{bmatrix} \bar{\bar{V}}_{32} - \bar{\bar{V}}_{23} \\ \bar{\bar{V}}_{13} - \bar{\bar{V}}_{31} \\ \bar{\bar{V}}_{21} - \bar{\bar{V}}_{12} \end{bmatrix} \quad (6)$$

where $\bar{\bar{X}}$ is the landmark product matrix and $\bar{\bar{V}}$ is the landmark velocity moment matrix. The landmark product matrix was determined used the following equation:

$$\bar{\bar{X}} = \frac{1}{n} \sum_{i=1}^{n} (\overline{x}_i - \overline{x}_o)(\overline{x}_i - \overline{x}_o)' \quad (7)$$

where n is the number of landmarks. The landmark velocity moment matrix was determined using the following equation:

$$\bar{\bar{V}} = \frac{1}{n} \sum_{i=1}^{n} \overline{v}_i (\overline{x}_i - \overline{x}_o)' \quad (8)$$

The magnitude of angular velocity (ω) was determined using the following equation:

$$\omega = |\overline{\omega}| = \sqrt{{\omega_x}^2 + {\omega_y}^2 + {\omega_z}^2} \quad (9)$$

where $\overline{\omega}$ is the angular velocity vector.

After the location of a point on the instantaneous helical axis was determined for multiple capture frames the optimal pivot point or in this instance the center of rotation ($\overline{p}_{opt}$) was determined using the following equation:

$$\overline{p}_{opt} = \left(\frac{1}{n}\sum_{i=1}^{n} I - n_i n_i'\right)^{-1} \left(\frac{1}{n}\sum_{i=1}^{n}(I - n_i n_i')\,\bar{p}_i\right) \tag{10}$$

where I is the identity matrix, n_i is the unit direction vector at i, and $\bar{p}_i$ is the location of a point on the instantaneous helical axis at i (Woltring, 1990). The unit direction vector (n_i) when the angular velocities of the landmarks are not equal to zero was determined using the following equation:

$$n_i = \frac{\overline{\omega}}{\omega} \tag{11}$$

In the special case of pure translation the unit direction vector was determined using the following equation (Sommer III, 1992):

$$n_i = \frac{\overline{v}_o}{|\overline{v}_o|} \tag{12}$$

3.3.1.2. Difference between Medial and Lateral Landmarks

The elbow and wrist joint centers on the scanning arm of the sonographer were determined by finding the midpoint between the reflective markers on the bony landmarks located medially and laterally from the joint center. This is a known and

accepted method used to determine hinge joints within the body. The following equation was used to determine the global position of the joint centers ($\overline{x}_{jc}$):

$$\overline{x}_{jc} = \frac{\overline{x}_m - \overline{x}_l}{2} + \overline{x}_l \quad (13)$$

where $\overline{x}_m$ is the global position of the medial marker and $\overline{x}_l$ is the global position of the lateral marker.

3.3.2. Reference Frames

Reference frames are the global or local coordinate systems which are used to describe the position of landmarks. The Vicon MX motion capture system determines the position of landmarks with respect to a global reference frame. The origin of the global reference frame was determined during the calibration process which is discussed in section 4.5 Procedure.

Local reference frames are fixed with respect to rotating and translating bodies and are used to describe the position of landmarks relative to body segments. Local reference frames can be defined as technical reference frames or anatomical reference frames. Local technical reference frames were determined for the thorax, humerus, and forearm using three non-collinear landmarks on the same body segment.

The equations to determine the three axes defining a local technical reference frame are given below:

$$Axis1 = \frac{\overline{x}_2 - \overline{x}_1}{|\overline{x}_2 - \overline{x}_1|} \quad (14)$$

where Axis1 is a vector that points from $\overline{x}_1$ to $\overline{x}_2$, where $\overline{x}_1$ and $\overline{x}_2$ are landmarks on the same body segment.

$$Axis2 = \frac{Axis\ 1 \times (\overline{x}_3 - \overline{x}_1)}{Axis\ 1 \times |\overline{x}_3 - \overline{x}_1|} \quad (15)$$

where Axis2 is a vector that is perpendicular to the plane defined by $\overline{x}_1$, $\overline{x}_2$, and $\overline{x}_3$, where $\overline{x}_3$ is a landmark on the same body segment as $\overline{x}_1$ and $\overline{x}_2$.

$$Axis3 = Axis1 \times Axis2 \quad (16)$$

where Axis3 is a vector mutually perpendicular to Axis1 and Axis2. The order of the cross products in Equations 15 and 16 is interchangeable depending on the desired direction of Axis2 and Axis3 (Winter, 2009).

3.3.3. Rotation Matrices

A global-to-local rotation matrix ($R_{L/G}$) can be used to determine the position of a landmark with respect to a global reference frame if the position of the landmark in a local reference frame is known. The opposite transformation can be performed with the corresponding local-to-global rotation matrix ($R_{G/L}$), which is simply the transpose of the global-to-local rotation matrix:

$$R_{G/L} = {R_{L/G}}' \quad (17)$$

Global-to-local rotation matrices are defined using the local reference frame axes. The global-to-local rotation matrix can be determined using the following matrix:

$$R_{L/G} = \begin{bmatrix} Axis1_x & Axis1_y & Axis1_z \\ Axis2_x & Axis2_y & Axis2_z \\ Axis3_x & Axis3_y & Axis3_z \end{bmatrix} \tag{18}$$

where Axis1, Axis2, and Axis3 are the three axes defining the local reference frame. In this example, the axes are in the sequence 123, but five additional sequences can be defined by rearranging the order of the three axes in the global-to-local rotation matrix.

The position of a landmark expressed with respect to a global reference frame can be defined in a local reference frame using the following equation:

$$[\vec{r}]_L = R_{L/G}[\vec{r}]_G - R_{L/G}[\vec{r}_o]_G \tag{19}$$

where $[\vec{r}]_L$ is the position of the landmark in the local reference frame, $[\vec{r}]_G$ is the position of the landmark in the global reference frame, and $[\vec{r}_o]_G$ is the position of the origin of the local reference frame expressed with respect to the global reference frame. The position of a landmark expressed with respect to a local reference frame can be defined with respect to the global reference frame using the equation below:

$$[\vec{r}]_G = R_{L/G}{}' [\vec{r}]_L + [\vec{r}_o]_G \tag{20}$$

As just described, technical reference frames are determined using three non-collinear landmarks located anywhere on the same body segment. Anatomical reference frames are determined using three key skeletal landmarks (Winter, 2009). The skeletal landmarks used in this study were the two joint centers (proximal and distal) and one landmark located medially or laterally from one of the joint centers.

The joint rotation matrix (R_{joint}) is determined using the global-to-local rotation matrices defined by two body segments located proximally and distally to the joint:

$$R_{joint} = \left(R_{distal/G}\right)\left(R_{proximal/G}\right)' \tag{21}$$

where $R_{distal/G}$ is the global-to-local rotation matrix of the distal segment and $R_{proximal/G}$ is the global-to-local rotation matrix of the proximal segment. The joint rotation matrix is used to determine the Euler angles.

3.3.4. Joint Angle Calculation Methods

The shoulder joint angles were determined using an Euler rotation sequence because the angles about three axes were of interest. The dot product was used to determine the elbow joint angles because only one angle (flexion/extension) was needed for this study. The cross and dot products were used to determine the wrist angles because only one angle (flexion/extension) was of interest.

3.3.4.1. Euler Angles

Euler angles are used to describe the orientation of a rigid body in 3D space by performing a series of three rotations about the axes of either a global or local reference

frame. The Euler rotation sequence used in this study was YX'Y" which was recommended by the International Society of Biomechanics (Wu, et al., 2005). This is the rotation of the reference frame about the y axis first, the new x axis second, and about the new y axis last. The first rotation sequence is φ about the y axis which results in the new reference frame x', y', z'. The second rotation sequence is θ about the new x' axis which results in the new reference frame x", y", z". The third rotation sequence is ψ about the new y" axis which results in the final reference frame x"', y"', z"'. Based on this sequence the Euler angles can be determined using the joint rotation matrix (R_{joint}):

$$R_{joint} = [R_{Y"}][R_{X'}][R_Y] = \begin{bmatrix} \mathrm{c}\,\psi & 0 & -\mathrm{s}\,\psi \\ 0 & 1 & 0 \\ \mathrm{s}\,\psi & 0 & \mathrm{c}\,\psi \end{bmatrix} \begin{bmatrix} 1 & 0 & 0 \\ 0 & \mathrm{c}\,\theta & \mathrm{s}\,\theta \\ 0 & -\mathrm{s}\,\theta & \mathrm{c}\,\theta \end{bmatrix} \begin{bmatrix} \mathrm{c}\,\varphi & 0 & -\mathrm{s}\,\varphi \\ 0 & 1 & 0 \\ \mathrm{s}\,\varphi & 0 & \mathrm{c}\,\varphi \end{bmatrix} \quad (22)$$

where $[R_{Y"}]$ is the rotation matrix for the third rotation about the y" axis, $[R_{X'}]$ is the rotation matrix for the second rotation about the x' axis, $[R_Y]$ is the rotation matrix for the first rotation about the y axis, c is the cosine function, and s is sine function (Winter, 2009). Equation (22) can be expanded into:

$$\begin{bmatrix} R_{joint_{11}} & R_{joint_{12}} & R_{joint_{13}} \\ R_{joint_{21}} & R_{joint_{22}} & R_{joint_{23}} \\ R_{joint_{31}} & R_{joint_{32}} & R_{joint_{22}} \end{bmatrix} = \begin{bmatrix} c\varphi c\psi - c\theta s\varphi s\psi & s\psi s\theta & -c\psi s\varphi - c\varphi c\theta s\psi \\ s\varphi s\theta & c\theta & c\varphi s\theta \\ c\varphi s\psi + c\psi c\theta s\varphi & -c\psi s\theta & c\varphi c\psi c\theta - s\varphi s\psi \end{bmatrix} \quad (23)$$

Using equation (21) the Euler angles can be determined. The second rotation angle is found with:

$$\theta = \cos^{-1}\left(R_{joint_{22}}\right) \tag{24}$$

The first rotation angle can then be determined with:

$$\varphi = \tan^{-1}\left(\frac{\sin\varphi}{\cos\varphi}\right) = \left(\frac{\frac{R_{joint_{21}}}{\sin\theta}}{\frac{R_{joint_{23}}}{\sin\theta}}\right) \tag{25}$$

The third rotation angle can be determined with:

$$\psi = \tan^{-1}\left(\frac{\sin\psi}{\cos\psi}\right) = \left(\frac{\frac{R_{joint_{12}}}{\sin\theta}}{\frac{R_{joint_{32}}}{-\sin\theta}}\right) \tag{26}$$

In this study the first Euler angle, φ, was used to describe shoulder flexion and extension. The second Euler angle, θ, describes shoulder abduction and adduction. The third Euler angle, ψ, describes shoulder internal and external rotation. Shoulder flexion, abduction, and internal rotation occur when the Euler angles are positive.

3.3.4.2. Dot Product

The dot product was used to determine flexion and extension for the elbow. The equation used to determine the flexion/extension angles at the elbow is:

$$\theta = \cos^{-1}\left(\frac{\vec{v}_{proximal}\cdot\vec{v}_{distal}}{|\vec{v}_{proximal}||\vec{v}_{distal}|}\right) \tag{27}$$

where $v_{proximal}$ is the vector representing the long axis of the proximal body segment, and v_{distal} is the vector representing the long axis of the distal body segment. The joint centers were used to create vectors in the proximal and distal body segments. Elbow flexion occurs when θ is positive. The elbow will always be positive as a result of the neutral position selected for the elbow joint.

3.3.4.3. Dot and Cross Products

The dot and cross products were used to determine flexion and extension for the wrist. The equation used to determine the flexion/extension angles at the wrist is:

$$\theta = sign\left(\cos^{-1}\left(\frac{\vec{v}_{distal} \cdot \vec{v}_{proximal}}{|\vec{v}_{distal}||\vec{v}_{proximal}|}\right)\right) \tag{28}$$

where sign is the direction of the vector normal to the proximal plane. The direction of the vector normal to the proximal plane was determined using the following equation:

$$d = \vec{v} \cdot \vec{v}_{normal} \tag{29}$$

where $\vec{v}$ is a vector above the proximal plane and its direction points away from the proximal plane and $\vec{v}_{normal}$ is a vector normal to the proximal plane. If d is negative then the normal vector is below the proximal plane, the wrist is in flexion, and sign is 1. If d is positive then the normal vector is above the proximal plane, the wrist is in extension, and sign is -1, reference Figure 2.

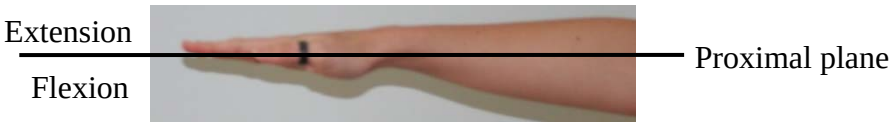

Figure 2: Location of the proximal plane used to determine if the wrist is in flexion or extension

The vector above the proximal plane, $\vec{v}$ was determined using the wrist joint center and a proximal body segment marker located above the proximal plane. The vector normal to the proximal plane, $\vec{v}_{normal}$ was determined using the following equation:

$$\vec{v}_{normal} = \vec{v}_{proximal} \times \vec{v}_{parallel} \tag{30}$$

where $\vec{v}_{parallel}$ is the vector parallel to the proximal plane. The following equation was used to determine the vector parallel to the proximal plane:

$$\vec{v}_{parallel} = \vec{v}_{distal} \times \vec{v}_{proximal} \tag{31}$$

The joint centers were used to create a vector in the proximal body segment. A marker on the distal body segment and the joint center were used to create a vector in the distal body segment. Wrist flexion occurs when θ is positive.

3.4. Electromyography and Co-contraction

Electromyography is a technique for evaluating and recording the electrical voltage generated by muscle fibers prior to the generation of muscle forces.

Electromyograms are produced from the recorded voltage. They can be used to detect co-contraction in muscle pairs by comparing if both muscles are producing an increase in voltage at the same instance. Co-contraction is when the antagonist and agonist muscles around a joint simultaneously contract. Co-contraction is an inefficiency in movement because the muscles are working against each other without producing a net moment (Winter, 2009).

3.5. Superficial Muscle Selection

Superficial muscle pairs in the dominant forearm and upper arm were investigated during this study because it has been hypothesized that frequent co-contraction of muscles has resulted in the pathophysiology of repetitive strain injury, which is a type of work-related musculoskeletal disorder (Malmivaara, van Tulder, & Koes, 2007). The muscles selected in the forearm were the flexor carpi ulnaris and extensor carpi ulnaris. This pair was selected because the flexor carpi ulnaris had been used in a previous sonography study to obtain electromyography data (Village & Trask, 2007). The muscles selected in the upper arm were the biceps brachii and triceps brachii.

4. Methodology

4.1. Participant Criterion and Recruitment

This study contained sonographer and patient participant groups. The criterion for the sonographer participant group required at least three years of experience in the field of sonography. This provided the study with conditioned sonographers that have adapted their techniques to accommodate the demands of their occupation. Multiple sonographers were obtained for this study from the West Michigan region.

The criterion for the volunteer patient required a body mass index equal to or greater than 30 which is considered obese (World Health Organization, 2012). A patient within this body mass index range created a scenario in which the sonographers would likely need to provide a greater force to the transducer to obtain an acceptable ultrasound image than they would with patients that have lower body mass indices. The patient characteristics needed to calculate body mass index were obtained using a tape measure and scale. Body mass index was calculated by dividing weight in kilograms by the squared height in meters. A single patient was used for this study to reduce variation.

The participant groups were recruited using fliers and personal connections to practicing sonographers. Lynn Carlton, an assistant professor at GVSU in the diagnostic medical sonography program, contacted sonographers to participate in the study. Fliers were posted on Grand Valley State University's (GVSU) Pew Campus to obtain a volunteer patient to be scanned. Participants were selected based on availability.

4.2. Sonographer Participation and Data Collection

This study had five sonographers participate, but complications with equipment prevented complete data collection for each participant. Motion capture data was

collected for all five sonographers, but the data collected for sonographer 1was insufficient for kinematic analysis. Electromyography was collected for sonographers 2, 4, and 5. Force and pressure applied to the transducers was collected for sonographers 1, 4, and 5.

Sonographers 2 and 3 were sitting in a backless, height adjustable, swivel, chair while they were scanning. Sonographers 1, 4, and 5 were standing while they were scanning. All of the sonographers used the C5-1 and S5-1 ultrasound transducers to scan the patient's left and right kidney.

4.3. Participant Demographics and Characteristics

All five sonographers were female, right hand dominant, and had at least three years of experience in diagnostic medical sonography. General sonography was the area of specialty for four of the sonographers. The additional sonographer participating in this study specialized in obstetric, abdominal, and vascular sonography. Pain had been experienced at some level either during scanning or as a result from scanning by four of the sonographers prior to the study. Demographics and characteristics of the sonographers can be found in Table 5. The patient that was scanned by each of the sonographers was a 23 year old male. He had a body mass index of 31.3 which was within the desired range for this study.

Table 5: Demographics and characteristics of participant sonographers

Sonographer	Age during Study (years)	Years of Experience	Hand Dominance	Gender	Areas of Specialty
1	57.4	16	Right	Female	General
2	44.4	14	Right	Female	Obstetric, abdominal, and vascular
3	60.2	34	Right	Female	General
4	32.8	3	Right	Female	General
5	25.9	3.5	Right	Female	General

4.4. Instrumentation and Materials

4.4.1. Vicon MX Motion Capture System

The Vicon MX motion capture system consists of a MX Giganet, eight Vicon T40 cameras, Vicon Nexus software, and reflective markers. The Vicon T40 cameras each have 320 LED strobe lights that are used to produce the signal that is sent to the MX Giganet. The MX Giganet connects the cameras and external devices to the capturing computer that contains the Vicon Nexus software (Vicon MX Hardware System Reference, 2007). An external device that was connected to the MX Giganet for this study was the MA300 multi-channel EMG system, which is discussed in the following section. The Vicon MX motion capture system was used to track and record the location of bony landmarks on sonographers and the recorded surface electromyography data.

4.4.2. MA300 Multi-Channel EMG System

The MA300 multi-channel EMG system consist of a MA300 desk top unit, MA300 backpack, surface electromyography electrodes, and coaxial cable. The MA300 multi-channel EMG system has 16 channels for data collection. Electrodes are conductive elements that are placed on the surface of the skin to record the electrical voltage generated by the muscle fibers prior to the generation of muscle forces. The

electrodes are non-invasive and a minimal risk to the sonographers being studied. The MA300 backpack processes and transmits the digital signal collected from the electrodes to the MA300 desk top unit. Additionally, it can be used to adjust gain on individual electrodes. The MA300 desk top unit transforms the digital input signals into analog output signals (Motion Lab Systems User Manual, 2007). The MA300 multi-channel EMG system was used to transmit the analog surface electromyography data to the MX Giganet.

4.4.3. Novel Pliance-X System

The Novel Pliance-X system consist of a s2054 Pliance-X sensor mat, Pliance-X sensor cable, Pliance-X box, Pliance-X fiber optic cable with fiber optic/USB adapter, belt, Pliance-X battery, Pliance-X battery cable, Bluetooth dongle, and Pliance data collection software. The Pliance-X box transmits data from the s2054 Pliance-X sensor mat via Bluetooth to the collection computer with Pliance data collection software (Pliance-X System Manual, 2011). The Novel Pliance-X system was used to determine the amount of force and pressure that the sonographers applied to the transducers. The s2054 Pliance-X sensor mat was secured to the ultrasound transducer using micropore tape. This resulted in a slight increase in the size of the transducer. This system collected data that was evaluated by the occupational therapy graduate students.

4.4.4. Jamar Dynamometer and Baseline Pinch Gauge

Jamar dynamometer and Baseline pinch gauge use hydraulic mechanisms that indicate the force applied by an individual to the instrument on a gauge dial (JAMAR

Hydrolic Hand Dynamometer User Instructions, 2004). A Jamar dynamometer was used to determine the isometric grip force of sonographers before the study. Then a Baseline pinch gauge was used to determine the three-jaw chuck, lateral pinch, and tip pinch forces. These forces were used by the occupational therapy graduate students in their study.

4.4.5. Philips iU22 Ultrasound System

A Philips iU22 ultrasound system was used by the sonographer to display real time imaging and save images of the patient's left and right kidney scans. C5-1 and S5-1 ultrasound transducers were used in conjunction with the Philips iU22 ultrasound system. The C5-1 transducer is a larger size than the S5-1 transducer. Difference transducer sizes were used during this study as a result of the joint collaboration with occupational therapy graduate students. The occupation therapy students were investigating whether the design of the transducer affects the amount of pressure exerted by the sonographer.

4.4.6. Miscellaneous Instrumentation

Miscellaneous instrumentation used during this study included a tape measure, scale, alcohol wipes, two-sided tape, micropore tape, and gaffer tape. The tape measure was used to measure the height of the sonographers and patient. A scale was used to determine the weight of the sonographers and patient. Alcoholic wipes were used to abrade and clean the sonographers' skin where the surface electromyography electrodes would be placed. Additionally, they were used to clean the surface electromyography electrodes. Two-sided tape was used to affix the reflective markers to the sonographers. Micropore tape was used to secure the s2054 Pliance-X sensor mat to the ultrasound

transducer that was being used. Micropore tape was used to prevent the remnants of tape residue on the s2054 Pliance-X sensor mat. Gaffer tape was used to secure the surface electromyography electrodes to the sonographers.

4.4.7. Questionnaire and Pain Measurements

A pre-scan questionnaire was administered to determine demographic information and if pain has been experienced in the upper extremities or torso of the sonographers. A post-scan questionnaire was administered to determine if pain had been experienced while scanning during the study and if there was a preference for transducer design. The pain level experienced was based on a functional pain scale ranging from no pain to intolerable and unable to verbally communicate because of the pain, zero to five respectively. The questionnaires were utilized by the occupational therapy graduate students in their thesis.

4.5. Procedure

Prior to the arrival of participants, the Vicon MX motion capture system located in the biomechanics laboratory at GVSU Cook DeVos Center for Health Sciences building was calibrated and reflective locations in laboratory were masked. The locations were masked using a built-in function within the Vicon Nexus software. Dynamic calibration of the capture field was obtained by continuously moving the calibration wand throughout the capture space until 1500 frames were detected by each Vicon T40 camera. The Vicon Nexus software then determined the image error for each camera. If the image error was less than 0.20 millimeters for each camera, then the next step was static calibration. Static calibration of the capture field was obtained by placing the calibration

wand on top of the south east corner of the first force plate to set the origin for the global coordinate system. The default sampling frequencies were used for the reflective markers and surface electromyography, 100 and 1200 Hertz respectively. After the Vicon MX motion capture system was setup, the MA300 multi-channel EMG system was assembled with the exclusion of the surface electromyography electrodes. Then, reflective markers were prepared using two-sided tape.

The sensor mat was calibrated before the study date using the trublu calibration device. The trublu calibration device applies an equally distributed pressure to all of sensors located on the sensor mat. The Pliance data collection software indicated several pressures that needed to be applied to the sensor to ensure calibration. The researchers adjusted the pressure accordingly. The Pliance data collection software then calibrated the individual sensors on the sensor mat based on the pressure applied to the sensors and the pressure recorded. The default sampling frequency used for calibration was 50 Hertz. The Novel Pliance-X system was then assembled and the s2054 Pliance-X sensor mat was zeroed. The sensor mat was zeroed by placing it flat on a table and using the Pliance data collection software. Then, it was secured to the C5-1 transducer using micropore tape and a baseline zero measurement was taken. When the sensor mat was secured, the researchers ensured that it was not creased which is shown is Figure 3.

S5-1 transducer

C5-1 transducer

C5-1 transducer

Figure 3: Pliance-X sensor mat wrapped around the transducers

When the volunteer patient arrived, he was asked to fill out a consent form and his height and weight were measured. When a sonographer arrived she filled out a consent form and pre-scan questionnaire. Grip and pinch forces were obtained from the sonographer using the Jamar dynamometer and Baseline pinch gauge following the procedures recommended by the American Society of Hand Therapists (American Society for Hand Therapists (ASHT): clinical assessment recommendations, 1981). The sonographer changed into the appropriate attire and reflective markers were placed on the lower extremities, upper dominant extremity, and torso. The sonographer's skin was prepared by lightly abrading it to remove dead skin cells and then rubbed with alcohol to reduce the impedance of the electrode/skin interface. The surface electromyography electrodes were cleaned using alcohol then secured above the prepared skin using gaffer tape. Placement of markers and electrodes is shown in Figure 4.

Figure 4: Reflective markers and surface electromyography electrodes on a sonographer participant while she is scanning the right kidney of the patient

After instrumentation was applied to the sonographer a static capture of the reflective markers was taken using the Vicon MX motion capture system. Then, the surface electromyography electrodes were connected to the MA300 backpack. The backpack was placed on the floor next to the sonographer or on the bed. The electromyography signals generated were examined using the Vicon MX motion capture system to ensure they would not become saturated during maximum voluntary isometric contraction. This required the sonographer to apply her maximum amount of force for the superficial muscle that was being examined. If the signal was saturated, then the gain for that individual electrode was decreased on the backpack. When it was determined that none of the signals would saturate, the maximum isometric voluntary contraction for each muscle was recorded in succession using the Vicon MX motion capture system.

After these signals were recorded the sonographer was given the opportunity to adjust the bed, ultrasound machine, and chair, if she was using it.

The final step before data collection was identifying the location of the sonographer's fingers on the sensor mat. The sonographer gripped the C5-1 transducer in the configuration that she would use scanning the patient. A researcher pressed on all of the sonographer's fingers located on the sensor mat individually while the Pliance data collection software was recording to determine the cell locations of the individual fingers. This would allow researchers to distinguish the force and pressure applied by the individual fingers to the sensor mat during scanning. The sonographer was instructed to maintain these finger positions on the sensor mat throughout the scan.

The sonographer instructed the patient to lie on his back on a standard examination bed with his abdomen exposed. The patient's right side was located next to the sonographer so that his right kidney could be scanned. An alternative position used for the right kidney scan was the patient lying on his left side with his back to the sonographer. The sonographer's arm was extended out from the body to expose her entire upper extremity reflective markers prior to scanning. The sonographer was directed to take four longitudinal scans of patient's right kidney using the same procedures she would in a clinical setting. The sonographer was asked to save images of the scan on the Philips iU22 ultrasound system so that the quality of the scans could be verified by a GVSU faculty member. The sonographer indicated when she finished scanning and data collection was stopped. The patient's abdomen was cleaned to remove any gel used by the sonographer. The sonographer was instructed to maintain the same finger configuration on the transducer for the left kidney scan. Researchers checked to

ensure that analog and marker data was collected by the Vicon Nexus software. If there was a problem with data collection, the scan was repeated.

The sonographer instructed the patient to lay on his right side facing the sonographer so that the ultrasound system would not have to be moved and the same process was repeated for the left kidney scan. The sensor mat was removed from the C5-1 transducer and secured to a S5-1 transducer using micropore tape. The C5-1 transducer was disconnected from the ultrasound system and the S5-1 transducer was connected. A baseline zero measurement was taken of the sensor mat using the Pliance data collection software. While the researchers were setting this up, the sonographer was able to have a 15 to 30 minute recovery period.

After the recovery period, the sonographer was asked to grip the S5-1 transducer in the configuration that she would use during scanning. Then, the same process to determine finger location was repeated. The sonographer, patient, and researchers repeated the same process for scanning the right and left kidney of the patient with the S5-1 transducer as they did for the C5-1 transducer. When the sonographer finished scanning, all of the instrumentation was removed from her skin and she filled out a post-scan questionnaire.

4.6. Motion Capture Data Analysis

A power spectral density analysis was performed to determine the cutoff frequency for the landmarks. The analysis was performed on data collections that had all landmark positions available throughout the scan. The power spectral density analysis determines the power distribution of a signal over frequency. The cutoff frequency was determined as the frequency in which 99 percent of the power was contained below

(Winter, 2009). The cutoff frequencies were obtained for all of the landmarks in every component. These cutoff frequencies were then averaged to obtain the cutoff frequency for the entire motion capture data collected which was 15.6 Hertz. A 4^{th} order low-pass zero phase lag Butterworth filter with a cutoff frequency at 15.6 Hertz was then applied to smooth the data and remove high frequency noise.

Kinematic analysis was then performed on the data to determine the joint angles. The joint centers were determined in the global coordinate system. The shoulder joint center was determined by finding the optimal pivot point using at least three landmarks on the scapula, reference equation (10). The elbow and wrist joint centers were determined in the global coordinate system for a static frame using equation (13).

Technical reference frames were then determined for the upper arm and forearm using the static frame, see equations (14) through (18). The positions of the shoulder and elbow joint centers with respect to the static technical reference frame were calculated, reference equation (19). The position of the wrist joint center was determined with respect to the local technical reference frame for the forearm. Upper arm and forearm dynamic technical reference frames were determined for each frame of data collection while the sonographers were scanning. The dynamic reference frame systems use the same landmark locations and axial orientations as the static technical reference frames. The dynamic technical reference frame for the upper arm was used to determine the global positions of the shoulder and elbow joint centers in every frame of data collection, reference equation (20). The dynamic technical reference frame for the forearm was used to determine the global positions of the wrist joint center. The technical reference frames developed are shown in Table 6, reference Table 4 in section 3.2 Landmark Selection for

nomenclature. The technical reference frames for the forearm varied because of the availability of visible markers on the forearm during each data collection.

Table 6: Technical reference frames for the upper arm (humerus) and forearm

Body Segment	Technical Reference Frame*
Upper Arm (Humerus)	$x_h = \frac{VH2-VH1}{\lvert VH2-VH1\rvert}, \quad y_h = \frac{x_h \times (VH3-VH1)}{x_h \times \lvert VH3-VH1\rvert}, \quad z_h = x_h \times y_h$
Forearm	$x_{f_1} = \frac{VF2-VF1}{\lvert VF2-VF1\rvert}, \quad y_{f_1} = \frac{x_{f_1} \times (VF3-VF1)}{x_{f_1} \times \lvert VF3-VF1\rvert}, \quad z_{f_1} = x_{f_1} \times y_{f_1}$
	$x_{f_2} = \frac{VF1-ejc}{\lvert VF1-ejc\rvert}, \quad y_{f_2} = \frac{x_{f_2} \times (VF2-ejc)}{x_{f_2} \times \lvert VF2-ejc\rvert}, \quad z_{f_2} = x_{f_2} \times y_{f_2}$
	$x_{f_3} = \frac{VF1-ejc}{\lvert VF1-ejc\rvert}, \quad y_{f_3} = \frac{x_{f_3} \times (VF3-ejc)}{x_{f_3} \times \lvert VF3-ejc\rvert}, \quad z_{f_3} = x_{f_3} \times y_{f_3}$
	$x_{f_4} = \frac{VF1-ejc}{\lvert VF1-ejc\rvert}, \quad y_{f_4} = \frac{x_{f_4} \times (RSP-ejc)}{x_{f_4} \times \lvert RSP-ejc\rvert}, \quad z_{f_4} = x_{f_4} \times y_{f_4}$

*ejc is the elbow joint center in the global coordinate system

The joint centers were established in the global coordinate system for every frame of data collection in order to determine the elbow and wrist joint angles and create anatomical reference frames. The elbow and wrist joint angles were determined for every frame of data collection using equation (27) and (28), respectively. To determine the: upper arm vector, the shoulder and the elbow joint centers were used. To determine the forearm vector, the elbow and wrist joint centers were used. To determine the hand vector, the wrist joint center and a marker on the hand were used. The elbow joint angle was determined using the humerus and forearm vector. The wrist joint angle was determined using the forearm and hand vector. The neutral position for the wrist and elbow joint center is shown in Figure 5.

A continuity test was applied to the wrist joint angles because in some instances it would suddenly change from extension to flexion or vice versa in a single frame of data

collection. The sudden changes were investigated using the Vicon Nexus software. In the Vicon Nexus software the hand marker would not transfer between extension and flexion. The continuity test applied prevented the wrist joint angle from transitioning between flexion and extension if the angular velocity was over 500 degrees per second.

Figure 5: Neutral and anatomical position of the upper extremities

Anatomical reference frames were determined for the thorax and upper arm to create a shoulder joint matrix, reference equation (21). The anatomical reference landmark locations and axial orientations used were recommended by the International Society of Biomechanics (Wu, et al., 2005). The positive directions for the axes were: posterior to anterior for the x axis, inferior to superior for the y axis, and medial to lateral for the z axis. The anatomical reference frames are shown in Table 7. Euler rotation sequence YX'Y" was then used to determine the shoulder joint angles, reference equations (22) through (26). As mentioned previously, φ describes shoulder flexion and

extension, θ describes shoulder abduction and adduction, and ψ describes shoulder internal and external rotation. Shoulder flexion, abduction, and internal rotation occur when the Euler angles are positive. The neutral position of the shoulder is shown in Figure 5.

Table 7: Anatomical reference frames for the thorax and humerus

Body Segment	Anatomical Reference Frame*
Humerus	$y_h = \frac{sjc-ejc}{\lvert sjc-ejc\rvert}, \quad x_h = \frac{y_h \times (ELH-ejc)}{y_h \times \lvert ELH-ejc\rvert}, \quad z_h = x_h \times y_h$
Thorax	$y_t = \frac{C7-T8}{\lvert C7-T8\rvert}, \quad z_t = \frac{y_t \times (SJ-T8)}{y_t \times \lvert SJ-T8\rvert}, \quad x_t = y_t \times z_t$

*ejc and sjc are the elbow and shoulder joint centers, in the global coordinate system.

4.7. Electromyography Data Analysis

A fast Fourier transform was applied to the electromyograms to determine the cutoff frequencies for the band-pass zero phase lag filter. The upper and lower bound cutoff frequencies selected were 20 Hertz and 300 Hertz, respectively. These are typical cutoff frequencies for surface electromyography (Cram, Kasman, & Holtz, 1998). Nearly all of the power within the signal is contained within the typical boundaries as shown in Figure 6. The lower bound cutoff removes electrical noise from wires swaying and biological artifacts. The upper bound cutoff removes tissue noise at the electrode site. A notch filter was applied to the electromyograms to remove the spike generated at 60 Hertz from electrical noise from the environment (Cram, Kasman, & Holtz, 1998). The data was smoothed and high and low frequency noise was reduced by removing the DC offset, applying a full wave rectification, applying a notch filter at 60 Hertz, and applying the band-pass zero phase lag filter. The DC offset is the subtraction of the mean voltage

for the electromyography data from every data point collected. Full wave rectification is taking the absolute value of the electromyography data after the DC offset has been removed.

Sonographer 5, C5-1 transducer, left kidney: Fast Fourier transform of raw maximum voluntary isometric contraction electromyography data for the extensor carpi ulnaris

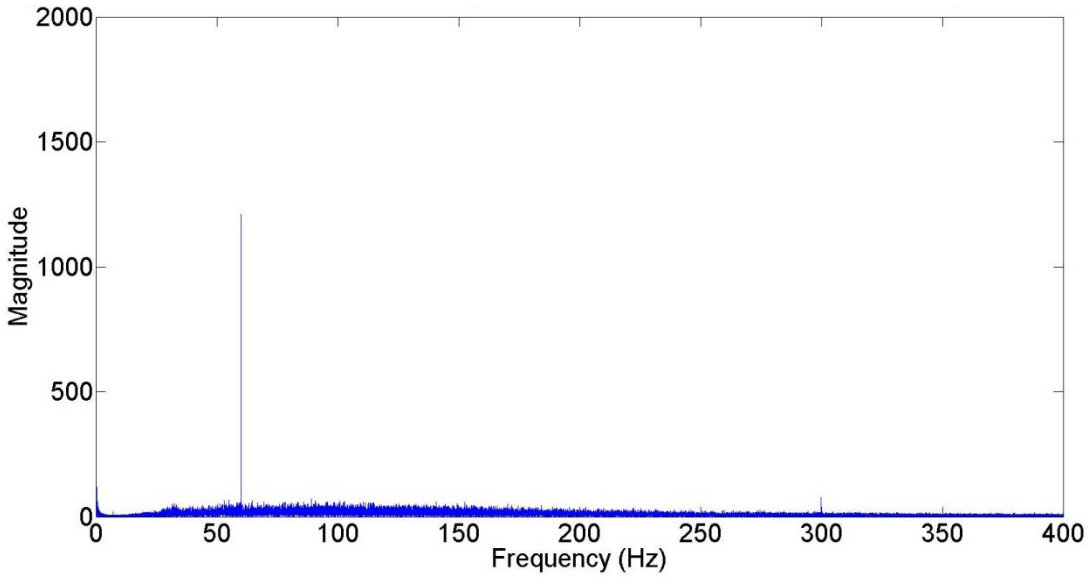

Figure 6: FFT of electromyogram used to determine upper and lower cutoff bounds

5. Results

5.1. Shoulder Joint Angles

During scanning, all of the sonographers experienced shoulder flexion. Additionally, sonographer 5 experienced shoulder extension. Maximum shoulder flexion and extension was 91.2 and -12.5 degrees, respectively. The maximum and minimum ranges of motion during a given scan were 60.9 and 16 degrees, which are shown in Table 8. A normalized histogram of shoulder flexion and extension for each scan is displayed in Figure 7.

Table 8: Shoulder joint flexion/extension during scanning

Sonographer	Transducer	Kidney Scan	Scanning Duration (s)	Shoulder Joint Angles (Degrees)			
				Flexion/Extension			Range of Motion
				Min	Max	Average	
2	C5-1	Left	57.9	29.2	90.0	36.8	60.9
		Right	87.2	35.0	91.2	51.2	56.2
	S5-1	Left	57.1	40.9	82.7	47.6	41.7
		Right	47.5	0.8	20.4	11.9	19.6
3	C5-1	Left	64.5	29.7	52.1	43.9	22.4
		Right	104.0	9.2	27.3	17.2	18.1
	S5-1	Left	93.8	33.4	49.3	40.6	16.0
		Right	157.9	32.2	61.0	45.3	28.7
4	C5-1	Left	47.1	4.7	39.7	21.2	35.0
		Right	57.9	7.5	39.9	20.3	32.4
	S5-1	Left	42.8	0.1	40.6	25.3	40.5
		Right	63.9	9.3	38.4	20.7	29.1
5	C5-1	Left	79.4	-4.4	24.6	9.0	29.0
		Right	95.7	-12.5	44.8	1.8	57.3
	S5-1	Left	73.4	3.3	22.6	13.4	19.3
		Right	54.3	10.2	42.0	20.0	31.8

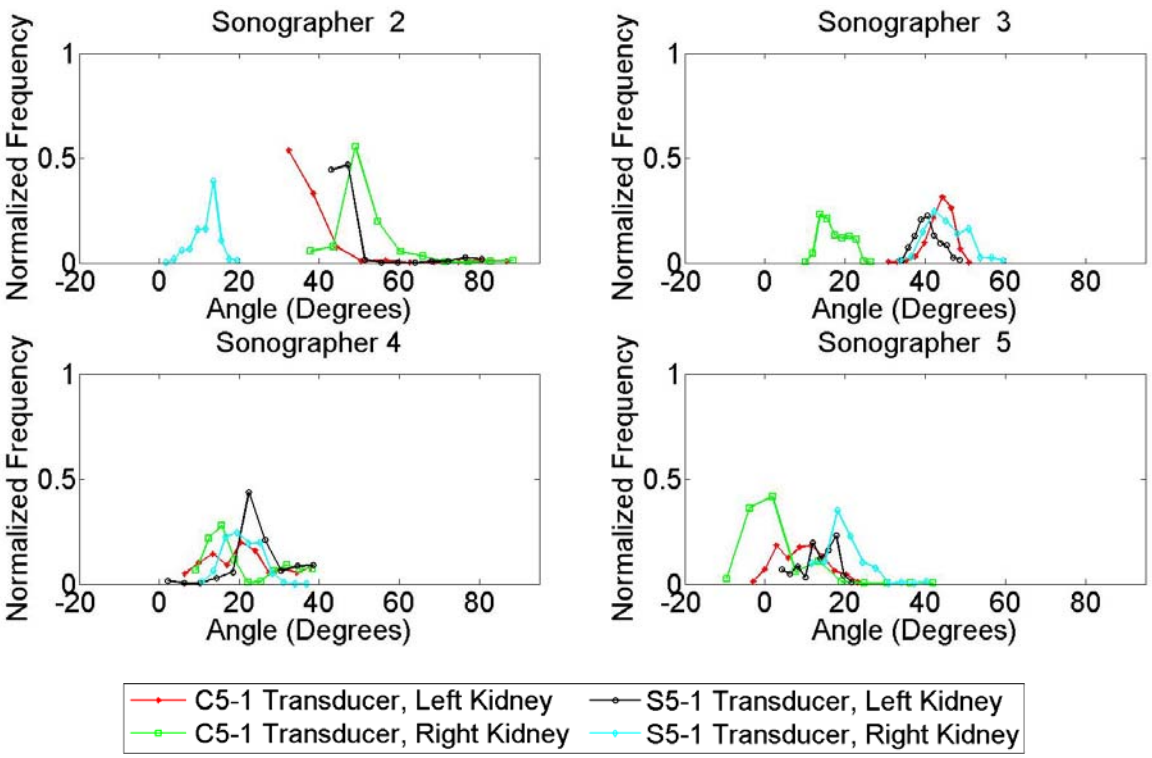

Figure 7: Normalized histogram of shoulder joint flexion/extension during scanning

Only shoulder abduction occurred during scanning with maximum and minimum angles of 112.5 and 38.6 degrees. The maximum and minimum ranges of motion were 37.2 and 11.7 degrees, which are shown in Table 9. A normalized histogram of shoulder abduction for each scan is displayed in Figure 8.

Table 9: Shoulder joint abduction during scanning

Sonographer	Transducer	Kidney Scan	Scanning Duration (s)	Shoulder Joint Angles (Degrees)			
				Abduction			Range of Motion
				Min	Max	Average	
2	C5-1	Left	57.9	43.5	68.9	48.6	25.4
		Right	87.2	70.7	86.5	78.0	15.9
	S5-1	Left	57.1	49.7	68.4	53.7	18.8
		Right	47.5	79.4	91.1	86.5	11.7
3	C5-1	Left	64.5	64.3	83.0	73.3	18.7
		Right	104.0	85.0	104.8	91.7	19.8
	S5-1	Left	93.8	91.7	112.0	103.9	20.3
		Right	157.9	93.4	112.5	104.7	19.1
4	C5-1	Left	47.1	44.0	62.4	50.0	18.5
		Right	57.9	39.2	75.3	55.5	36.1
	S5-1	Left	42.8	45.3	65.4	52.7	20.1
		Right	63.9	43.1	80.3	60.4	37.2
5	C5-1	Left	79.4	38.6	57.7	47.0	19.1
		Right	95.7	41.0	68.5	53.6	27.5
	S5-1	Left	73.4	42.7	68.9	52.8	26.2
		Right	54.3	56.5	78.7	64.7	22.2

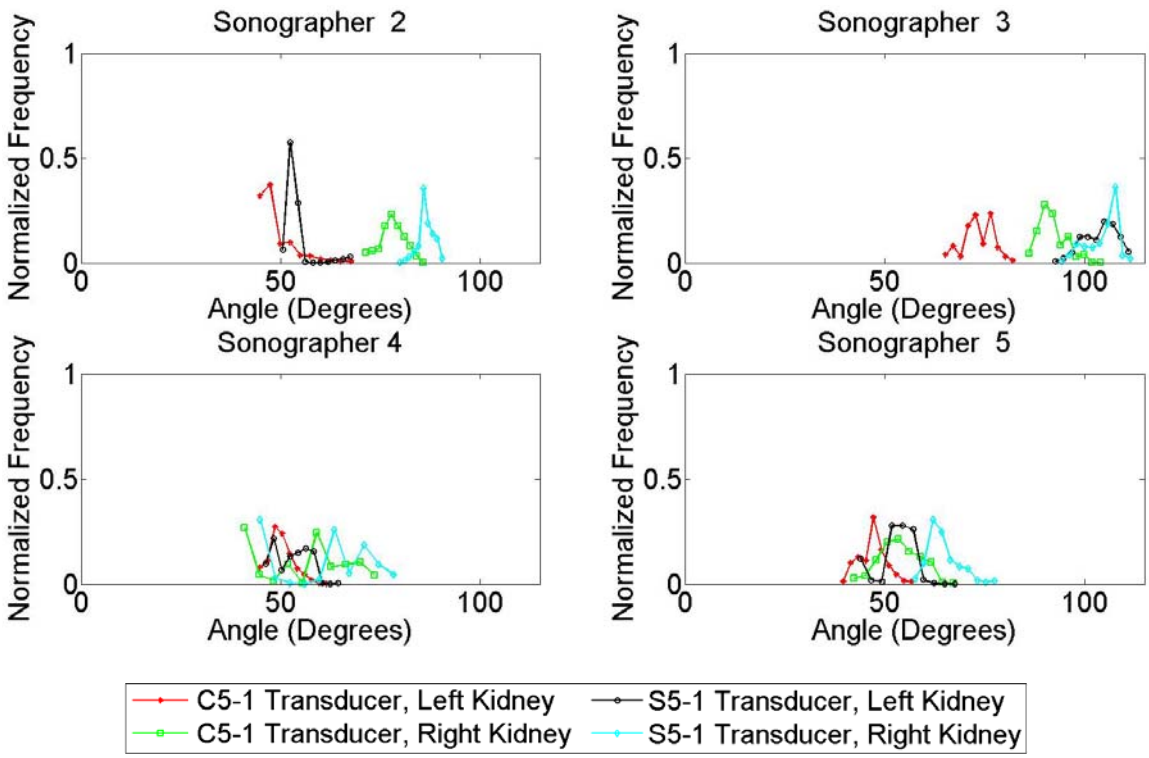

Figure 8: Normalized histogram of shoulder joint abduction during scanning

External shoulder rotation was experienced by all of the sonographers. Internal shoulder rotation was only experienced by sonographers 2 and 4. The maximum shoulder internal rotation generated was 22.4 degrees and the maximum external rotation was 90 degrees. The maximum and minimum ranges of motion for internal and external rotation were 66.3 and 12.6 degrees, respectively. These values can be found in Table 10. A normalized histogram of internal and external shoulder rotation for each scan is displayed in Figure 9.

Table 10: Shoulder joint internal/external rotation during scanning

Sonographer	Transducer	Kidney Scan	Scanning Duration (s)	Shoulder Joint Angles (Degrees)			
				Internal/External Rotation			Range of Motion
				Min	Max	Average	
2	C5-1	Left	57.9	-66.4	-42.3	-53.1	-24.1
		Right	87.2	-61.8	-31.3	-43.8	-30.5
	S5-1	Left	57.1	-66.5	-50.2	-60.2	-16.3
		Right	47.5	-29.9	6.9	-2.5	36.8
3	C5-1	Left	64.5	-88.8	-76.2	-84.5	-12.6
		Right	104.0	-47.5	-27.3	-38.8	-20.2
	S5-1	Left	93.8	-90.0	-76.1	-83.7	-13.8
		Right	157.9	-60.7	-36.4	-46.7	-24.3
4	C5-1	Left	47.1	-61.7	-17.4	-41.9	-44.3
		Right	57.9	-43.9	22.4	-7.9	66.3
	S5-1	Left	42.8	-74.0	-26.3	-53.5	-47.7
		Right	63.9	-47.9	16.3	-16.0	64.3
5	C5-1	Left	79.4	-59.2	-33.1	-47.7	-26.1
		Right	95.7	-42.5	-10.3	-19.4	-32.2
	S5-1	Left	73.4	-61.7	-45.2	-52.6	-16.4
		Right	54.3	-37.9	-19.9	-31.1	-18.0

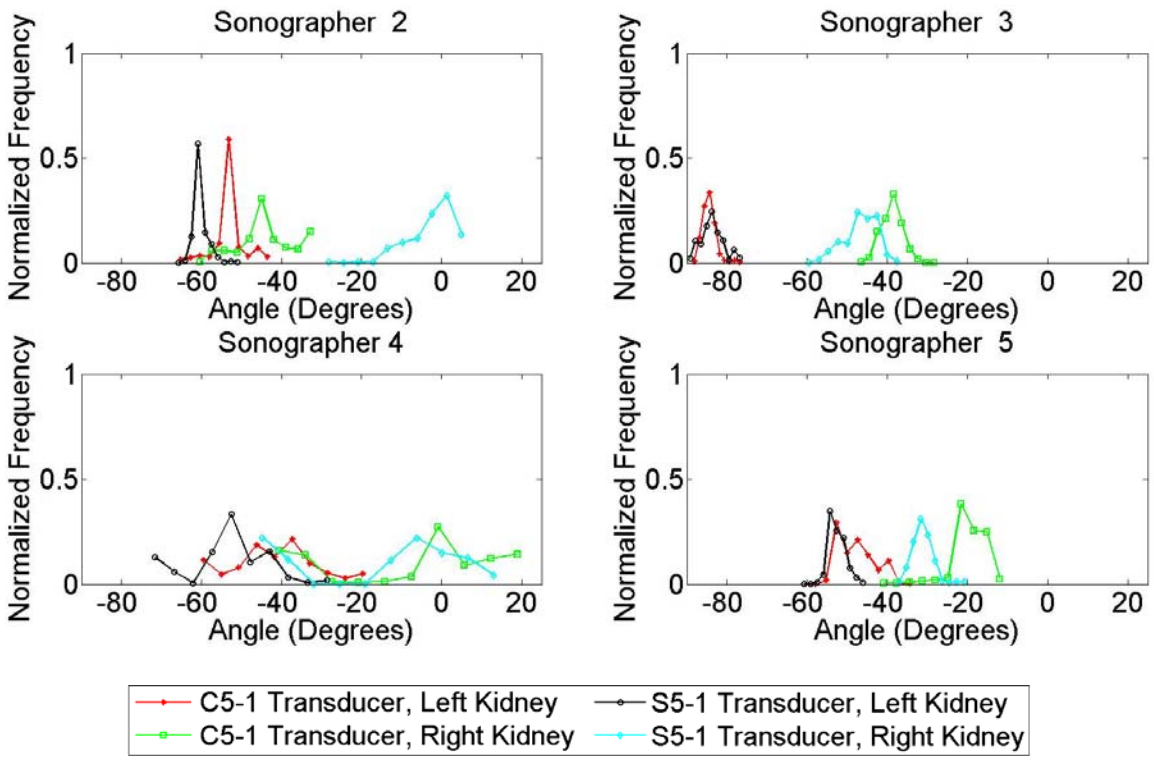

Figure 9: Normalized histogram of shoulder joint internal/external rotation during scanning

5.2. Elbow Joint Angles

All of the sonographers experienced flexion at the elbow joint as a result of the neutral position that was selected. During this study, the maximum and minimum elbow flexion generated was 102.2 and 9.3 degrees. The maximum and minimum ranges of motion for flexion were 49.1 and 16.5 degrees, which are displayed in Table 11. A normalized histogram of elbow flexion for each scan is shown in Figure 10.

Table 11: Elbow joint flexion during scanning

Sonographer	Transducer	Kidney Scan	Scanning Duration (s)	Elbow Joint Flexion (Degrees)			
				Min	Max	Average	Range of Motion
2	C5-1	Left	57.9	NA	NA	NA	NA
		Right	87.2	9.3	39.2	25.1	29.9
	S5-1	Left	57.1	NA	NA	NA	NA
		Right	47.5	56.6	74.7	65.4	18.1
3	C5-1	Left	64.5	46.0	70.4	60.7	24.3
		Right	104.0	31.7	80.8	65.9	49.1
	S5-1	Left	93.8	9.5	33.0	15.5	23.5
		Right	157.9	11.0	46.2	32.4	35.2
4	C5-1	Left	47.1	68.9	86.9	77.9	18.0
		Right	57.9	69.0	95.9	83.4	27.0
	S5-1	Left	42.8	51.7	75.2	63.8	23.5
		Right	63.9	59.6	84.9	71.6	25.4
5	C5-1	Left	79.4	56.5	85.0	64.2	28.4
		Right	95.7	57.7	102.2	79.4	44.5
	S5-1	Left	73.4	50.6	72.4	57.8	21.8
		Right	54.3	49.5	66.0	56.0	16.5

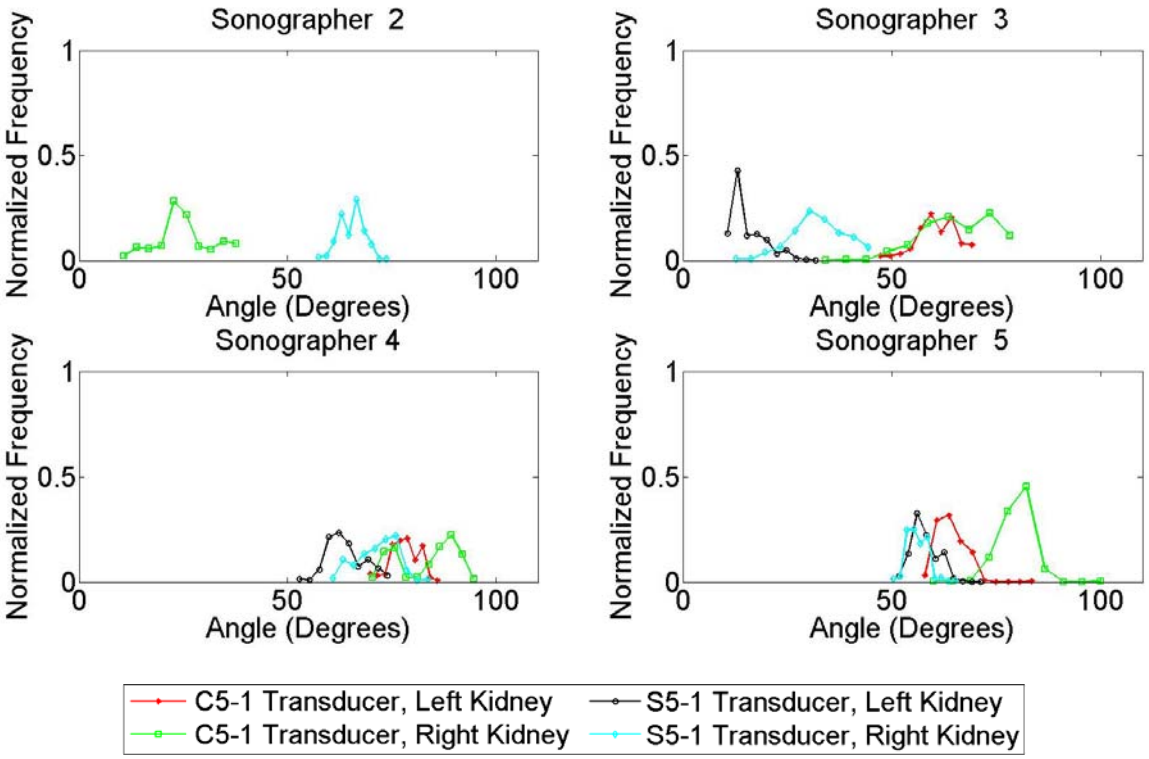

Figure 10: Normalized histogram of elbow joint flexion during scanning

5.3. Wrist Joint Angles

All of the sonographers experienced extension at the wrist joint. Additionally, sonographer 4 experienced flexion. The maximum wrist flexion generated was 8.8 degrees and the maximum extension was 70.4 degrees. The maximum and minimum ranges of motion for extension were 58.3 and 20.5 degrees, which are displayed in Table 12. A normalized histogram of wrist extension for each scan is shown in Figure 11.

Table 12: Wrist joint flexion/extension during scanning

Sonographer	Transducer	Kidney Scan	Scanning Duration (s)	Wrist Joint Angles (Degrees)			
				Flexion/Extension			Range of Motion
				Min	Max	Average	
2	C5-1	Left	57.9	NA	NA	NA	NA
		Right	87.2	-59.7	-1.4	-31.4	58.3
	S5-1	Left	57.1	NA	NA	NA	NA
		Right	47.5	-43.0	-6.1	-21.3	36.8
3	C5-1	Left	64.5	-63.9	-12.7	-49.5	51.2
		Right	104.0	-53.6	-3.7	-25.9	49.9
	S5-1	Left	93.8	-35.5	-10.4	-19.9	25.1
		Right	157.9	-56.9	-15.6	-38.3	41.3
4	C5-1	Left	47.1	-55.3	-12.0	-40.7	43.3
		Right	57.9	-63.0	-19.8	-35.6	43.2
	S5-1	Left	42.8	-38.5	8.8	-22.9	47.3
		Right	63.9	-70.4	-43.2	-56.5	27.2
5	C5-1	Left	79.4	-47.7	-21.8	-35.1	25.8
		Right	95.7	-30.4	-1.7	-10.8	28.7
	S5-1	Left	73.4	-43.1	-22.6	-33.3	20.5
		Right	54.3	-34.3	-9.8	-15.6	24.5

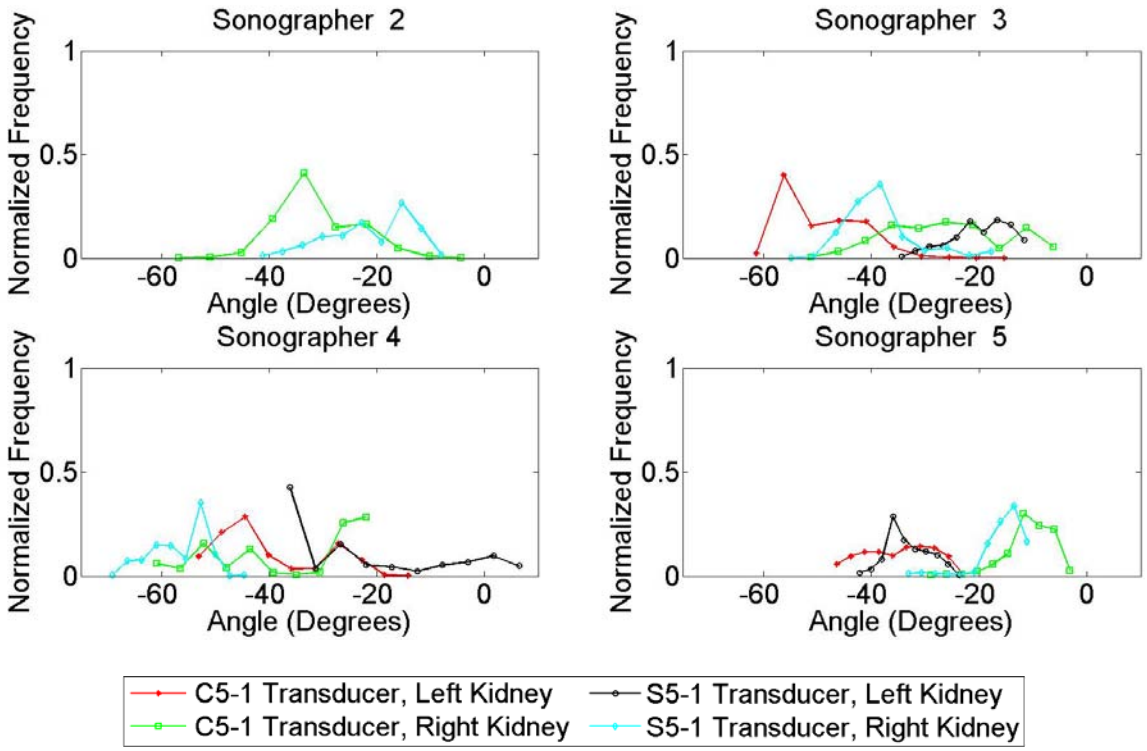

Figure 11: Normalized histogram of wrist joint extension during scanning

5.4. Joint Angles for the Different Scanning Factors

The maximum and minimum joint angles obtained for the different scanning factors are shown in Table 13. The sonographer's scanning position had the greatest difference for maximum shoulder flexion/extension and the least difference for shoulder abduction. Ultrasound transducer design had the greatest and least difference for maximum and minimum elbow flexion. The kidney that was scanned had the greatest difference for maximum internal/external shoulder rotation and the least difference for minimum elbow flexion.

Table 13: Minimum and maximum joint angles achieved for all of the scans based on the different scanning factors

Scan Factors	Joint Angles (Degrees)									
	Shoulder Flexion(+)/Extension(-)		Shoulder Abduction		Shoulder Internal(+)/External(-)		Elbow Flexion		Wrist Flexion(+)/Extension(-)	
	Min	Max	Min	Max	Min	Max	Min	Max	Min	Max
Seated	0.8	91.2	43.5	112.5	-90.0	6.9	9.3	80.8	-63.9	-1.4
Standing	-12.5	44.8	38.6	80.3	-74.0	22.4	49.5	102.2	-70.4	8.8
C5-1 Transducer	-12.5	91.2	38.6	104.8	-88.8	22.4	9.3	102.2	-63.9	-1.4
S5-1 Transducer	0.1	82.7	42.7	112.5	-90.0	16.3	9.5	84.9	-70.4	8.8
Left Kidney	-4.4	90.0	38.6	112.0	-90.0	-17.4	9.5	86.9	-63.9	8.8
Right Kidney	-12.5	91.2	39.2	93.4	-61.8	22.4	9.3	102.2	-70.4	-1.4

5.5. Electromyography Results

Electromyograms produced by the muscles pairs for sonographer 5 using the C5-1 transducer are shown in Figures 12 and 13. The muscles pairs were the flexor and extensor carpi ulnaris for the forearm and the biceps and triceps brachii for the upper arm. The data was collected while scanning the patient's left kidney. The rest of the electromyograms produced during this study can be found in Appendix 10.1.

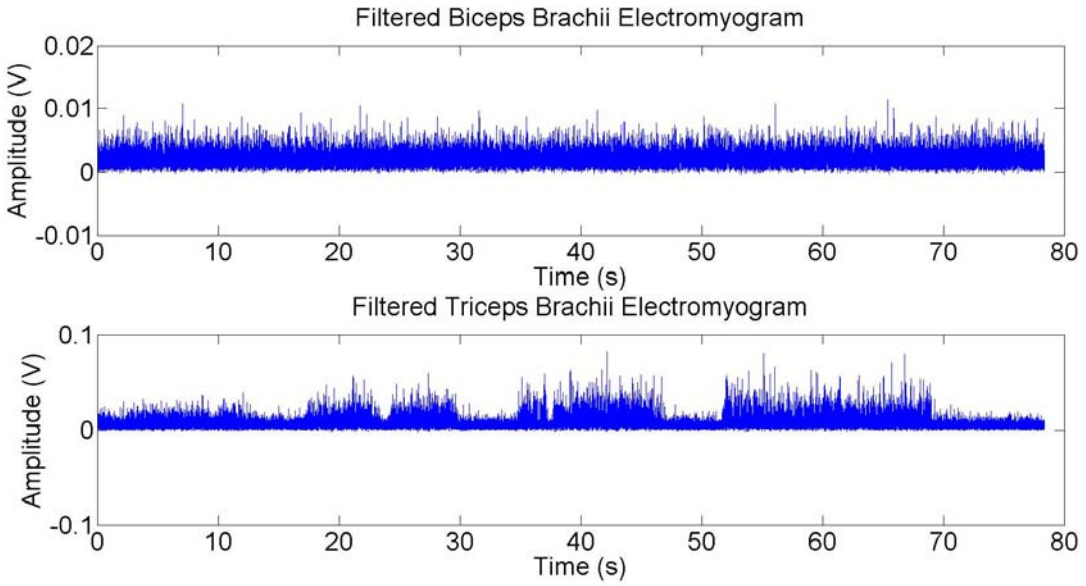

Figure 12: Upper arm electromyograms from sonographer 5 scanning the left kidney of the patient using the C5-1 transducer

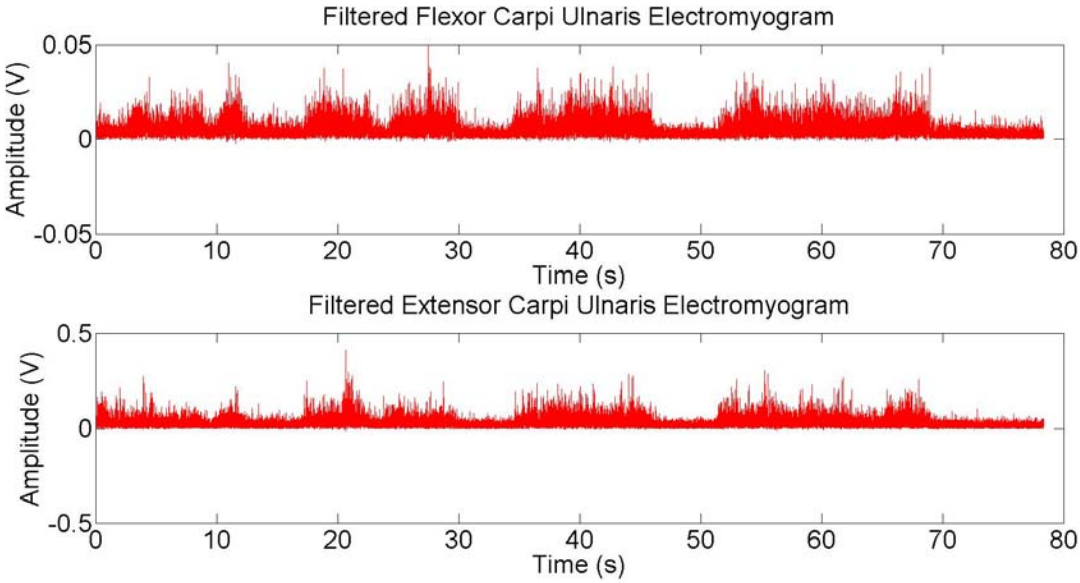

Figure 13: Forearm electromyograms from sonographer 5 scanning the left kidney of the patient using the C5-1 transducer

6. Discussion

6.1. Comparison of Shoulder Joint Angles

The flexion and extension angles achieved by each sonographer varied. Sonographer 2 generated larger flexion angles because she tilted her thorax forward when she needed to use the keyboard on the ultrasound machine. Additionally, sonographer 2 maintained a smaller angle range for a longer duration of time compared to the other sonographers. In other words, she was not flexing and extending her shoulder as much as the other sonographer. Sonographer 3 had a similar flexion angle range for all of the scans except when she scanned the patient's right kidney using the C5-1 transducer. For this scan, the angle range was offset about 20 degrees less than the other scans because the sonographer decreased the distance between her thorax and the patient's kidneys. In the scans performed by sonographers 4, shoulder flexion was within the same angle range regardless of the transducer used or the kidney scanned. Higher flexion angles were achieved by sonographers 2 and 3 who were seated during the scanning procedures.

The abduction angles that were generated by sonographers 2, 4, and 5 are similar during left kidney scans. Sonographer 3 had larger abduction angles because she rested her arm on the patient while she scanned. Higher abduction angles were obtained when the S5-1 transducer was used to scan the patient's right kidney. Shoulder abduction exceeded the acceptable limits for all of the scanning factors, reference Figure 8. The acceptable limits for shoulder abduction are between 0 and 20 degrees (McCulloch, Xie, & Adams, 2002). When the shoulder is elevated over 30 degrees of abduction it can cause fatigue and a reduction in blood flow to shoulder muscles leading to injury or pain

(Garg, Hegmann, & Kapellusch, 2006; Village & Trask, 2007). During this study, the sonographers were always over 30 degrees of abduction.

The internal and external rotation angles varied for each sonographer. When sonographer 2 scanned the patient's left kidney she maintained a smaller angle range. External rotation was greater for sonographers 2 and 3, who were seated. Sonographer 4 experienced larger ranges of motion because she would shift her weight from one foot to the other when she needed to use the keyboard resulting in her twisting her torso. Additionally, external rotation was greater when the sonographers were scanning the patient's left kidney because of the position of the patient.

6.2. Comparison of Elbow Joint Angles

There were no similarities between the sonographers for elbow flexion. Elbow angles were not obtained for sonographer 2 when she scanned the patient's left kidney because not enough markers were detectable by the cameras on the forearm. When sonographer 3 scanned the patient's right kidney, she had a larger range of motion because she would move her chair or tilt her torso more often. Sonographer 5 had larger flexion angles than the other sonographers, which could be because of the location of the patient kidneys in relation to the sonographer's shoulder joint. Her shoulder joint was at a higher elevation in comparison to the other sonographers, so she did not need to extend her elbow as much while scanning.

6.3. Comparison of Wrist Joint Angles

All of the sonographers experienced wrist extension. Only sonographer 4 experienced wrist flexion when she scanned the patient's left kidney using the S5-1

transducer. Wrist angles were not obtained for sonographer 2 during the scanning of the patient's left kidney for the same reason described above. Sonographer 4 had greater extension angles when she scanned the patient's right kidney. Sonographer 5 obtained larger extension angles and had a similar angle range when she scanned the patient's left kidney. Sonographers 2, 3, and 4 had large ranges of motion. Acceptable wrist extension is between 0 and 15 degrees (Hedge, 1998). The average wrist angles for all of the scans were over 15 degrees except when sonographer 5 used the C5-1 transducer to scan the patient's right kidney, which can be seen in Table 12.

6.4. Comparison of Joint Angles to the Burnett Study

The joint angles in the left kidney scans from this study were 1.8 degrees higher than the minimum shoulder abduction angle, 12.8 degrees higher than the maximum shoulder abduction angle, and 1.3 degrees higher than the maximum elbow flexion angle obtained in the left abdominal scans recorded by Burnett and Campbell-Kyureghyan (2010). For the right kidney scans, shoulder abduction was 0.4 degrees less than the minimum and 5.7 degrees less than the maximum and elbow flexion was 4.1 degrees higher than the maximum obtained in the right abdominal scans. The wrist angles obtained in this study were substantially different in comparison to the Burnett study. During this study the average wrist angle all of the scans were in extension, reference Table 12. In the Burnett study the average wrist angles for the left and right abdominal scans were in flexion, reference Table 3. The differences for the wrist angles could be a result of the anatomy scanned, position of the patient, or the position of the sonographer.

6.5. Electromyography Discussion

The maximum voluntary isometric contraction signals for the muscles investigated were inaccurate because the sonographers were not applying their peak force. As a result, only qualitative conclusions can be drawn from the electromyography results. The electromyograms indicated that co-contraction was occurring in the forearm muscles pair and the upper arm muscles pair at multiple instances throughout the short scanning durations, for all of the sonographers. The tricep brachii, flexor carpi ulnaris, and extensor carpi ulnaris appear to generate electrical voltage at the same instance for all of the electromyograms, reference Appendix 10.1. As mentioned previously, co-contraction was investigated because it has been hypothesized as a potential cause of repetitive strain injury, which is a type of work-related musculoskeletal disorder. The high presence of co-contraction while the sonographers were scanning could be a contributing factor to injuries.

7. Limitations of the Study

Limitations for this study include the sonographer participant sample size, difficulty of the cameras in detecting marker locations throughout the scans for the forearm, inability of the sonographers to reposition their fingers, sonographers not applying their maximum voluntary isometric contraction, shoulder translation, and sonographers scanning outside of their typical work environment.

The sample size of sonographers for kinematics was four and for electromyography was three. As a result, statistical analyses could not be performed on the results. During the study, forearm markers were not consistently located by the Vicon MX motion capture system for 7 out of the 16 scans. This was a result of the scanning technique that the sonographers used and equipment location.

As mentioned previously, this study was a joint collaboration with occupational therapy graduate students who investigated if there was a difference in the amount of pressure applied to the transducers by individual fingers and the entire hand. The individual sensors on the pressure mat were correlated to fingers prior to scanning inhibiting the ability of sonographer to reposition their fingers. During the maximum voluntary isometric contractions, the sonographers did not apply their maximum force for the superficial muscles that were investigated. This resulted in saturation of the electromyography signal in some instances.

If the sonographers continually moved their body backwards and forwards during scanning, it would cause the shoulder to translate affecting the shoulder joint center calculations. Furthermore, the study was performed outside of the sonographers' typical work environment in order to utilize the Vicon MX motion capture system. As a result

the sonographers could have been working with unfamiliar equipment causing them to scan differently.

8. Future Research

This study provides a baseline of kinematic results for the dominant upper extremity of sonographers while they are scanning. Further research could include joint analysis for the thorax, wrist ulnar and radial deviation angles, joint torques, and using a fixture that would restrain the sonographer's arm during maximum voluntary isometric contraction readings.

Since one of the contributing factors to sonographer injuries is awkward posture that results in twisting the torso, investigating movement about the thorax could quantify the amount of movement that contributes to injuries. Further analysis of the wrist joint to determine ulnar and radial deviation could be used to determine if sonographers experience more movement about the wrist or the shoulder joint when they scan. Determining the joint torques would help quantify the amount of loading in the upper extremity of sonographer while they scan.

Additionally, using a fixture that constrains the sonographer's arm during maximum voluntary isometric contraction would ensure that the electromyography signal does not saturate. This would also make it possible to determine the percent maximum voluntary isometric contraction for each muscle. Furthermore, determining joint torques and investigating co-contraction between muscle pairs can be used to determine the percent of co-contraction that is occurring (Winter, 2009).

9. Conclusion

This study evaluated upper extremity kinematics and determined if co-contraction was present in upper extremity muscle pairs during kidney scanning because of the prevalence of work-related musculoskeletal disorders in sonographers. There were three scanning factors in this study: sonographer's position, ultrasound transducer design, and kidney that was scanned. Sonographers' upper extremity movements and muscular activity were recorded using a Vicon MX motion capture system. The kinematics investigated in this study was shoulder, elbow, and wrist joint angles. The results were compared: 1) for each joint angle to determine if there was a trend present as a result of the scanning factors, 2) for shoulder abduction/adduction and wrist flexion/extension to acceptable published limits, and 3) to results published in a previous study by Burnett and Campbell-Kyureghyan (2010).

The kinematic evaluation concluded that the sonographers were scanning with their shoulders in flexion, abduction, and external rotation, with their elbows in flexion, and with their wrists in extension for the majority of their scanning procedures. Shoulder abduction was always greater than published acceptable limits. Wrist extension exceeded published acceptable limits during all of the scans. The shoulder and elbow joint angles determined for this study were similar to the angles determined by other researchers in a previous study. Although there were some trends observed within single joint movement by the different scanning factors, within this study none of the factors had a significant impact on the entire movement of the upper extremity. The electromyograms indicated that the agonistic muscle in the upper arm and forearm generated electrical voltage simultaneously with the antagonistic muscle in the pair at multiple instances during the

scans, indicating co-contraction was occurring. These results could be used to improve transducer design, which could minimize the risk of musculoskeletal work-related disorders in sonographers.

10. Appendices

10.1. Electromyograms

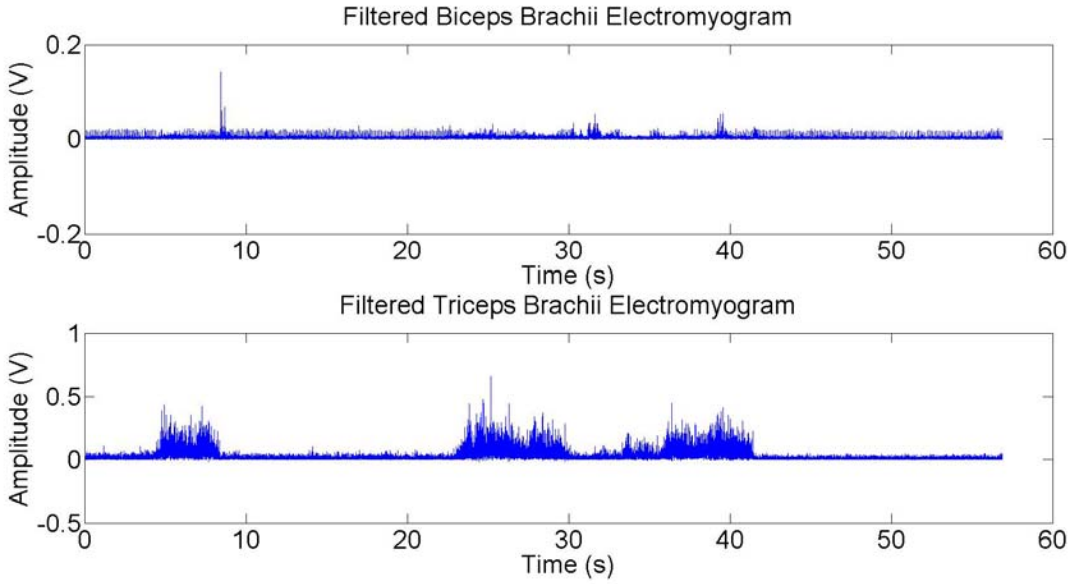

Figure A: Sonographer 2 filtered upper arm muscles pair electromyogram using a C5-1 transducer to scan the patient's left kidney

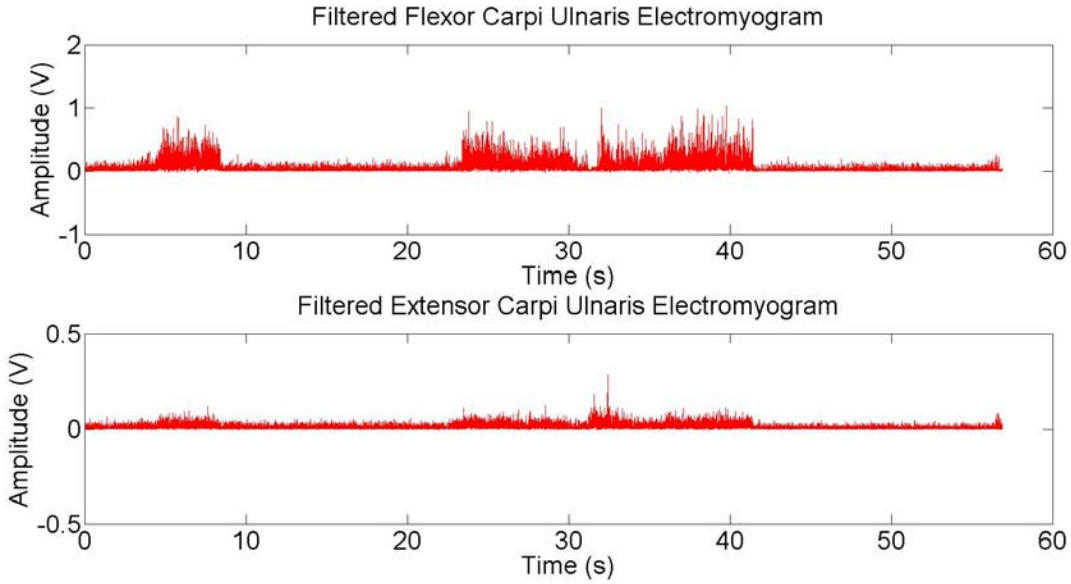

Figure B: Sonographer 2 filtered forearm muscles pair electromyogram using a C5-1 transducer to scan the patient's left kidney

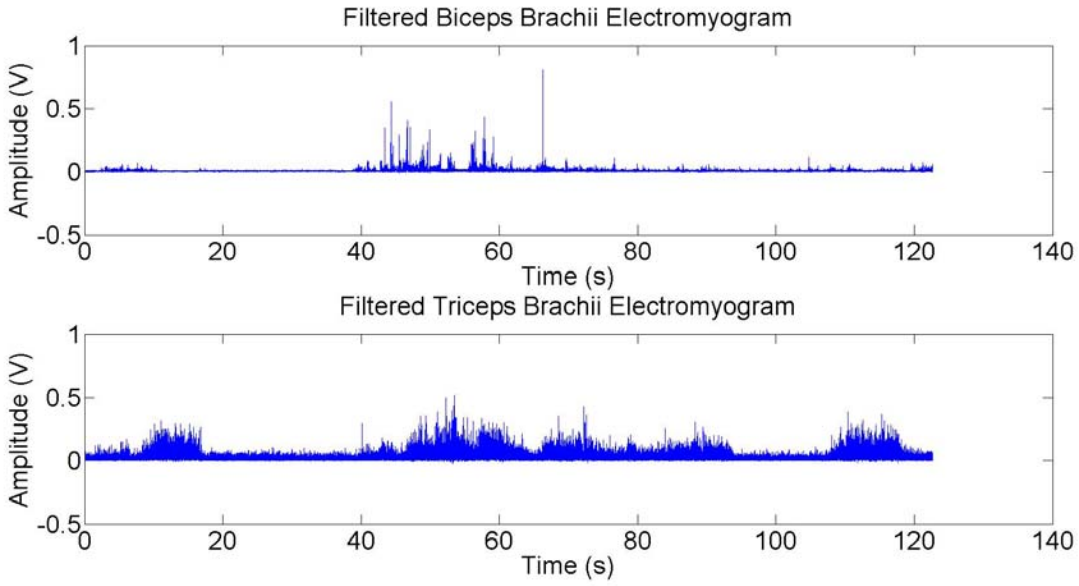

Figure C: Sonographer 2 filtered upper arm muscles pair electromyogram using a C5-1 transducer to scan the patient's right kidney

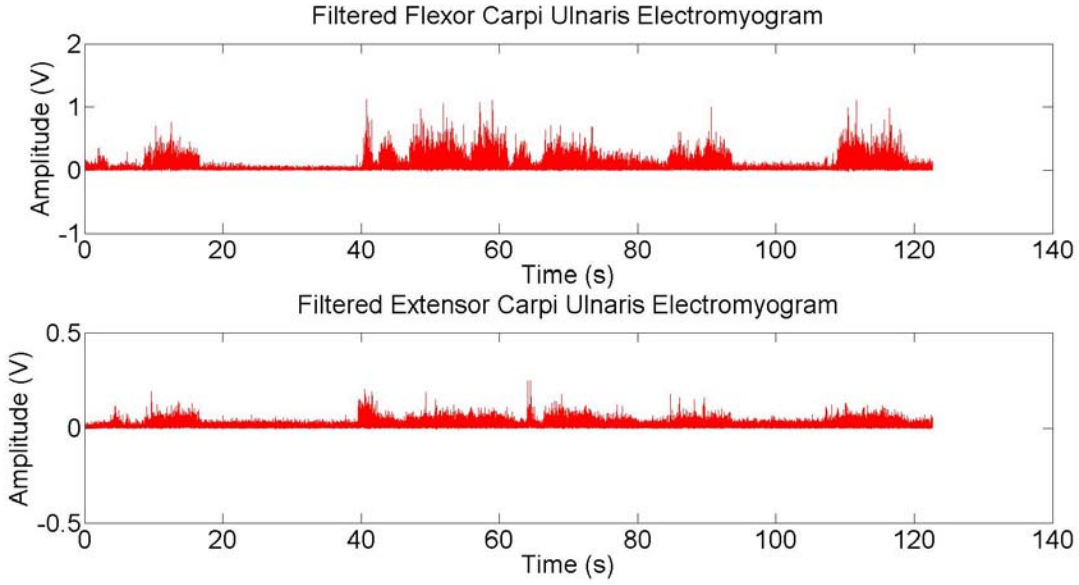

Figure D: Sonographer 2 filtered forearm muscles pair electromyogram using a C5-1 transducer to scan the patient's right kidney

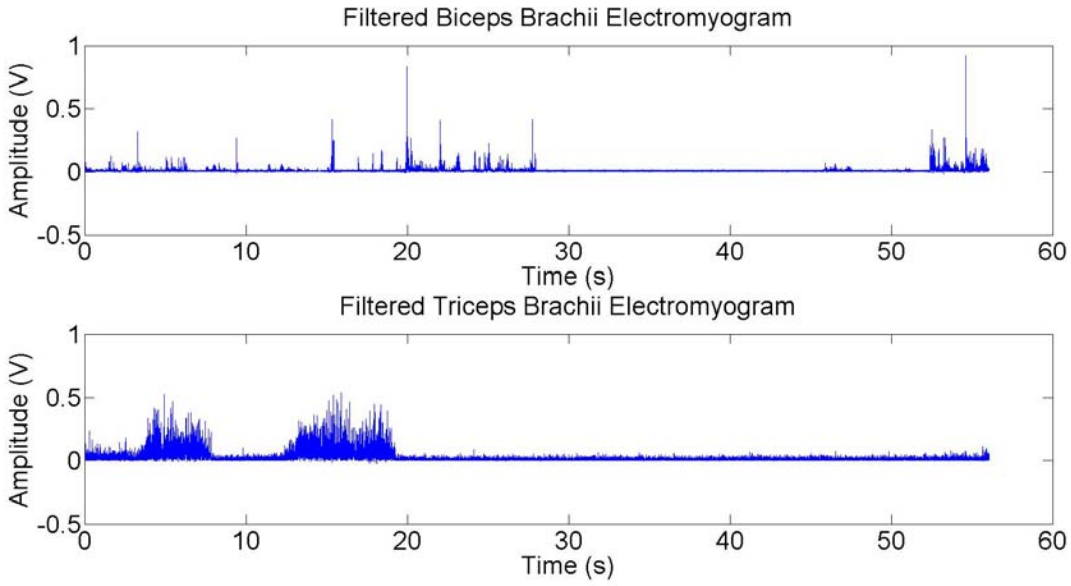

Figure E: Sonographer 2 filtered upper arm muscles pair electromyogram using a S5-1 transducer to scan the patient's left kidney

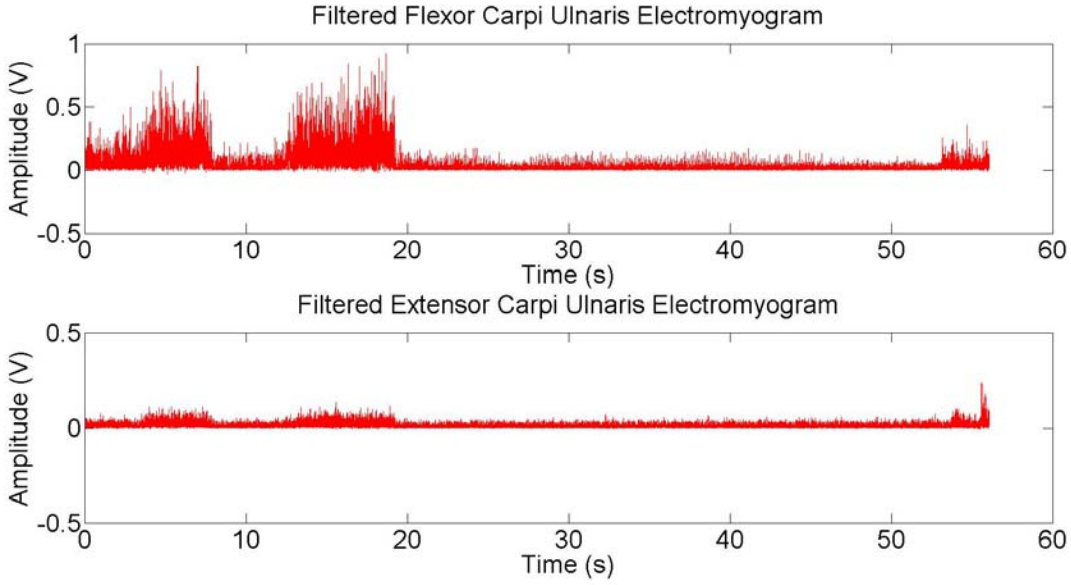

Figure F: Sonographer 2 filtered forearm muscles pair electromyogram using a S5-1 transducer to scan the patient's left kidney

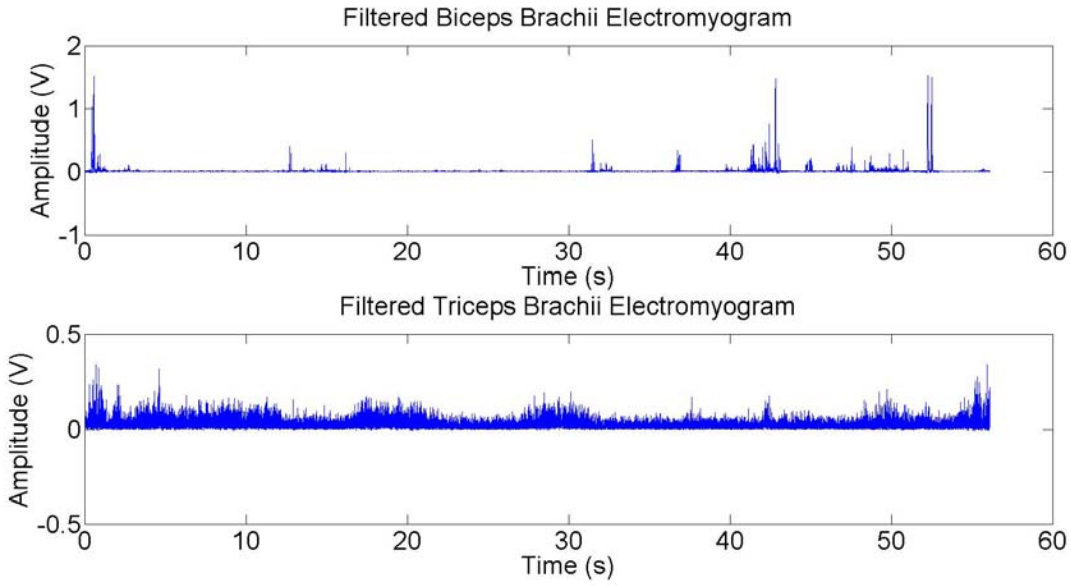

Figure G: Sonographer 2 filtered upper arm muscles pair electromyogram using a S5-1 transducer to scan the patient's right kidney

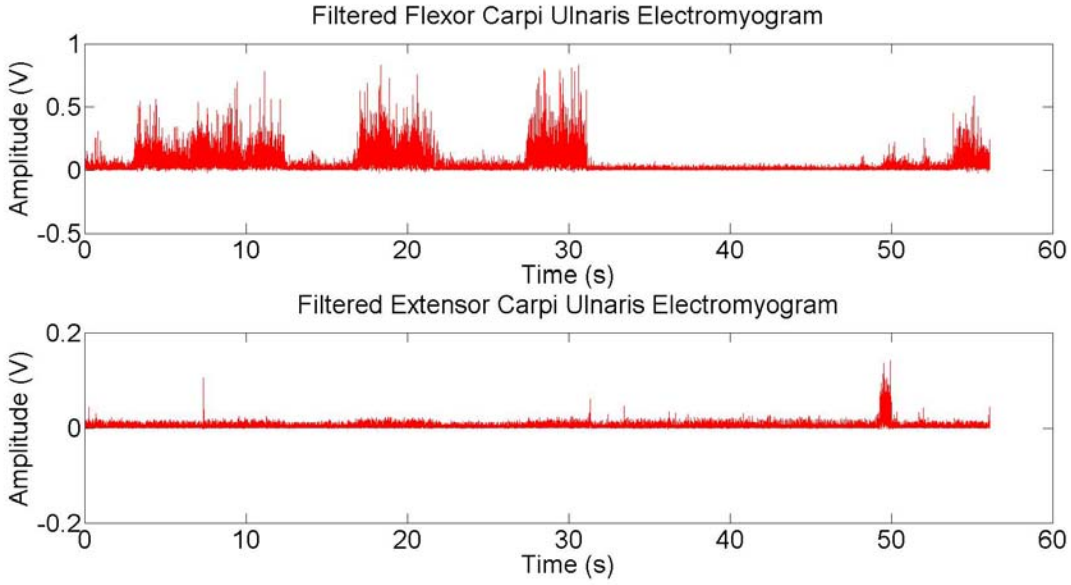

Figure H: Sonographer 2 filtered forearm muscles pair electromyogram using a S5-1 transducer to scan the patient's right kidney

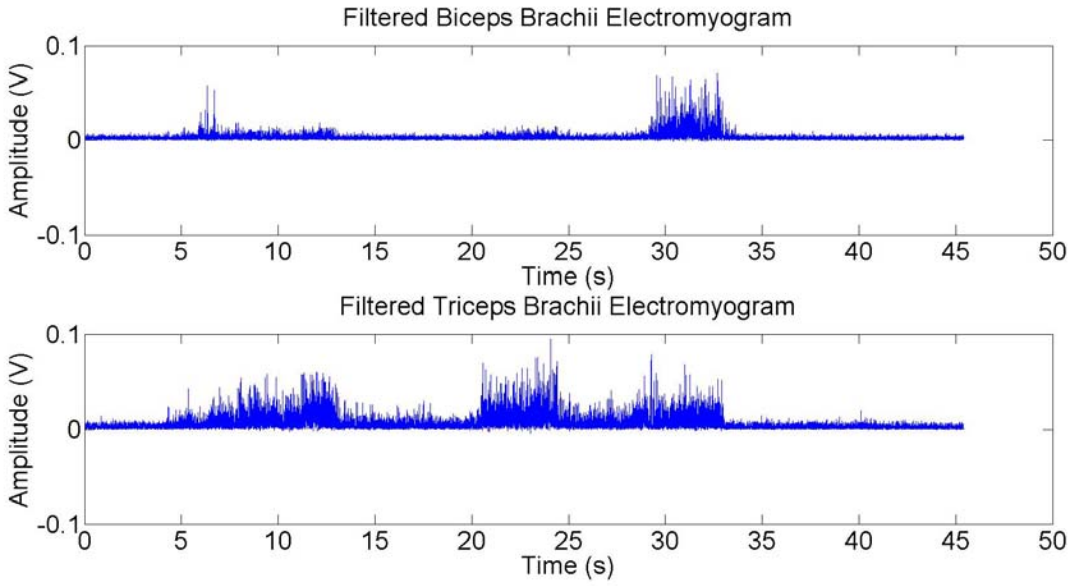

Figure I: Sonographer 4 filtered upper arm muscles pair electromyogram using a C5-1 transducer to scan the patient's left kidney

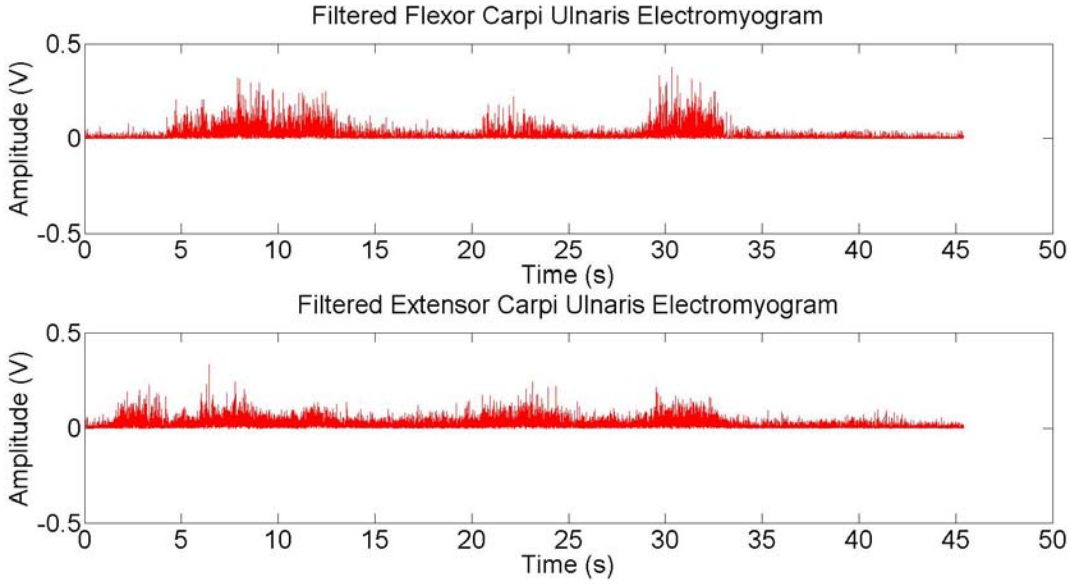

Figure J: Sonographer 4 filtered forearm muscles pair electromyogram using a C5-1 transducer to scan the patient's left kidney

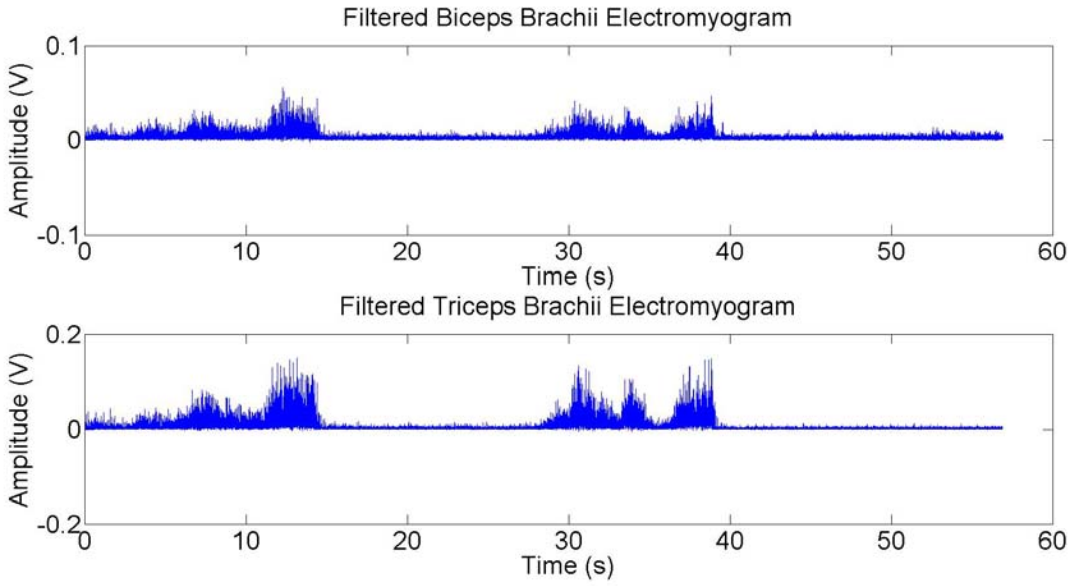

Figure K: Sonographer 4 filtered upper arm muscles pair electromyogram using a C5-1 transducer to scan the patient's right kidney

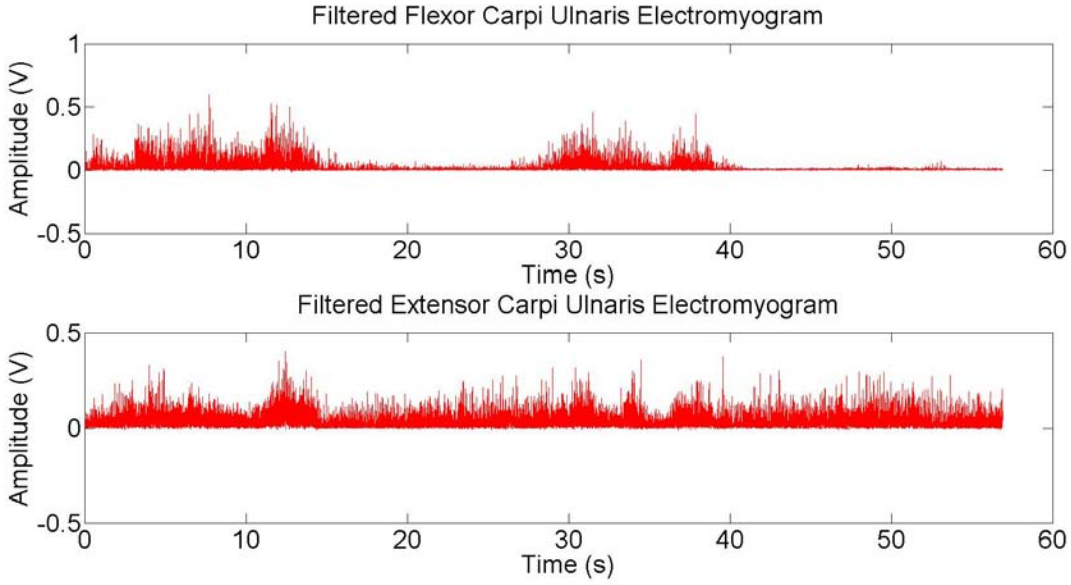

Figure L: Sonographer 4 filtered forearm muscles pair electromyogram using a C5-1 transducer to scan the patient's right kidney

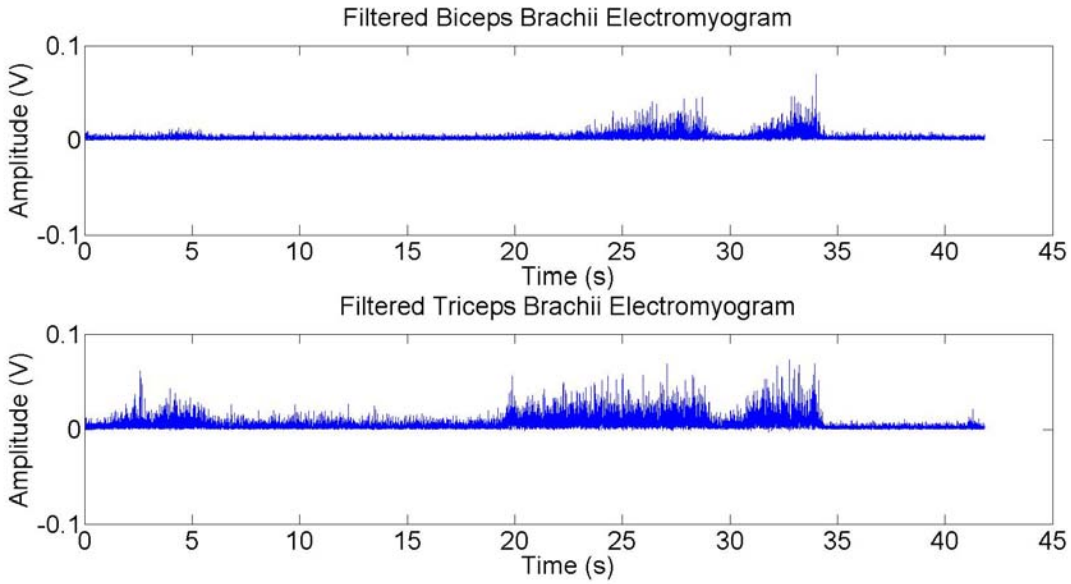

Figure M: Sonographer 4 filtered upper arm muscles pair electromyogram using a S5-1 transducer to scan the patient's left kidney

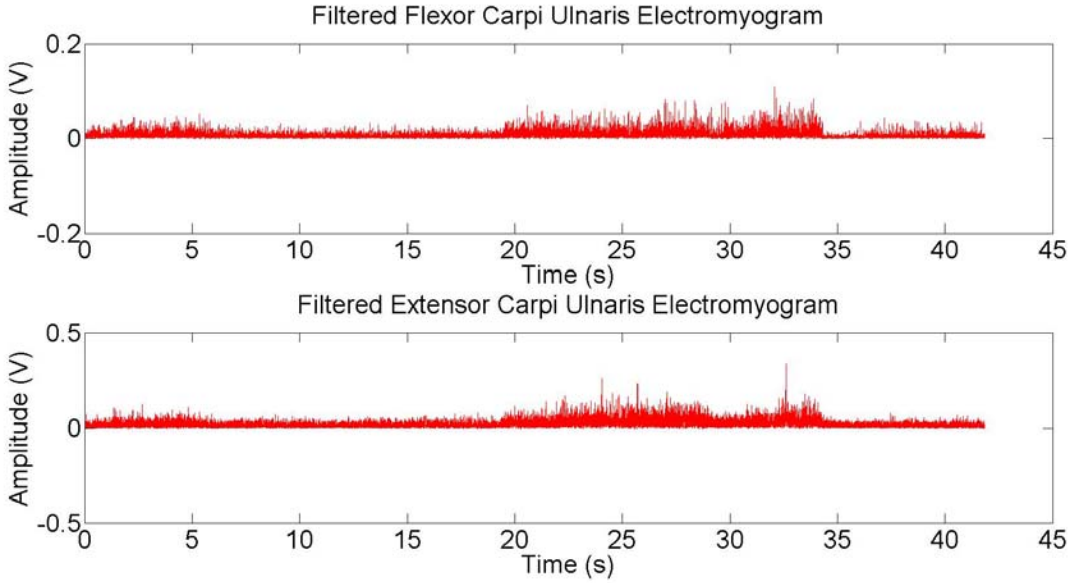

Figure N: Sonographer 4 filtered forearm muscles pair electromyogram using a S5-1 transducer to scan the patient's left kidney

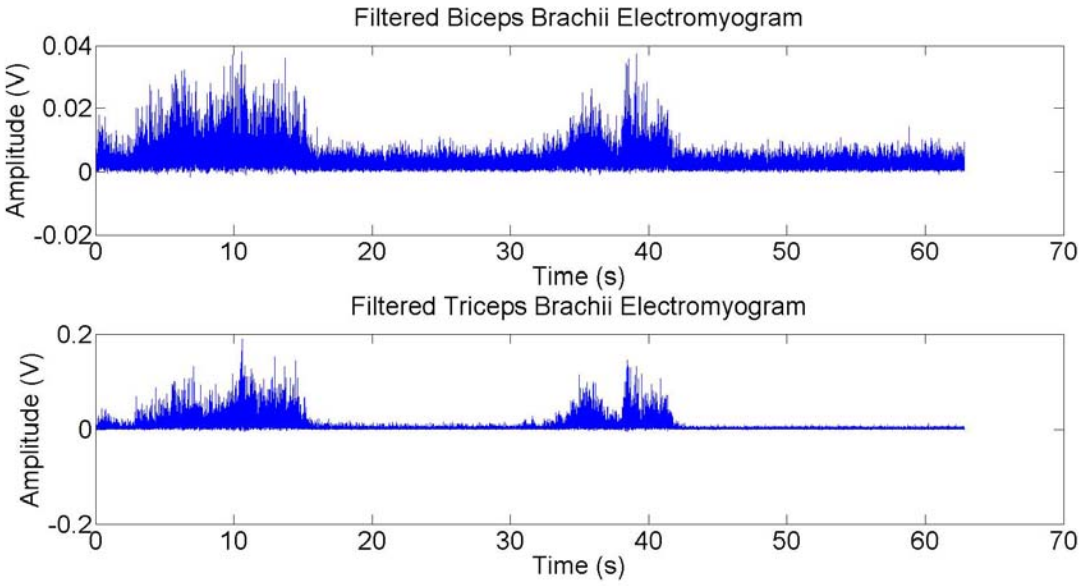

Figure O: Sonographer 4 filtered upper arm muscles pair electromyogram using a S5-1 transducer to scan the patient's right kidney

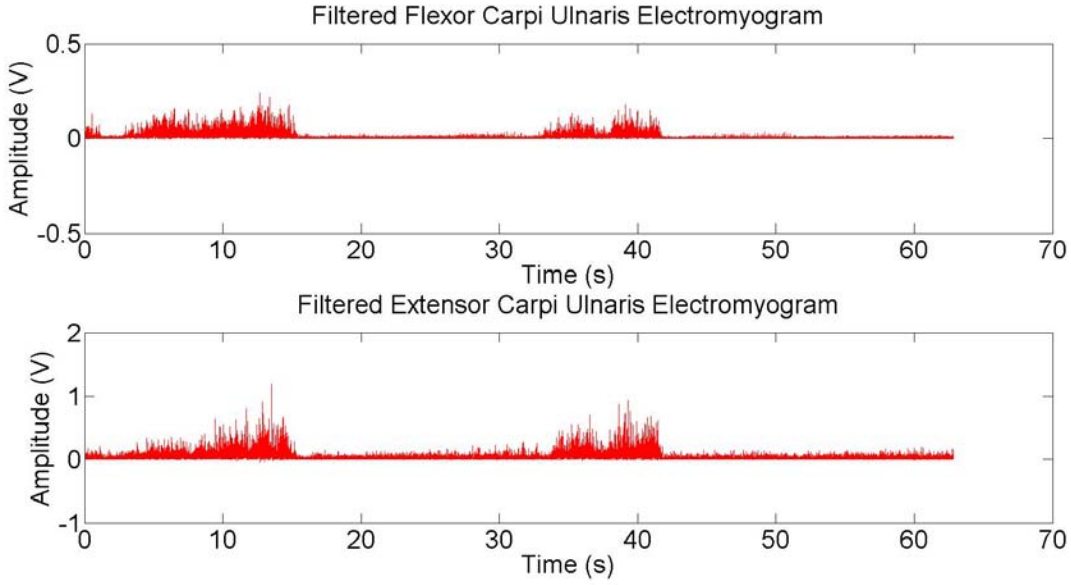

Figure P: Sonographer 4 filtered forearm muscles pair electromyogram using a S5-1 transducer to scan the patient's right kidney

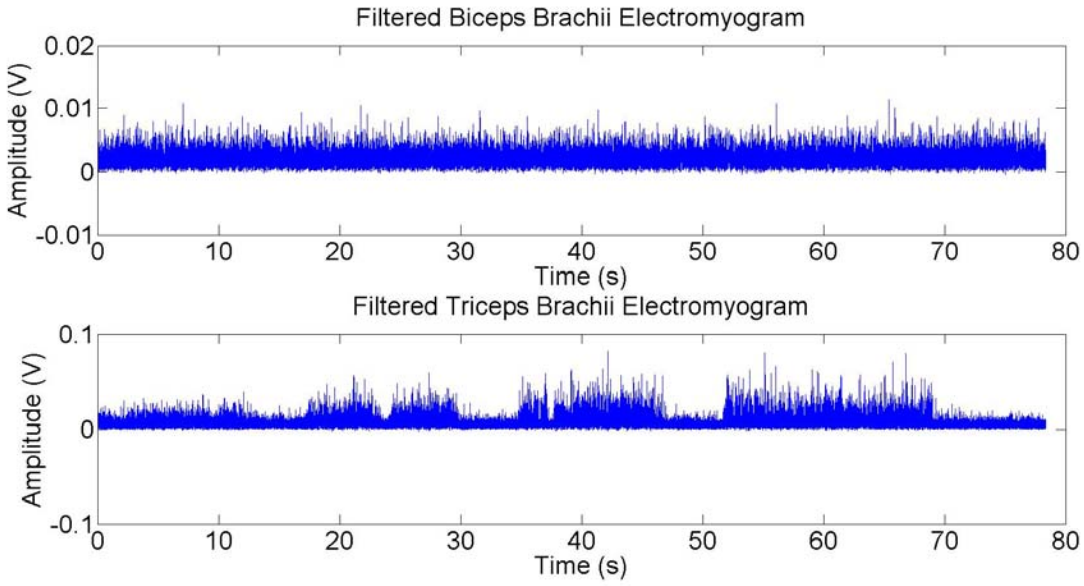

Figure Q: Sonographer 5 filtered upper arm muscles pair electromyogram using a C5-1 transducer to scan the patient's left kidney

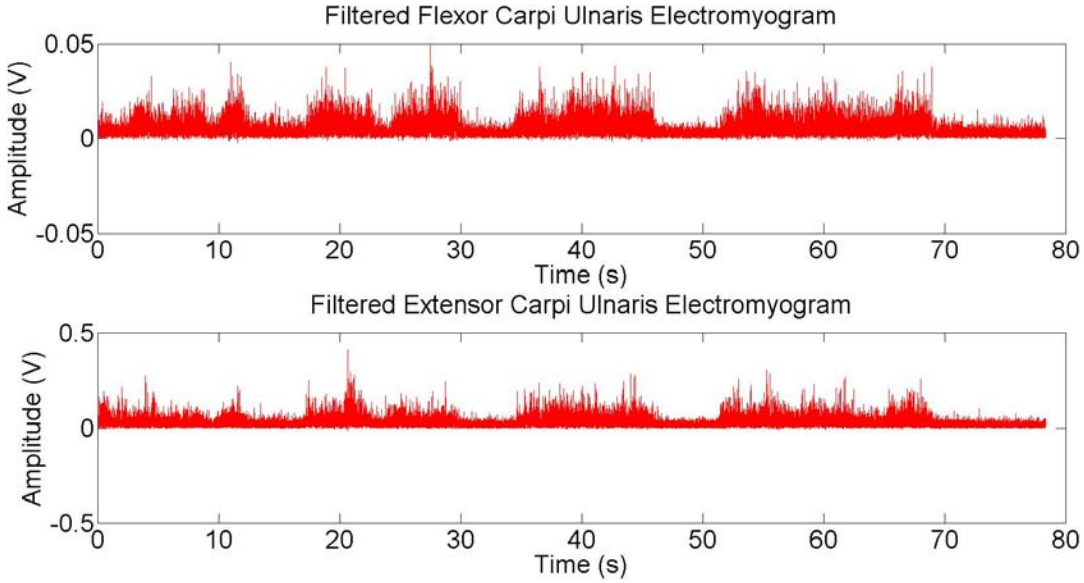

Figure R: Sonographer 5 filtered forearm muscles pair electromyogram using a C5-1 transducer to scan the patient's left kidney

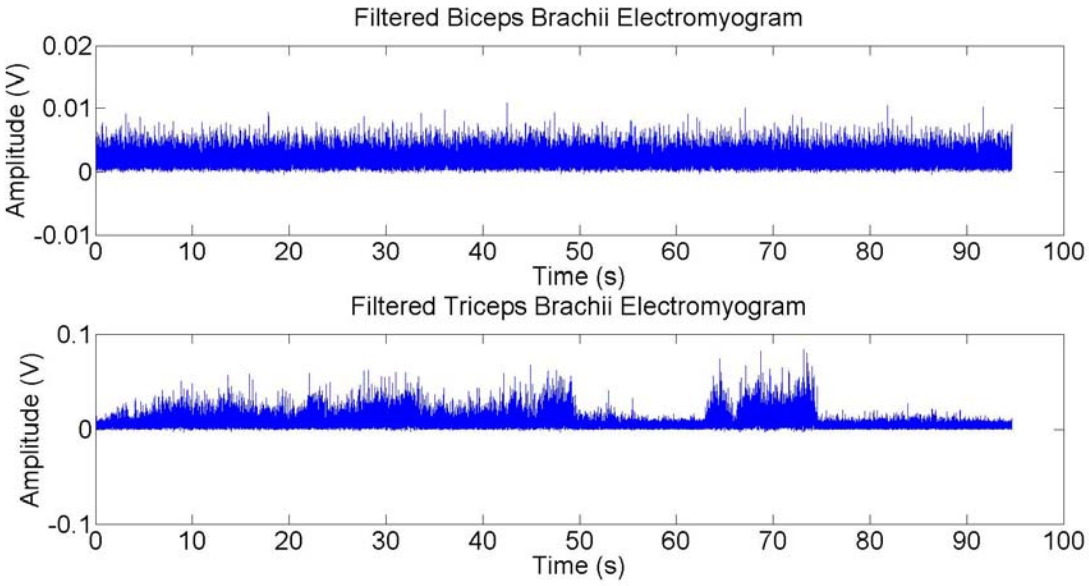

Figure S: Sonographer 5 filtered upper arm muscles pair electromyogram using a C5-1 transducer to scan the patient's right kidney

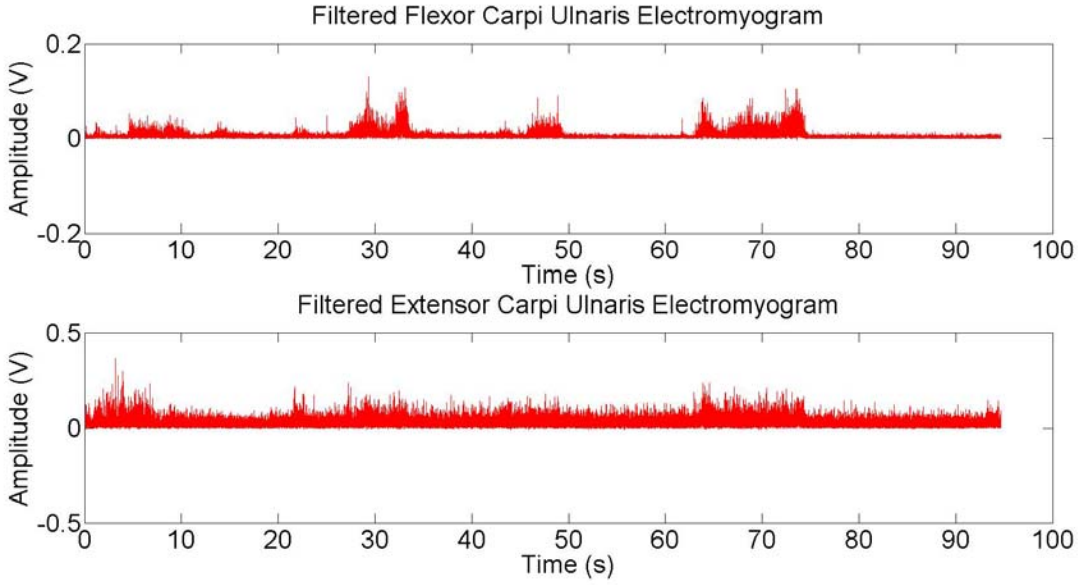

Figure T: Sonographer 5 filtered forearm muscles pair electromyogram using a C5-1 transducer to scan the patient's right kidney

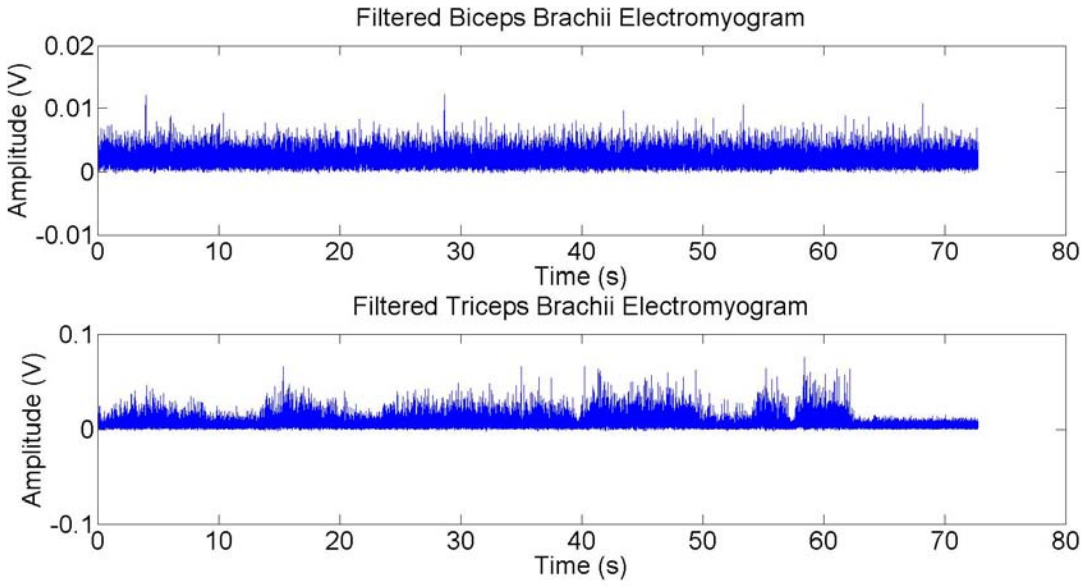

Figure U: Sonographer 5 filtered upper arm muscles pair electromyogram using a S5-1 transducer to scan the patient's left kidney

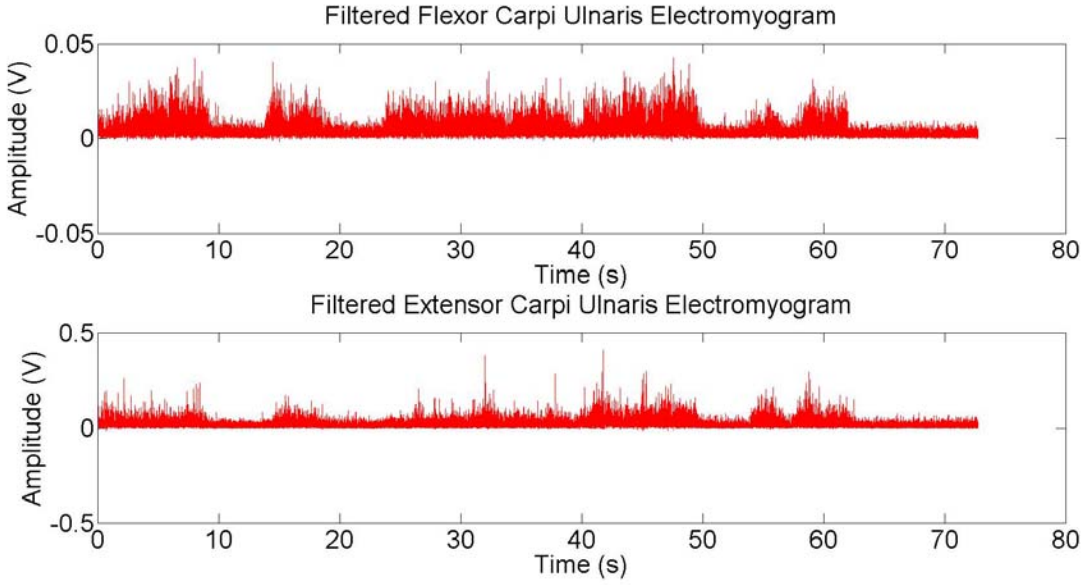

Figure V: Sonographer 5 filtered forearm muscles pair electromyogram using a S5-1 transducer to scan the patient's left kidney

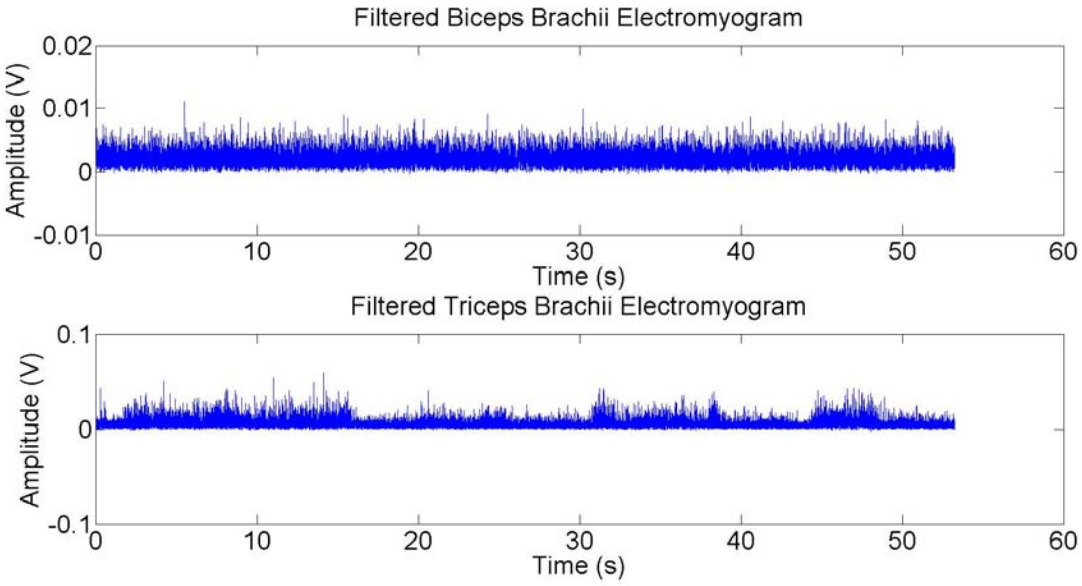

Figure W: Sonographer 5 filtered upper arm muscles pair electromyogram using a S5-1 transducer to scan the patient's right kidney

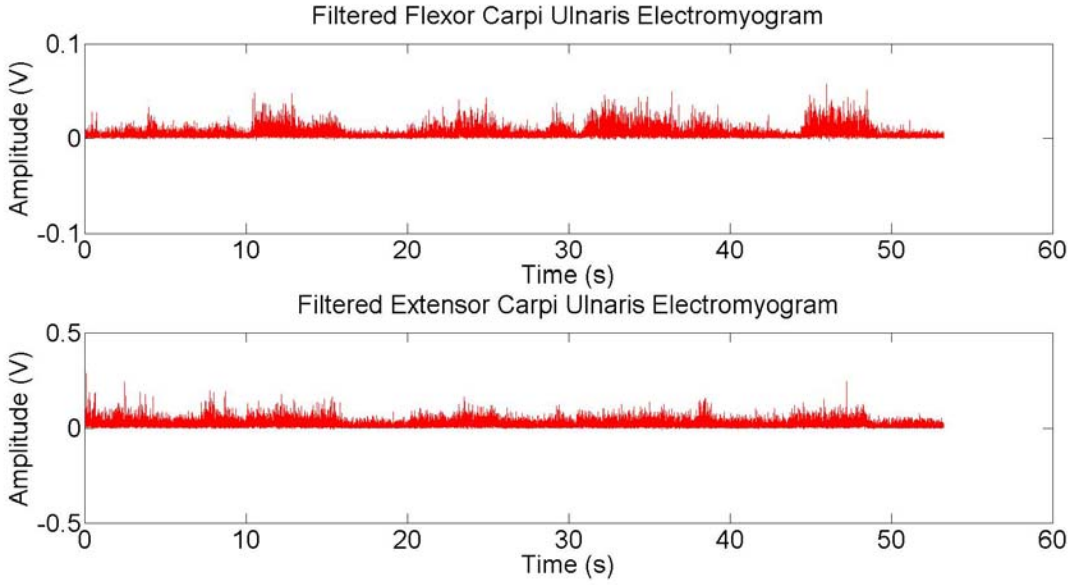

Figure X: Sonographer 5 filtered forearm muscles pair electromyogram using a S5-1 transducer to scan the patient's right kidney

10.2. Matlab Code

10.2.1. Kinematic Evaluating Program

```
%This program determines the joint angles for the wrist, elbow,
%and shoulder joints.

%Constant
Fs = 100;        %sampling frequency
Fc = 15.6;       %cutoff frequency

%Loads the raw marker data from the sonography research study
   %Subject 1 (is subject 3 in thesis)
   P1_lt_lk_markers = importdata('P1_lt_lk_markers.CSV');
   P1_lt_rk_markers = importdata('P1_lt_rk_markers.CSV');
   P1_st_lk_markers = importdata('P1_st_lk_markers.CSV');
   P1_st_rk_markers = importdata('P1_st_rk_markers.CSV');

   %Subject 2
   P2_lt_lk_markers = importdata('P2_lt_lk_markers.CSV');
   P2_lt_rk_markers = importdata('P2_lt_rk_markers.CSV');
   P2_st_lk_markers = importdata('P2_st_lk_markers.CSV');
   P2_st_rk_markers = importdata('P2_st_rk_markers.CSV');

   %Subject 4
   P4_lt_lk_markers = importdata('P4_lt_lk_markers.CSV');
   P4_lt_rk_markers = importdata('P4_lt_rk_markers.CSV');
   P4_st_lk_markers = importdata('P4_st_lk_markers.CSV');
   P4_st_rk_markers = importdata('P4_st_rk_markers.CSV');

   %Subject 5
   P5_lt_lk_markers = importdata('P5_lt_lk_markers.CSV');
   P5_lt_rk_markers = importdata('P5_lt_rk_markers.CSV');
   P5_st_lk_markers = importdata('P5_st_lk_markers.CSV');
   P5_st_rk_markers = importdata('P5_st_rk_markers.CSV');

%-------------------------------------------------------------------------
%Constants
   %Subject 1 (is sonographer 2 in thesis)angle_ranges angles joint_centers
      [P1_lt_lk_rows,P1_lt_lk_columns] = size(P1_lt_lk_markers);
      [P1_lt_rk_rows,P1_lt_rk_columns] = size(P1_lt_rk_markers);
      [P1_st_lk_rows,P1_st_lk_columns] = size(P1_st_lk_markers);
      [P1_st_rk_rows,P1_st_rk_columns] = size(P1_st_rk_markers);

      P1_IHA_landmarks = 5;
      P1_lt_rk_IHA_landmarks = 4;
      P1_lt_lk_IHA_landmarks = 4;

      P1_IHA_start = 1;

      P1_lt_lk_forearm = 1;
      P1_lt_rk_forearm = 1;
      P1_st_lk_forearm = 3;
      P1_st_rk_forearm = 4;
```

```
P1_st_lk_wrist_marker = 4;
P1_wrist_marker = 2;


%Subject 2 (is sonographer 3 in thesis)angle_ranges angles joint_centers
[P2_lt_lk_rows,P2_lt_lk_columns] = size(P2_lt_lk_markers);
[P2_lt_rk_rows,P2_lt_rk_columns] = size(P2_lt_rk_markers);
[P2_st_lk_rows,P2_st_lk_columns] = size(P2_st_lk_markers);
[P2_st_rk_rows,P2_st_rk_columns] = size(P2_st_rk_markers);

P2_IHA_landmarks = 3;

P2_lt_lk_IHA_start = 1;
P2_lt_rk_IHA_start = 1;
P2_st_lk_IHA_start = 2151;
P2_st_rk_IHA_start = 1;

P2_lt_lk_IHA_end = 5710;
P2_lt_rk_IHA_end = 6122;
P2_st_lk_IHA_end = 9379;
P2_st_rk_IHA_end = 7337;

P2_lt_lk_forearm = 1;
P2_lt_rk_forearm = 2;
P2_st_lk_forearm = 4;
P2_st_rk_forearm = 2;

P2_wrist_marker = 3;


%Subject 4
[P4_lt_lk_rows,P4_lt_lk_columns] = size(P4_lt_lk_markers);
[P4_lt_rk_rows,P4_lt_rk_columns] = size(P4_lt_rk_markers);
[P4_st_lk_rows,P4_st_lk_columns] = size(P4_st_lk_markers);
[P4_st_rk_rows,P4_st_rk_columns] = size(P4_st_rk_markers);

P4_IHA_landmarks = 5;
P4_IHA_start = 1;

P4_forearm_frame_option = 4;
P4_lk_forearm_frame_option = 1;

P4_wrist_marker = 1;


%Subject 5
[P5_lt_lk_rows,P5_lt_lk_columns] = size(P5_lt_lk_markers);
[P5_lt_rk_rows,P5_lt_rk_columns] = size(P5_lt_rk_markers);
[P5_st_lk_rows,P5_st_lk_columns] = size(P5_st_lk_markers);
[P5_st_rk_rows,P5_st_rk_columns] = size(P5_st_rk_markers);

P5_IHA_landmarks = 5;
P5_IHA_start = 1;
P5_forearm_frame_option = 4;

P5_wrist_marker = 3;
```

```
%-------------------------------------------------------------------------
%Determines the joint angles for the marker data from the sonography
%research study
   %Subject 1
      %Large transducer left kidney scan
      [P1_lt_lk_angle_ranges P1_lt_lk_angles P1_lt_lk_joint_centers]= ...
         upper_extremity_joint_angles (Fs, Fc, P1_st_rk_markers(1,:), ...
         P1_lt_lk_markers, P1_IHA_landmarks, P1_IHA_start, ...
         P1_lt_lk_rows, P1_lt_lk_forearm, P1_wrist_marker);

      %Large transducer right kidney scan
      [P1_lt_rk_angle_ranges P1_lt_rk_angles P1_lt_rk_joint_centers]= ...
         upper_extremity_joint_angles (Fs, Fc, P1_st_rk_markers(1,:), ...
         P1_lt_rk_markers, P1_lt_rk_IHA_landmarks, P1_IHA_start, ...
         P1_lt_rk_rows, P1_lt_rk_forearm, P1_wrist_marker);

      %Small transducer left kidney scan
      [P1_st_lk_angle_ranges P1_st_lk_angles P1_st_lk_joint_centers]= ...
         upper_extremity_joint_angles (Fs, Fc, P1_st_rk_markers(1,:), ...
         P1_st_lk_markers, P1_IHA_landmarks, P1_IHA_start, ...
         P1_st_lk_rows, P1_st_lk_forearm, P1_st_lk_wrist_marker);

      %Small transducer right kidney scan
      [P1_st_rk_angle_ranges P1_st_rk_angles P1_st_rk_joint_centers]= ...
         upper_extremity_joint_angles (Fs, Fc, P1_st_rk_markers(1,:), ...
         P1_st_rk_markers, P1_IHA_landmarks, P1_IHA_start, ...
         P1_st_rk_rows, P1_st_rk_forearm, P1_wrist_marker);


   %Subject 2
      %Large transducer left kidney scan
      [P2_lt_lk_angle_ranges P2_lt_lk_angles P2_lt_lk_joint_centers]= ...
         upper_extremity_joint_angles (Fs, Fc, P2_lt_lk_markers(742,:), ...
         P2_lt_lk_markers, P2_IHA_landmarks, P2_lt_lk_IHA_start, ...
         P2_lt_lk_IHA_end, P2_lt_lk_forearm, P2_wrist_marker);

      %Large transducer right kidney scan
      [P2_lt_rk_angle_ranges P2_lt_rk_angles P2_lt_rk_joint_centers]= ...
         upper_extremity_joint_angles (Fs, Fc, P2_lt_lk_markers(742,:), ...
         P2_lt_rk_markers, P2_IHA_landmarks, P2_lt_rk_IHA_start, ...
         P2_lt_rk_IHA_end, P2_lt_rk_forearm, P2_wrist_marker);

      %Small transducer left kidney scan
      [P2_st_lk_angle_ranges P2_st_lk_angles P2_st_lk_joint_centers]= ...
         upper_extremity_joint_angles (Fs, Fc, P2_lt_lk_markers(742,:), ...
         P2_st_lk_markers, P2_IHA_landmarks, P2_st_lk_IHA_start, ...
         P2_st_lk_IHA_end, P2_st_lk_forearm, P2_wrist_marker);

      %Small transducer right kidney scan
      [P2_st_rk_angle_ranges P2_st_rk_angles P2_st_rk_joint_centers]= ...
         upper_extremity_joint_angles (Fs, Fc, P2_lt_lk_markers(742,:), ...
         P2_st_rk_markers, P2_IHA_landmarks, P2_st_rk_IHA_start, ...
         P2_st_rk_IHA_end, P2_st_rk_forearm, P2_wrist_marker);
```

```
%Subject 4
    %Large transducer left kidney scan
    [P4_lt_lk_angle_ranges P4_lt_lk_angles P4_lt_lk_joint_centers]= ...
        upper_extremity_joint_angles (Fs, Fc, P4_lt_lk_markers(13,:), ...
        P4_lt_lk_markers, P4_IHA_landmarks, P4_IHA_start, ...
        P4_lt_lk_rows, P4_lk_forearm_frame_option, P4_wrist_marker);

    %Large transducer right kidney scan
    [P4_lt_rk_angle_ranges P4_lt_rk_angles P4_lt_rk_joint_centers]= ...
        upper_extremity_joint_angles (Fs, Fc, P4_lt_lk_markers(13,:), ...
        P4_lt_rk_markers, P4_IHA_landmarks, P4_IHA_start, ...
        P4_lt_rk_rows, P4_forearm_frame_option, P4_wrist_marker);

    %Small transducer left kidney scan
    [P4_st_lk_angle_ranges P4_st_lk_angles P4_st_lk_joint_centers]= ...
        upper_extremity_joint_angles (Fs, Fc, P4_lt_lk_markers(13,:), ...
        P4_st_lk_markers, P4_IHA_landmarks, P4_IHA_start, ...
        P4_st_lk_rows, P4_lk_forearm_frame_option, P4_wrist_marker);

    %Small transducer right kidney scan
    [P4_st_rk_angle_ranges P4_st_rk_angles P4_st_rk_joint_centers]= ...
        upper_extremity_joint_angles (Fs, Fc, P4_lt_lk_markers(13,:), ...
        P4_st_rk_markers, P4_IHA_landmarks, P4_IHA_start, ...
        P4_st_rk_rows, P4_forearm_frame_option, P4_wrist_marker);


%Subject 5
    %Large transducer left kidney scan
    [P5_lt_lk_angle_ranges P5_lt_lk_angles P5_lt_lk_joint_centers]= ...
        upper_extremity_joint_angles (Fs, Fc, P5_lt_lk_markers(1,:), ...
        P5_lt_lk_markers, P5_IHA_landmarks, P5_IHA_start, ...
        P5_lt_lk_rows, P5_forearm_frame_option, P5_wrist_marker);

    %Large transducer right kidney scan
    [P5_lt_rk_angle_ranges P5_lt_rk_angles P5_lt_rk_joint_centers]= ...
        upper_extremity_joint_angles (Fs, Fc, P5_lt_lk_markers(1,:), ...
        P5_lt_rk_markers, P5_IHA_landmarks, P5_IHA_start, ...
        P5_lt_rk_rows, P5_forearm_frame_option, P5_wrist_marker);

    %Small transducer left kidney scan
    [P5_st_lk_angle_ranges P5_st_lk_angles P5_st_lk_joint_centers]= ...
        upper_extremity_joint_angles (Fs, Fc, P5_lt_lk_markers(1,:), ...
        P5_st_lk_markers, P5_IHA_landmarks, P5_IHA_start, ...
        P5_st_lk_rows, P5_forearm_frame_option, P5_wrist_marker);

    %Small transducer right kidney scan
    [P5_st_rk_angle_ranges P5_st_rk_angles P5_st_rk_joint_centers]= ...
        upper_extremity_joint_angles (Fs, Fc, P5_lt_lk_markers(1,:), ...
        P5_st_rk_markers, P5_IHA_landmarks, P5_IHA_start, ...
        P5_st_rk_rows, P5_forearm_frame_option, P5_wrist_marker);


%-------------------------------------------------------------------------
%Determines the x and y axes for the joint angle histograms
    %Subject 1 (is subject 3 in thesis)
    [P1_lt_lk_n P1_lt_lk_xoutput] = scan_hist(P1_lt_lk_angles);
```

```
    [P1_lt_rk_n P1_lt_rk_xoutput] = scan_hist(P1_lt_rk_angles);
    [P1_st_lk_n P1_st_lk_xoutput] = scan_hist(P1_st_lk_angles);
    [P1_st_rk_n P1_st_rk_xoutput] = scan_hist(P1_st_rk_angles);

  %Subject 2
    [P2_lt_lk_n P2_lt_lk_xoutput] = scan_hist(P2_lt_lk_angles);
    [P2_lt_rk_n P2_lt_rk_xoutput] = scan_hist(P2_lt_rk_angles);
    [P2_st_lk_n P2_st_lk_xoutput] = scan_hist(P2_st_lk_angles);
    [P2_st_rk_n P2_st_rk_xoutput] = scan_hist(P2_st_rk_angles);

  %Subject 4
    [P4_lt_lk_n P4_lt_lk_xoutput] = scan_hist(P4_lt_lk_angles);
    [P4_lt_rk_n P4_lt_rk_xoutput] = scan_hist(P4_lt_rk_angles);
    [P4_st_lk_n P4_st_lk_xoutput] = scan_hist(P4_st_lk_angles);
    [P4_st_rk_n P4_st_rk_xoutput] = scan_hist(P4_st_rk_angles);

  %Subject 5
    [P5_lt_lk_n P5_lt_lk_xoutput] = scan_hist(P5_lt_lk_angles);
    [P5_lt_rk_n P5_lt_rk_xoutput] = scan_hist(P5_lt_rk_angles);
    [P5_st_lk_n P5_st_lk_xoutput] = scan_hist(P5_st_lk_angles);
    [P5_st_rk_n P5_st_rk_xoutput] = scan_hist(P5_st_rk_angles);

%-------------------------------------------------------------------------
%Plots the normalized histograms for the joint angles
%Determines what angle column to plot
 for i=1:5;

   %Sets the x and y axis limits
   if i == 1         %Shoulder flexion and extension angles
      x_min = -20;
      x_max = 95;
   elseif i == 2     %Shoulder abduction and adduction angles
      x_min = 0;
      x_max = 115;
   elseif i == 3     %Shoulder internal and external rotation angles
      x_min = -90;
      x_max = 25;
  elseif i == 4      %Elbow flexion angles
      x_min = 0;
      x_max = 110;
   else              %Wrist flexion and extension angles
     x_min = -75;
      x_max = 10;
   end

  figure;
  subplot(221)
  plot(P1_lt_lk_xoutput(:,i),P1_lt_lk_n(:,i)/P1_lt_lk_rows, '-r*', ...
    P1_lt_rk_xoutput(:,i),P1_lt_rk_n(:,i)/P1_lt_rk_rows, '-gs',...
    P1_st_lk_xoutput(:,i),P1_st_lk_n(:,i)/P1_st_lk_rows, '-ko', ...
    P1_st_rk_xoutput(:,i),P1_st_rk_n(:,i)/P1_st_rk_rows, '-cd','LineWidth',2)
    xlabel('Angle (Degrees)','fontsize',30)
    ylabel('Normalized Frequency','fontsize',30)
    xlim([x_min x_max])
    ylim([0 1])
    title('Sonographer  2','fontsize',30)
```

```
    subplot(222)
    plot(P2_lt_lk_xoutput(:,i),P2_lt_lk_n(:,i)/P2_lt_lk_rows,'-r*', ...
        P2_lt_rk_xoutput(:,i),P2_lt_rk_n(:,i)/P2_lt_rk_rows, '-gs',...
        P2_st_lk_xoutput(:,i),P2_st_lk_n(:,i)/P2_st_lk_rows, '-ko', ...
        P2_st_rk_xoutput(:,i),P2_st_rk_n(:,i)/P2_st_rk_rows, '-cd','LineWidth',2)
        xlabel('Angle (Degrees)','fontsize',30)
        xlim([x_min x_max])
        ylim([0 1])
        ylabel('Normalized Frequency','fontsize',30)
        title('Sonographer  3','fontsize',30)

    subplot(223)
    plot(P4_lt_lk_xoutput(:,i),P4_lt_lk_n(:,i)/P4_lt_lk_rows,'-r*', ...
        P4_lt_rk_xoutput(:,i),P4_lt_rk_n(:,i)/P4_lt_rk_rows, '-gs',...
        P4_st_lk_xoutput(:,i),P4_st_lk_n(:,i)/P4_st_lk_rows, '-ko', ...
        P4_st_rk_xoutput(:,i),P4_st_rk_n(:,i)/P4_st_rk_rows, '-cd','LineWidth',2)
        xlabel('Angle (Degrees)','fontsize',30)
        xlim([x_min x_max])
        ylim([0 1])
        ylabel('Normalized Frequency','fontsize',30)
        title('Sonographer 4','fontsize',30)

    subplot(224)
    plot(P5_lt_lk_xoutput(:,i),P5_lt_lk_n(:,i)/P5_lt_lk_rows,'-r*', ...
        P5_lt_rk_xoutput(:,i),P5_lt_rk_n(:,i)/P5_lt_rk_rows, '-gs',...
        P5_st_lk_xoutput(:,i),P5_st_lk_n(:,i)/P5_st_lk_rows, '-ko', ...
        P5_st_rk_xoutput(:,i),P5_st_rk_n(:,i)/P5_st_rk_rows, '-cd','LineWidth',2)
        h = legend('C5-1 Transducer, Left Kidney','C5-1 Transducer, Right Kidney','S5-1 Transducer, Left
Kidney','S5-1 Transducer, Right Kidney');
        set(h,'Interpreter','none')
        xlabel('Angle (Degrees)','fontsize',30)
        xlim([x_min x_max])
        ylim([0 1])
        ylabel('Normalized Frequency','fontsize',30)
        title('Sonographer  5','fontsize',30)
 end
```

10.2.2. Kinematic Main Program

```
function [angle_ranges angles joint_centers]= upper_extremity_joint_angles(fs, fc, static_raw_data,
dynamic_raw_data,IHA_landmarks,IHA_start,IHA_end,forearm_frame_option,wrist_marker_option)
%This function determines the joint centers and joint angles for the
%wrist, elbow, and shoulder joints.

%Constants
   [r,c] = size(dynamic_raw_data); %Determines the length of the inputs
                                   %source assuming all inputs are of
                                   %equal length/time duration


%Static trial raw data
   %Seperates the filtered data into individual markers
   [ELH_S EMH_S VH1_S VH2_S VH3_S USP_S RSP_S VF1_S VF2_S VF3_S]= ...
      marker_seperation_static (static_raw_data);


%Dynamic trial raw data
   %Generates a power spectral density analysis to determine cutoff
   %frequencies then filters the raw marker data using the cutoff frequencies
   for i=1:c
      [filt_dynamic(:,i)]= filtering (fs,fc,dynamic_raw_data(:,i));
   end

   %Seperates the filtered data into individual markers
   [SJ_D C7_D T8_D AA_D TS_D AI_D ELH_D VH1_D VH2_D VH3_D RSP_D...
      VF1_D VF2_D VF3_D hand_D]= marker_seperation_dynamic (filt_dynamic);

   %Seperates the data into one matrix with: AA_D TS_D AI_D AC_D PC_D for
   %the input matrix for the instantaneous helical axes method
      scapula_markers_filtered= marker_seperation(filt_dynamic,IHA_landmarks);
      scapula_markers_raw= marker_seperation(dynamic_raw_data,IHA_landmarks);

%-------------------------------------------------------------------------
%Determines the joint centers
   %Instantaneous helical axes method (IHA)
      %Determines the glenohumeral joint center in the global coordinate
      %system
      if IHA_end < r;
         [global_gleno_IHA]= IHA_pivot_pt(fs, scapula_markers_raw(IHA_start:IHA_end,:));
      else
         [global_gleno_IHA]= IHA_pivot_pt(fs, scapula_markers_filtered(IHA_start:IHA_end,:));
      end

   %Difference between medial and lateral markers about the joint
      %Determines the elbow joint center in the global coordinate system
      [jc_elbow_global]= interpolated_joint_center(ELH_S,EMH_S);

      %Determines the wrist joint center in the global coordinate system
      [jc_wrist_global]= interpolated_joint_center(USP_S,RSP_S);

%-------------------------------------------------------------------------
%Determines the technical reference frame for a static frame
   %Humerus
```

```
    [Rhs_GtoL]= reference_frame(VH1_S',VH2_S',VH3_S',4);
    %Forearm
    if forearm_frame_option == 1;
        [Rfs_GtoL]= reference_frame(jc_elbow_global',VF1_S',VF2_S',4);

    elseif forearm_frame_option == 2;
        [Rfs_GtoL]= reference_frame(jc_elbow_global',VF1_S',VF3_S',4);

    elseif forearm_frame_option == 3;
        [Rfs_GtoL]= reference_frame(jc_elbow_global',VF1_S',RSP_S',4);

    else
        [Rfs_GtoL]= reference_frame(VF1_S',VF2_S',VF3_S',4);
    end

%--------------------------------------------------------------------------
%Determines the local position of the joint centers using the static
%technical reference frame
    %For the glenohumeral joint calculated using IHA
        %Humerus
        [rhs_local_glen_IHA]= local_position(Rhs_GtoL,global_gleno_IHA,VH1_S');

    %For the elbow joint center calculated using the difference between
    %medial and lateral markers about the joint
        %Humerus
        [rhs_local_elbow_diff]= local_position(Rhs_GtoL,jc_elbow_global',VH1_S');

    %For the wrist joint center calculated using the difference between
    %medial and lateral markers about the joint
        %Forearm
        [rfs_local_wrist]= local_position(Rfs_GtoL, jc_wrist_global',VF1_S');

%--------------------------------------------------------------------------
%Determines the dynamic technical reference frames

    %Humerus
    j=1;
        for i=1:r;
            Rhd_GtoL(j:j+2,1:3)= reference_frame(VH1_D(i,:)',VH2_D(i,:)',VH3_D(i,:)',4);
            j=j+3;
        end

%--------------------------------------------------------------------------
%Determines the global position of the joint center using the technical
%reference frames from the dynamic trial: creating nrx3 matrix
    %Glenohumeral joint center
        %IHA method
          j=1;
          for i=1:r;
              rd_global_gleno_IHA(i,1:3) = global_position(Rhd_GtoL(j:j+2,1:3), ...
                rhs_local_glen_IHA, VH1_D(i,:)')';
              j=j+3;
          end
```

```
%-------------------------------------------------------------------------
%Determines the global position of the joint center using the technical
%reference frames from the dynamic trial: creating nrx3 matrix
   %Elbow joint center
    j=1;
    for i=1:r;
       rd_global_elbow(i,1:3) = global_position(Rhd_GtoL(j:j+2,1:3), ...
          rhs_local_elbow_diff, VH1_D(i,:)')';
       j=j+3;
    end

%-------------------------------------------------------------------------
%Determines the dynamic technical reference frames
   %Forearm
   if forearm_frame_option == 1;
      j=1;
      for i=1:r;
         Rfd_GtoL(j:j+2,1:3)= reference_frame(rd_global_elbow(i,:)',VF1_D(i,:)',VF2_D(i,:)',4);
      j=j+3;
      end

   elseif forearm_frame_option == 2;
      j=1;
      for i=1:r;
         Rfd_GtoL(j:j+2,1:3)= reference_frame(rd_global_elbow(i,:)',VF1_D(i,:)',VF3_D(i,:)',4);
      j=j+3;
      end

   elseif forearm_frame_option == 3;
      j=1;
      for i=1:r;
         Rfd_GtoL(j:j+2,1:3)= reference_frame(rd_global_elbow(i,:)',VF1_D(i,:)',RSP_D(i,:)',4);
      j=j+3;
      end

   else
      j=1;
      for i=1:r;
         Rfd_GtoL(j:j+2,1:3)= reference_frame(VF1_D(i,:)',VF2_D(i,:)',VF3_D(i,:)',4);
         j=j+3;
      end
   end
%-------------------------------------------------------------------------
   %Wrist joint center
   j=1;
   for i=1:r;
      rd_global_wrist(i,1:3) = global_position(Rfd_GtoL(j:j+2,1:3), ...
         rfs_local_wrist, VF1_D(i,:)')';
      j=j+3;
   end

%-------------------------------------------------------------------------
%Determines the anatomical reference frame for the dynamic trial at each
%frame
   %Thorax
   j=1;
```

```
    for i=1:r;
        R_GtoL_thorax(j:j+2,1:3) = reference_frame(T8_D(i,:)', C7_D(i,:)', ...
            SJ_D(i,:)',5);
        j=j+3;
    end


    %Humerus
    j=1;
    for i=1:r;
        R_GtoL_humerus(j:j+2,1:3) = reference_frame_humerus(rd_global_elbow(i,:)', ...
            rd_global_gleno_IHA(i,:)', ELH_D(i,:)', 3);
        j=j+3;
    end

%-------------------------------------------------------------------------
%Determines the joint angles at every single frame of the dynamic trial
    %Glenohumeral joint
        %Using humerus and thorax reference frames
        j=1;
        for i=1:r;
            [phi_gleno(i,1) theta_gleno(i,1) psi_gleno(i,1)]= ...
                yxy_euler_sequence(R_GtoL_humerus(j:j+2,1:3), R_GtoL_thorax(j:j+2,1:3));
            j=j+3;
        end


    %Elbow joint
     for i=1:r
        humerus_vector= rd_global_elbow(i,1:3)-rd_global_gleno_IHA(i,1:3);
        forearm_vector= rd_global_wrist(i,1:3)-rd_global_elbow(i,1:3);

        vector_mag= norm(forearm_vector)*norm(humerus_vector);

        elbow_flex_rads= acos(dot(humerus_vector,forearm_vector) / ...
            vector_mag);

        elbow_flex(i,:)= elbow_flex_rads * (180/pi);
     end

    %Wrist joint
        %Determines what wrist marker is used to determine the marker
        %vector
        if wrist_marker_option == 1;
            wrist_marker = VF1_D;
        elseif wrist_marker_option == 2;
            wrist_marker = VF2_D;
        elseif wrist_marker_option == 3;
            wrist_marker = VF3_D;
        elseif wrist_marker_option == 4;
            wrist_marker = RSP_D;
        end

        for i=1:r
```

```
        %Vector representing the long axis of the proximal body segment
        forearm_vector= rd_global_wrist(i,1:3)-rd_global_elbow(i,1:3);

        %Vector representing the long axis of the distal body segment
        hand_vector= hand_D(i,1:3)-rd_global_wrist(i,1:3);

        %Vector that points lateral to medial about the wrist
        %(points from thumb to pinky)
        vector_norm_zaxis= cross(hand_vector, forearm_vector);

        %Vector that points from anterior to posterior at the wrist
        %(points from the palm to the top of the hand)
        vector_norm_xaxis= cross(forearm_vector, vector_norm_zaxis);

        %Marker vector to check direction of vector_norm_xaxis
        marker_vector= wrist_marker(i,1:3) - rd_global_wrist(i,1:3);

        %The direction of vector_norm_zaxis determines if the wrist is
        %in flexion or extension
        check = dot(marker_vector,vector_norm_xaxis);

        if check < 0
           sign = 1;
        else
           sign = -1;
        end
         sign_check(i,1)= sign;

        vector_mags= norm(hand_vector)*norm(forearm_vector);

        wrist_flex_rads= sign*acos(dot(hand_vector,forearm_vector) / ...
           vector_mags);

        wrist_flex(i,:)= wrist_flex_rads * (180/pi);


        %Continuity test
        %Determines the difference between two angles in succession and
        %if the angle changes more than 5 degrees in 0.20 seconds then
        %the sign of the previous angle is applied to the current angle
        if i > 1
           wrist_diff= abs(wrist_flex(i,:) - wrist_flex(i-1,:));
           wrist_diff_check(i,:)= wrist_diff;
           if wrist_diff >= 5
              wrist_rads= acos(dot(hand_vector,forearm_vector) ...
                 / vector_mags) * sign_check(i-1,1);


              sign_check(i,1) = sign_check(i-1,1);

              wrist_flex(i,:)= wrist_rads * (180/pi);
           end
        end
     end

%--------------------------------------------------------------------
```

```
%Determines the min, max, and average for each joint angles
   %Minimum joint angles
      %Glenohumeral
      gleno_angles = zeros(3,3);
      gleno_angles(1,1) = min(phi_gleno);
      gleno_angles(1,2) = min(theta_gleno);
      gleno_angles(1,3) = min(psi_gleno);

      %Elbow joint
      elbow_flexion(1,1) = min(elbow_flex);

      %Wrist joint
      wrist_flexion(1,1) = min(wrist_flex);

   %Maximum joint angles
      %Glenohumeral
      gleno_angles(2,1) = max(phi_gleno);
      gleno_angles(2,2) = max(theta_gleno);
      gleno_angles(2,3) = max(psi_gleno);

      %Elbow joint
      elbow_flexion(2,1) = max(elbow_flex);

      %Wrist joint
      wrist_flexion(2,1) = max(wrist_flex);

   %Average joint angles
      %Glenohumeral
      gleno_angles(3,1) = mean(phi_gleno);
      gleno_angles(3,2) = mean(theta_gleno);
      gleno_angles(3,3) = mean(psi_gleno);

      %Elbow joint
      elbow_flexion(3,1) = mean(elbow_flex);

      %Wrist joint
      wrist_flexion(3,1) = mean(wrist_flex);

%-------------------------------------------------------------------------
%Output
   %Min and max angles
      angle_ranges(:,1:3) = gleno_angles;
      angle_ranges(:,4) = elbow_flexion;
      angle_ranges(:,5) = wrist_flexion;

   %All angles for the scan
      angles(:,1) = phi_gleno;
      angles(:,2) = theta_gleno;
      angles(:,3) = psi_gleno;
      angles(:,4) = elbow_flex;
      angles(:,5) = wrist_flex;

      %Joint Centers
      joint_centers(:,1:3)= rd_global_gleno_IHA;
      joint_centers(:,4:6)= rd_global_elbow;
      joint_centers(:,7:9)= rd_global_wrist;
```

10.2.3. Kinematic Sub-programs

10.2.3.1. Marker Separation

```
function [AA_TS_AI_AC_PC]= marker_seperation (raw_marker_data, number_of_IHA_landmarks)
%This function seperates the data into individual markers that are needed
%for determining the wrist, elbow, glenohumeral, sternoclavicular, and
%acromioclavicular joint angles.

%Sections the data into individual markers
i = 1;
j = 3;

SJ = raw_marker_data(:,i:j);
i = i+3;
j = j+3;

C7 = raw_marker_data(:,i:j);
i = i+3;
j = j+3;

T8 = raw_marker_data(:,i:j);
i = i+3;
j = j+3;

AA = raw_marker_data(:,i:j);
i = i+3;
j = j+3;

TS = raw_marker_data(:,i:j);
i = i+3;
j = j+3;

AI = raw_marker_data(:,i:j);
i = i+3;
j = j+3;

AC = raw_marker_data(:,i:j);
i = i+3;
j = j+3;

PC = raw_marker_data(:,i:j);
i = i+3;
j = j+3;

ELH = raw_marker_data(:,i:j);
i = i+3;
j = j+3;

EMH = raw_marker_data(:,i:j);
i = i+3;
j = j+3;

VH1 = raw_marker_data(:,i:j);
i = i+3;
```

```
j = j+3;

VH2 = raw_marker_data(:,i:j);
i = i+3;
j = j+3;

VH3 = raw_marker_data(:,i:j);
i = i+3;
j = j+3;

USP = raw_marker_data(:,i:j);
i = i+3;
j = j+3;

RSP = raw_marker_data(:,i:j);
i = i+3;
j = j+3;

VF1 = raw_marker_data(:,i:j);
i = i+3;
j = j+3;

VF2 = raw_marker_data(:,i:j);
i = i+3;
j = j+3;

VF3 = raw_marker_data(:,i:j);
i = i+3;
j = j+3;

hand = raw_marker_data(:,i:j);
i = i+3;
j = j+3;


%Determines the single matrix for the instantaneous helical axes method
if number_of_IHA_landmarks == 5;
   m = 1;
   n = 3;

   AA_TS_AI_AC_PC(:,m:n) = AA;
   m = m+3;
   n = n+3;

   AA_TS_AI_AC_PC(:,m:n) = TS;
   m = m+3;
   n = n+3;

   AA_TS_AI_AC_PC(:,m:n) = AI;
   m = m+3;
   n = n+3;

   AA_TS_AI_AC_PC(:,m:n) = AC;
   m = m+3;
   n = n+3;
```

```
    AA_TS_AI_AC_PC(:,m:n) = PC;

elseif number_of_IHA_landmarks == 4;
        m = 1;
    n = 3;

    AA_TS_AI_AC_PC(:,m:n) = AA;
    m = m+3;
    n = n+3;

    AA_TS_AI_AC_PC(:,m:n) = TS;
    m = m+3;
    n = n+3;

    AA_TS_AI_AC_PC(:,m:n) = AI;
    m = m+3;
    n = n+3;

    AA_TS_AI_AC_PC(:,m:n) = AC;


else
    m = 1;
    n = 3;

    AA_TS_AI_AC_PC(:,m:n) = TS;
    m = m+3;
    n = n+3;

    AA_TS_AI_AC_PC(:,m:n) = AI;
    m = m+3;
    n = n+3;

    AA_TS_AI_AC_PC(:,m:n) = PC;
end
```

10.2.3.2. Marker Separation Static

```
function [ELH EMH VH1 VH2 VH3 USP RSP VF1 VF2 VF3]= marker_seperation_static
(raw_marker_data)
%This function seperates the data into individual markers that are needed
%for determining the wrist, elbow, glenohumeral, sternoclavicular, and
%acromioclavicular joint angles.

%Sections the data into individual markers
i = 1;
j = 3;

SJ = raw_marker_data(:,i:j);
i = i+3;
j = j+3;

C7 = raw_marker_data(:,i:j);
i = i+3;
j = j+3;

T8 = raw_marker_data(:,i:j);
i = i+3;
j = j+3;

AA = raw_marker_data(:,i:j);
i = i+3;
j = j+3;

TS = raw_marker_data(:,i:j);
i = i+3;
j = j+3;

AI = raw_marker_data(:,i:j);
i = i+3;
j = j+3;

AC = raw_marker_data(:,i:j);
i = i+3;
j = j+3;

PC = raw_marker_data(:,i:j);
i = i+3;
j = j+3;

ELH = raw_marker_data(:,i:j);
i = i+3;
j = j+3;

EMH = raw_marker_data(:,i:j);
i = i+3;
j = j+3;

VH1 = raw_marker_data(:,i:j);
i = i+3;
j = j+3;
```

```
VH2 = raw_marker_data(:,i:j);
i = i+3;
j = j+3;

VH3 = raw_marker_data(:,i:j);
i = i+3;
j = j+3;

USP = raw_marker_data(:,i:j);
i = i+3;
j = j+3;

RSP = raw_marker_data(:,i:j);
i = i+3;
j = j+3;

VF1 = raw_marker_data(:,i:j);
i = i+3;
j = j+3;

VF2 = raw_marker_data(:,i:j);
i = i+3;
j = j+3;

VF3 = raw_marker_data(:,i:j);
i = i+3;
j = j+3;

hand = raw_marker_data(:,i:j);
i = i+3;
j = j+3;
```

10.2.3.3. Marker Separation Dynamic

```
function [SJ C7 T8 AA TS AI ELH VH1 VH2 VH3 RSP VF1 VF2 VF3 hand]=
marker_seperation_dynamic (raw_marker_data)
%This function seperates the data into individual markers that are needed
%for determining the wrist, elbow, glenohumeral, sternoclavicular, and
%acromioclavicular joint angles.

%Sections the data into individual markers
i = 1;
j = 3;

SJ = raw_marker_data(:,i:j);
i = i+3;
j = j+3;

C7 = raw_marker_data(:,i:j);
i = i+3;
j = j+3;

T8 = raw_marker_data(:,i:j);
i = i+3;
j = j+3;

AA = raw_marker_data(:,i:j);
i = i+3;
j = j+3;

TS = raw_marker_data(:,i:j);
i = i+3;
j = j+3;

AI = raw_marker_data(:,i:j);
i = i+3;
j = j+3;

AC = raw_marker_data(:,i:j);
i = i+3;
j = j+3;

PC = raw_marker_data(:,i:j);
i = i+3;
j = j+3;

ELH = raw_marker_data(:,i:j);
i = i+3;
j = j+3;

EMH = raw_marker_data(:,i:j);
i = i+3;
j = j+3;

VH1 = raw_marker_data(:,i:j);
i = i+3;
j = j+3;
```

```
 VH2 = raw_marker_data(:,i:j);
i = i+3;
j = j+3;

VH3 = raw_marker_data(:,i:j);
i = i+3;
j = j+3;

USP = raw_marker_data(:,i:j);
i = i+3;
j = j+3;

RSP = raw_marker_data(:,i:j);
i = i+3;
j = j+3;

VF1 = raw_marker_data(:,i:j);
i = i+3;
j = j+3;

VF2 = raw_marker_data(:,i:j);
i = i+3;
j = j+3;

VF3 = raw_marker_data(:,i:j);
i = i+3;
j = j+3;

hand = raw_marker_data(:,i:j);
i = i+3;
j = j+3;
```

10.2.3.4. Power Spectral Density Analysis

```
function [Fc]= psd_analysis (Fs,raw_data)
%This program performs a power spectral density analysis to determine the
%cutoff frequency for each marker in each component direction


%Applies a rectangular window and takes the FFT of the raw data
sigLength = length(raw_data);
win = rectwin(sigLength);

%Fast Fourier Transformation of rectangular window
FFT = fft(win .* raw_data);

%Frequency
figLength = sigLength/2 + 1;
frequency = [1:figLength]*Fs/(2*figLength);

%FFTs are normally two-sided this returns a one-sided FFT
FFT_onesided = FFT(1:figLength);

%Normalizes FFT data
FFT_norm=(abs(FFT_onesided))/sum(abs(FFT_onesided));


%Determines cutoff frequency
   %Initial values
   sum_FFT = 0;
   j = 1;
   power_cutoff = 0.99;

   %Sums the normalized FFT values until it is over 99 percent of the power
   while sum_FFT < power_cutoff
      sum_FFT = sum_FFT + FFT_norm(j);
      location = j;

      j = j+1;
   end


%Returns the frequency at which 99 percent of the power is contained
%below this frequency
   Fc = frequency(1,location);
```

10.2.3.5. Filtering

```
function [filtered_data]= filtering (Fs,Fc,raw_data)
%This program performs a power spectral density analysis to determine the
%cutoff frequency for each marker in each component direction

%Constant
Fn= Fs/2;   %Nyquist frequency
order = 4;  %Order of the filter

%Filters the data using a 4th order lowpass Butterworth filter and a
%zero-phase digital filter
   [b,a] = butter(order,Fc/Fn,'low');
   filtered_data = filtfilt(b,a,raw_data);
```

10.2.3.6. Instantaneous Helical Axis Pivot Point

```
function [opp rms]= IHA_pivot_pt(Fs, xi)
%This function determines the optimum pivot point using the positions
%determined from the instantaneous helical axes method (IHA).

%Reference article-
   %Woltring, H. "Model and measurement error influences in data
   %processing." In Biomechanics of human movement : applications
   %in rehabilitation, sports and ergonomics, by A., Berme, N. (Eds.)
   %Cappozzo, 203-237. Worthington, 1990.

%Constants
   t = 1/Fs;          %Time interval between frames
   [r,c] = size(xi);   %Number of landmarks, there should be at least 3

   %Identity matrix
   I = zeros(3,3);
   for j=1:3
      I(j,j) = 1;
   end

%Determines the velocity of the landmarks using the numerical difference
%method
[vi] = linear_velocity(xi, t);


%Determines the velocity of the landmarks using the numerical difference
%method
[ai]= linear_acceleration(xi, t);


%Determines the IHA position in the global coordinate system for each frame
%excluding the first and last frame because of the velocities and
%accelerations determined
for k=2:r-1
   [IHA_p(k-1,:) u(k-1,:)]= IHA_position(xi(k,:), vi(k,:), ai(k,:));
end


%Determines Q (I have no idea what it stands for)
Q_sum=0;
for j=1:r-2
   Qi(j:j+2,1:3)= I - (u(j,:)*u(j,:)');

   Q_sum = Qi(j:j+2,1:3) + Q_sum;
end

Q_inital = Q_sum/(r-2);


%Checking for singularity which will result in Q being undefined if the
%inverse is taken
check_matrix = zeros(3,3);
if Q_inital == check_matrix
```

```
    Q = I;
else
    Q = Q_inital;
end


%Determines the optimum pivot point
k=1;
Qi_si_sum=0;
for j=1:r-2
    Qi(k:k+2,1:3)= I - (u(j,:)*u(j,:)');

    Qi_si_sum= Qi(k:k+2,1:3)*IHA_p(j,:)' + Qi_si_sum;

    k=k+3;
end

Qi_si = Qi_si_sum/(r-2);

opp = (Q^-1) * Qi_si; %Returns a 3x1 matrix


%Root mean square
sum_diff_sq = zeros(1,3);

for i=1:r-2
    sum_diff_sq(1,1) = sum_diff_sq(1,1) + (IHA_p(i,1) -opp(1,1))^2;
    sum_diff_sq(1,2) = sum_diff_sq(1,2) + (IHA_p(i,2) -opp(2,1))^2;
    sum_diff_sq(1,3) = sum_diff_sq(1,3) + (IHA_p(i,3) -opp(3,1))^2;
end

rms = sqrt(sum_diff_sq/(r-2));
```

10.2.3.7. Linear Velocity

```
function [vi]= linear_velocity(xi, t)
%This function determines the linear velocity of landmarks using the
%numerical difference method.

%Constants
   [r,c] = size(xi);   %Number of landmarks, there should be at least 4
   m = c/3;

%Initial values
   vi = zeros(r,c);

%Linear velocity in the global reference frame
for i=2:r-1;

   j=1;    %Initializes landmark location

   for k=1:m;
      vi(i,j)   = (xi(i+1,j) - xi(i-1,j))/(2*t);      %Component x
      vi(i,j+1) = (xi(i+1,j+1) - xi(i-1,j+1))/(2*t);  %Component y
      vi(i,j+2) = (xi(i+1,j+2) - xi(i-1,j+2))/(2*t);  %Component z

      j=j+3;  %Increments to the next landmark
   end
end
```

10.2.3.8. Linear Acceleration

```
function [ai]= linear_acceleration(xi, t)
%This function determines the linear acceleration of landmarks using the
%numerical difference method.

%Constants
   [r,c] = size(xi);   %Number of landmarks, there should be at least 4
   m = c/3;

%Initial values
   ai = zeros(r,c);

%Linear acceleration in the global reference frame
for i=2:r-1;

   j=1;    %Initializes landmark location

   for k=1:m;
      ai(i,j)   = (xi(i+1,j) - (2 * xi(i,j)) + xi(i-1,j))/(t^2);       %Component x
      ai(i,j+1) = (xi(i+1,j+1) - (2 * xi(i,j+1)) + xi(i-1,j+1))/(t^2); %Component y
      ai(i,j+2) = (xi(i+1,j+2) - (2 * xi(i,j+2)) + xi(i-1,j+2))/(t^2); %Component z

      j=j+3;  %Increments to the next landmark
   end
end
```

10.2.3.9. Instantaneous Helical Axis Position

```
function [IHA_p u]= IHA_position(xi, vi, ai)
%This function determines the location of a point on the instantaneous
%helical axis (IHA). This point will lie at root of perpendicular to
%IHA through the centroid of the landmarks.

%Reference article-
   %Sommer III, H. "Determination of first and second order instant
   %screw parameters from landmark trajectories." ASME Journal of
   %Mechanical Design, 1992: 274-282.

%Inputs-
   %xi is global location of landmarks
   %vi is velocity of landmarks
   %ai is acceleration of landmarks

%Output-
   %IHA_P is the IHA location: 1x3 matrix


%Constants
   [r,c] = size(xi);   %Number of landmarks, there should be at least 3
   m = c/3;
   fi(1:m) = 1;       %Landmark weighting factors vector of length m
   eps = 1.0E-5;      %Epsilon converge tolerance- distance between points
                      %will need to be less than epsilon tolerance

   %Variance-covariance weighting matrix for landmark measurements
   ss = zeros(3,3);
   for i=1:3;
      ss(i,i) = 1;
   end


%Initial values
   xo = zeros(3,1);    %Global location of centroid of landmarks
   vo = zeros(3,1);    %Mean velocity of landmarks
   ao = zeros(3,1);    %Mean acceleration of landmarks

   X = zeros(3,3);     %Landmark inertia matrix
   V = zeros(3,3);     %Landmark velocity moment matrix
   A = zeros(3,3);     %Landmark acceleration moment matrix


%Least squares statistical weighting
   %Applies scalar statistical weighting factor to each landmark
      fo = sum(fi)/m;     %Mean statistical weighting factor for landmarks
                          %eq. 50

      %Scales and sums xi, vi, and ai for each component (x,y,z), eq. 51-53
      j=1;
      for i=1:m;
            xo(1) = xo(1) + (fi(i)*xi(j));      %Component x
            xo(2) = xo(2) + (fi(i)*xi(j+1));    %Component y
```

```
        xo(3) = xo(3) + (fi(i)*xi(j+2));    %Component z

        vo(1) = vo(1) + (fi(i)*vi(j));      %Component x
        vo(2) = vo(2) + (fi(i)*vi(j+1));    %Component y
        vo(3) = vo(3) + (fi(i)*vi(j+2));    %Component z

        ao(1) = ao(1) + (fi(i)*ai(j));      %Component x
        ao(2) = ao(2) + (fi(i)*ai(j+1));    %Component y
        ao(3) = ao(3) + (fi(i)*ai(j+2));    %Component z

        j=j+3;  %Increments to the next landmark
    end

    %Determines the mean and normalizing xo, vo, and ao
    xo = xo/m/fo;
    vo = vo/m/fo;
    ao = ao/m/fo;

    %Determines the accumulation summation matrices over all landmarks
    %eq. 54-56
    for i=1:m;
       for j=1:3:3*m;
          X = X + (fi(i)*(xi(j:j+2)-xo(:)')'*(xi(j:j+2)-xo(:)'));

          V = V + fi(i)*vi(j:j+2)'*(xi(j:j+2)-xo(:)');

          A = A + fi(i)*ai(j:j+2)'*(xi(j:j+2)-xo(:)');
       end
    end

    %Normalizes summation matrices
    X = X/m/fo;
    V = V/m/fo;
    A = A/m/fo;


%Provides least squares smoothing of measurement errors inherent in
%experimental position and velocity measurements
    %Variance-covariance weighting for coordinate measurements, eq. 58-59
    Xw = X/ss;
    Vw = V/ss;

    %Weighted landmark point mass inertia matrix, eq. 61
    X_pmi = -Xw;
    X_pmi(3,2) = Xw(3,2);
    X_pmi(1,1) = Xw(2,2) + Xw(3,3);
    X_pmi(2,2) = Xw(1,1) + Xw(3,3);
    X_pmi(3,3) = Xw(1,1) + Xw(2,2);

    %Velocity right hand vector, eq. 61
    V_rh(1,1) = Vw(3,2) - Vw(2,3);
    V_rh(2,1) = Vw(1,3) - Vw(3,1);
    V_rh(3,1) = Vw(2,1) - Vw(1,2);

    %Angular velocity vector, eq. 61
    w = X_pmi\V_rh;
```

```
        %Magnitude of angular velocity
        w_mag = norm(w);

        %Skew-symmetric angular velocity matrix, eq. 3
        w_skew = skew_symmetric(w);


%Determines IHA location
    %Constraint: to use the point on the IHA at the root of its
    %perpendicular through the centroid of the landmarks
    if(w_mag > eps)
        %Unit direction vector, eq. 2
        u = w'/w_mag;

        %IHA position, eq. 16
        IHA_p = xo + (w_skew*vo)/(w_mag^2);

    %Constraint: pure translation- magnitude of angular velocity is zero
    else
        %Unit direction vector, eq. 29
        u = vo'/norm(vo');

        %IHA position, eq. 16
        IHA_p = xo;
    end


%Transposes IHA_p into a 1x3 matrix
IHA_p = IHA_p';
```

10.2.3.10. Skew Symmetric

```
function [skew_sm]= skew_symmetric(vector)
%This function creates a skew-symmetric matrix from the input vector that
%is a [3,1] or [1,3] matrix.

%Determines the size of the vector
   %m is the number of rows
   %n is the number of columns
[m,n]=size(vector);

%Returns the skew-symmetric matrice of the vector
   %The vector has to be a [3,1] or [1,3] matrix
if ((m == 3 && n == 1) || (m == 1  && n == 3))
   if (m > n)
      skew_sm = zeros(m,m);
      skew_sm(1,2) = -vector(3,1);
      skew_sm(1,3) =  vector(2,1);
      skew_sm(2,3) = -vector(1,1);
      skew_sm(2,1) =  vector(3,1);
      skew_sm(3,1) = -vector(2,1);
      skew_sm(3,2) =  vector(1,1);
   end

   if (m < n)
      skew_sm = zeros(n,n);
      skew_sm(1,2) = -vector(1,3);
      skew_sm(1,3) =  vector(1,2);
      skew_sm(2,3) = -vector(1,1);
      skew_sm(2,1) =  vector(1,3);
      skew_sm(3,1) = -vector(1,2);
      skew_sm(3,2) =  vector(1,1);
   end

%If the vector is not a [3,1] or [1,3] matrix then NAN is returned
else
   skew_sm = 0/0;
end
```

10.2.3.11. Interpolated Joint Center

```
function [inter_jc]= interpolated_joint_center(pt1, pt2)
%This function determines the midpoint between the reflective markers on the
%bony landmarks located medially and laterally from the joint center

inter_jc = ((pt2 - pt1)/2) + pt1;
```

10.2.3.12. Reference Frame

```
function [R_GtoL]= reference_frame(pt1, pt2, pt3, axial_order)
%Uses three non-collinear points to determine the global to local reference
%frames from the points selected. The origin of the reference frame is set
%to pt1.

%Determines Axis 1 by connecting the origin to point 2
Axis1= (pt2-pt1)/norm(pt2-pt1);

%Determines a temporary vector from the origin and point 3
temp= pt3-pt1;

%Vector perpendicular to Axis 1 by taking the cross product of the
%temporary vector and Axis 1
Axis2= cross(temp, Axis1)/norm(cross(temp, Axis1));

%Mutually perpendicular vector from the cross product of Axis 1 and Axis 2
Axis3= cross(Axis1, Axis2);

%Set the size of the global to local reference frame
R_GtoL=zeros(3,3);

%Determines the global to local reference frame from Axis 1, Axis 2, and
%Axis 3
if axial_order == 1;
   R_GtoL=[Axis1'; Axis2'; Axis3'];
elseif axial_order == 2;
   R_GtoL=[Axis1'; Axis3'; Axis2'];
elseif axial_order == 3;
   R_GtoL=[Axis2'; Axis1'; Axis3'];
elseif axial_order == 4;
   R_GtoL=[Axis2'; Axis3'; Axis1'];
elseif axial_order == 5;
   R_GtoL=[Axis3'; Axis1'; Axis2'];
else
   R_GtoL=[Axis3'; Axis2'; Axis1'];
end
```

10.2.3.13. Reference Frame Humerus

```
function [R_GtoL]= reference_frame_humerus(pt1, pt2, pt3, axial_order)
%Uses three non-collinear points to determine the global to local reference
%frames from the points selected. The origin of the reference frame is set
%to pt1.

%Determines Axis 1 by connecting the origin to point 2
Axis1= (pt2-pt1)/norm(pt2-pt1);

%Determines a temporary vector from the origin and point 3
temp= pt3-pt1;

%Vector perpendicular to Axis 1 by taking the cross product of the
%temporary vector and Axis 1
Axis2= cross(Axis1, temp)/norm(cross(Axis1, temp));

%Mutually perpendicular vector from the cross product of Axis 1 and Axis 2
Axis3= cross(Axis2, Axis1);

%Set the size of the global to local reference frame
R_GtoL=zeros(3,3);

%Determines the global to local reference frame from Axis 1, Axis 2, and
%Axis 3
if axial_order == 1;
   R_GtoL=[Axis1'; Axis2'; Axis3'];
elseif axial_order == 2;
   R_GtoL=[Axis1'; Axis3'; Axis2'];
elseif axial_order == 3;
   R_GtoL=[Axis2'; Axis1'; Axis3'];
elseif axial_order == 4;
   R_GtoL=[Axis2'; Axis3'; Axis1'];
elseif axial_order == 5;
   R_GtoL=[Axis3'; Axis1'; Axis2'];
else
   R_GtoL=[Axis3'; Axis2'; Axis1'];
end
```

10.2.3.14. Global Position

```
function [r_global]= global_position(R_GtoL, r_local, origin)
%Determining the location of the joint center in the global reference frame

r_global= (R_GtoL' * r_local) + origin;
```

10.2.3.15. Local Position

```
function [r_local]= local_position(R_GtoL, r_global, origin)
%Determining the location of the joint center in the local reference frame

r_local= (R_GtoL * r_global) - (R_GtoL * origin);
```

10.2.3.16. Euler Sequences

```
%This program determines the joint rotation matrix for Euler angle
%sequences that are used for the sonographer research study.

phi = sym('phi');       %First rotation angle
theta = sym('theta');   %Second rotation angle
psi = sym('psi');       %Third rotation angle


%YX'Y'' rotation sequence
   %Primary rotation- Y axis
   y1 = [cos(phi) 0 -sin(phi); 0 1 0; sin(phi) 0 cos(phi)];
   %Secondary rotation- X axis
   x = [1 0 0; 0 cos(theta) sin(theta); 0 -sin(theta) cos(theta)];
   %Tertiary rotation- Y axis
   y3 = [cos(psi) 0 -sin(psi); 0 1 0; sin(psi) 0 cos(psi)];
   %YX'Y'' joint rotation matrix
   YXY_rotation = y3*(x*y1)
```

10.2.3.17. YXY Euler Sequence

```
function [phi theta psi]= yxy_euler_sequence(R_GtoDistal, R_GtoProximal)
%Determines the joint rotation matrix and the Euler angles for ONLY a YX'Y"
%sequence

%Determines the joint rotation matrix, distal segment's orientation
%relative to the proximal segment
R_joint= R_GtoDistal * R_GtoProximal';

%Secondary rotation- X axis
%Determines the Euler angle for theta in radians
theta_rad= acos(R_joint(2,2));

%Primary rotation- Y axis
%Determines the Euler angle for phi in radians
phi_rad= atan((R_joint(2,1)/(sin(theta_rad)))/(R_joint(2,3)/(sin(theta_rad))));

%Tertiary rotation- Y axis
%Determines the Euler angle for psi in radians
psi_rad= atan((R_joint(1,2)/(sin(theta_rad)))/(R_joint(3,2)/(-sin(theta_rad))));


%Converts the angles to degrees
phi= phi_rad * (180/pi);
theta= theta_rad *(180/pi);
psi= psi_rad * (180/pi);
```

10.2.3.18. Histogram

```
function [n xoutput] = scan_hist(data)
%This function determines the x and y axis for the histograms

for i=1:5
   [n(:,i), xoutput(:,i)]=hist(data(:,i));
end
```

10.2.4. Electromyography Evaluating Program

```
%This program filters all of the raw emg data and plots the electromyograms

fs = 1200;          %sampling frequency
loc_bicep = 1;      %column location of the bicep emg data
loc_tricep = 2;     %column location of the tricep emg data
loc_flexor = 3;     %column location of the flexor emg data
loc_extensor = 4;   %column location of the tricep emg data


%Loads the raw EMG data files from the sonography research study
   %Subject 1
   load P1_lt_lk_emg.CSV
   load P1_lt_rk_emg.CSV
   load P1_st_lk_emg.CSV
   load P1_st_rk_emg.CSV

   %Subject 4
   load P4_lt_lk_emg.CSV
   load P4_lt_rk_emg.CSV
   load P4_st_lk_emg.CSV
   load P4_st_rk_emg.CSV

   %Subject 5
   load P5_lt_lk_emg.CSV
   load P5_lt_rk_emg.CSV
   load P5_st_lk_emg.CSV
   load P5_st_rk_emg.CSV


%Plots filtered emg
   %Subject 1
   [P1_lt_lk_emg_filtered] = emg_filt_plot(fs, P1_lt_lk_emg);
   [P1_lt_rk_emg_filtered] = emg_filt_plot(fs, P1_lt_rk_emg);
   [P1_st_lk_emg_filtered] = emg_filt_plot(fs, P1_st_lk_emg);
   [P1_st_rk_emg_filtered] = emg_filt_plot(fs, P1_st_rk_emg);

   %Subject 4
   [P4_lt_lk_emg_filtered] = emg_filt_plot(fs, P4_lt_lk_emg);
   [P4_lt_rk_emg_filtered] = emg_filt_plot(fs, P4_lt_rk_emg);
   [P4_st_lk_emg_filtered] = emg_filt_plot(fs, P4_st_lk_emg);
   [P4_st_rk_emg_filtered] = emg_filt_plot(fs, P4_st_rk_emg);

   %Subject 5
   [P5_lt_lk_emg_filtered] = emg_filt_plot(fs, P5_lt_lk_emg);
   [P5_lt_rk_emg_filtered] = emg_filt_plot(fs, P5_lt_rk_emg);
   [P5_st_lk_emg_filtered] = emg_filt_plot(fs, P5_st_lk_emg);
   [P5_st_rk_emg_filtered] = emg_filt_plot(fs, P5_st_rk_emg);
```

10.2.5. Electromyography Sub-programs

10.2.5.1. Electromyography Filtered Data Plots

```
function [filtered_data] = emg_filt_plot(fs, rawdata)
%This function filters the EMG data and plots the electromyograms

%Filters raw EMG data
   [filtered_data]= emg_filtered(fs, rawdata);

%Determines the time for each data collection
   ts = 1/fs;
   N = length(filtered_data);
   t = (0:N-1)*ts;            %Time vector
   time = t';

%plots
   figure;
   subplot(2,1,1);
   plot(time,filtered_data(:,1));
   xlabel('Time (s)','fontsize',24);
   ylabel('Amplitude (V)','fontsize',24);
   title('Filtered Biceps Brachii Electromyogram','fontsize',24);

   subplot(2,1,2);
   plot(time,filtered_data(:,2));
   xlabel('Time (s)','fontsize',24);
   ylabel('Amplitude (V)','fontsize',24);
   title('Filtered Triceps Brachii Electromyogram','fontsize',24);

   figure
   subplot(2,1,1);
   plot(time,filtered_data(:,3),'r');
   xlabel('Time (s)','fontsize',24);
   ylabel('Amplitude (V)','fontsize',24);
   title('Filtered Flexor Carpi Ulnaris Electromyogram','fontsize',24);

   subplot(2,1,2);
   plot(time,filtered_data(:,4),'r');
   xlabel('Time (s)','fontsize',24);
   ylabel('Amplitude (V)','fontsize',24);
   title('Filtered Extensor Carpi Ulnaris Electromyogram','fontsize',24);
```

10.2.5.2. Electromyography Filtering

```
function [emg_bandpass]= emg_filtered(fs, raw_emgdata)
%This function filters the EMG data using a notch filter and passband filter.

%Removes leading zeros from the data which are the first 1200 points
   emg_data    = raw_emgdata(fs+1:end,:);


%Determines the DC offset of the EMG output, the DC offset is the
%difference of the mean from zero.
   emg_dc_offset  = mean(emg_data);


%Accounts for the DC offset in the EMG output, the mean is subtracted
%from the original data.
   emg_dc_adjust(:,1)  = emg_data(:,1) - emg_dc_offset(1,1);
   emg_dc_adjust(:,2)  = emg_data(:,2) - emg_dc_offset(1,2);
   emg_dc_adjust(:,3)  = emg_data(:,3) - emg_dc_offset(1,3);
   emg_dc_adjust(:,4)  = emg_data(:,4) - emg_dc_offset(1,4);

%Full wave rectification, absolute value of EMG output.
   emg_fwr  = abs(emg_dc_adjust);

%Applys a notch filter at 60 Hz
   wo = 60/600;
   bw = wo/35;
   [b,a] = iirnotch(wo,bw);
   notch_filtered = filtfilt(b,a, emg_fwr);

%Apply a passband filter with a 20Hz lower bound cutoff and 300Hz upper
%bound cutoff
   wc = [20/600 300/600];
   a = 1;
   b = fir1(8, wc, 'bandpass');
   emg_bandpass = filtfilt(b, a, notch_filtered);
```

10.2.5.3. Fast Fourier Transform of Raw Electromyography Data

```
function [bicep_fft tricep_fft flexor_fft extensor_fft] = fft_raw_emg(fs, raw_data)
%Divides the signal into the seperate muscles
bicep_raw = raw_data(:,1);
tricep_raw = raw_data(:,2);
flexor_raw = raw_data(:,3);
extensor_raw = raw_data(:,4);

%Constants for the signal
ts = 1/fs;                  %Sample time
N = length(bicep_raw);      %Length of signal
NFFT = 2^nextpow2(N);
fre = fs/2*linspace(0,1,NFFT/2+1);    %frequency

%------------------------------------------------------------------------
%Determines the FFT for the bicep
bicep_fft = abs(fft(bicep_raw(1201:end,1),NFFT));

%Plots the FFT
figure;
subplot(411);
plot(fre,bicep_fft(1:length(fre),:));
xlabel('Frequency (Hz)'); ylabel('Magnitude');
title('FFT of Bicep Raw MVIC EMG Data');

%------------------------------------------------------------------------
%Determines the FFT for the tricep
tricep_fft = abs(fft(tricep_raw(1201:end,1),NFFT));

%Plots the FFT
subplot(412);
plot(fre,tricep_fft(1:length(fre),:));
xlabel('Frequency (Hz)'); ylabel('Magnitude');
title('FFT of Tricep Raw MVIC EMG Data');

%------------------------------------------------------------------------
%Determines the FFT for the flexor
flexor_fft = abs(fft(flexor_raw(1201:end,1),NFFT));
subplot(413);

%Plots the FFT
plot(fre,flexor_fft(1:length(fre),:));
xlabel('Frequency (Hz)'); ylabel('Magnitude');
title('FFT of Flexor Raw MVIC EMG Data');

%------------------------------------------------------------------------
%Determines the FFT for the extensor
extensor_fft = abs(fft(extensor_raw(1201:end,1),NFFT));
subplot(414);

%Plots the FFT
plot(fre,extensor_fft(1:length(fre),:));
xlabel('Frequency (Hz)'); ylabel('Magnitude');
title('FFT of Extensor Raw MVIC EMG Data');
```

10.3. Occupational Therapy Results

Table A: Pinch and grip strength in the dominant hand of the sonographer

Sonographer	Pinch Strength (lbs)						Grip Strength (lbs)	
	Three-Jaw Chuck	Norms	Lateral Pinch	Norms	Tip Pinch	Norms	Grip	Norms
1	14	16	14	15.7	11	11.7	60	57.3
4	12.3	19.3	15	18.7	12.3	12.6	83.3	78.7
5	16.3	17.7	18.6	17.7	12.6	11.9	80	74.5

Table B: Pressures and forces for the entire sensor mat during left kidney scans

Sonographer	Left Kidney Scans							
	C5-1 Transducer				S5-1 Transducer			
	Max. Force (N)	Average Force (N)	Max. Pressure (kPa)	Average Max. Pressure (kPa)	Max. Force (N)	Average Force (N)	Max. Pressure (kPa)	Average Max. Pressure (kPa)
1	62.67	30.99	88.33	47.67	81	60.88	126.67	91.68
4	89.83	45.81	190	69.81	100.33	57.69	130	58.16
5	88.83	53.69	140	63.01	74.5	47.8	76.67	39.67

Table C: Pressures and forces for the entire sensor mat during right kidney scans

Sonographer	Right Kidney Scans							
	C5-1 Transducer				S5-1 Transducer			
	Max. Force (N)	Average Force (N)	Max. Pressure (kPa)	Average Max. Pressure (kPa)	Max. Force (N)	Average Force (N)	Max. Pressure (kPa)	Average Max. Pressure (kPa)
1	52.67	11.7	121.67	28.58	65.67	46.8	150	81.79
4	115.5	43.37	175	60.87	127.67	63.6	165	58.4
5	86.67	36.9	181.67	77.22	84	48.93	106.67	57.77

Table D: Maximum pressure exerted by the thumb and on the entire sensor mat

Sonographer	Maximum Pressure (kPa)							
	Left Kidney				Right Kidney			
	C5-1 Transducer		S5-1 Transducer		C5-1 Transducer		S5-1 Transducer	
	Full	Thumb	Full	Thumb	Full	Thumb	Full	Thumb
1	88.33	88.33	126.67	126.67	121.67	121.67	150	150
4	190	190	130	130	175	175	165	165
5	140	140	76.67	68.33	181.67	181.67	106.67	106.67

Table E: Maximum force exerted by the thumb and on the entire sensor mat

Sonographer	Maximum Force (N)							
	Left Kidney				Right Kidney			
	C5-1 Transducer		S5-1 Transducer		C5-1 Transducer		S5-1 Transducer	
	Full	Thumb	Full	Thumb	Full	Thumb	Full	Thumb
1	62.67	25.83	81	17.17	52.67	20.67	65.67	17
4	89.83	38	100.33	31.67	115.5	44.5	127.67	38
5	88.83	23.5	74.5	14.83	86.67	30.67	84	19.33

10.4. Participant Consent Forms

Participant Consent Form

Dear Sonographer:

You are invited to participate in an occupational therapy research study. Your participation in this study is completely voluntary. This study has been approved by the Human Research Review Committee at GVSU. Please read the information below and ask questions about anything you don't understand. You are free to decide not to participate in this study at any time.

1. **Title of Study:** Hand Grip Pressures Between Various Transducers And The Related Perception Of Pain Experienced By Sonographers

2. **Researchers:** Hannah Bullock, OTS, Chad Conroy, OTS, Lauren Vetter, OTS. Committee Chair: Dr. Jeanine Beasley, EdD, OTR, CHT.

3. **Purpose of Study:** One purpose of this study is to determine if the design of an ultrasound transducer affects the amount of pressure exerted by sonographers to achieve a quality scan. An additional purpose of this study would be examining the possibility of repetitive strain injuries resulting from awkward posture, repetitive movement, and griping force. The study will also examine if the amount of pressure exerted by the sonographer correlates with any possible subjective level pain as reported by the sonographer.

4. **Reason for Invitation**: You are being invited to participate in this study, because you are a sonographers with a minimum of 5 years experience practicing in the field of sonography.

5. **How Participants Were Selected**: Participants were selected due to personal relationships with Grand Valley State University Radiological Imaging Faculty and experience in the field of sonography.

6. **Procedure Of Study:**
   - The study will take place in Cook-DeVos Center for Health Sciences, 4th Floor Sonography Room in Grand Rapids, MI.
   - You will be asked to complete a pre-scanning form and a post-scanning form.
   - You will be asked to obtain a quality scan of each kidney of a model/volunteer. You will be asked to use two different types of transducers, and use your right and left hand to scan. You will be asked to obtain 14 scans overall. Reflective markers will be placed on the arms to determine joint angles and surface EMGs will be placed on the arms to record muscle activity.
   - Each scan should not exceed 5-10 minutes. The entire data collection process should not exceed 3 hours.
   - There are no out of pocket costs to you for participation in this study.

7. **Risks and Benefits:**
   - There is no direct benefit of your participation in this study. However, the information obtained may benefit sonographers in the future.
   - We feel this study involves minimal risk. You may experience physical upper-extremity pain/fatigue from scanning, fatigue from standing during the scanning procedures, and anxiety from being watched.

8. **Compensation for Harm:** If you are harmed from participating in this research emergency first aid will be provided to you and you will be referred to an appropriate medical care center. **Any costs for additional medical care that may be required are your responsibility and that of your medical insurance company.**

9. **Voluntary Participation:** Your participation in this research study is completely voluntary. You do not have to participate. You may quit at any time without any penalty to you.

10. **Privacy and Confidentiality:** Your name will not be given to anyone other than the research team. All the information collected from you or about you will be kept confidential, and filed in a locked cabinet in the Occupational Therapy Department Research file.

11. **Research Study Results:** If you wish to learn about the results of this research study, or if you have any questions after the study, you may request that information by contacting Dr. Jeanine Beasley at beasleyj@gvsu.edu or 616-331-3117.

12. **Payment:** There will be no payment for participation in the research.

13. **Agreement To Participate:** By signing this consent form below you are stating the following:
    - The details of this research study have been explained to me including what I am being asked to do and the anticipated risks and benefits;
    - I have had an opportunity to have my questions answered;
    - I am voluntarily agreeing to participate in the research as described on this form;
    - I may ask more questions or quit participating at any time without penalty.

_____ (Initial here) I have been given a copy of this document for my records.

Print Name: _____

Sign Name in ink: _____

Date Signed: _____

Email:_____

Phone:_____

If you have any questions about your rights as a research participant, please contact the **Research Protections Office** at Grand Valley State University, Grand Rapids, MI

Phone: 616-331-3197 e-mail: HRRC@GVSU.EDU

Participant Consent Form

Dear Volunteer:

You are invited to participate in an occupational therapy research study. Your participation in this study is completely voluntary. This study has been approved by the Human Research Review Committee at GVSU. Please read the information below and ask questions about anything you don't understand. You are free to decide not to participate in this study at any time.

1. **Title of Study:** Hand Grip Pressures Between Various Transducers And The Related Perception Of Pain Experienced By Sonographers

2. **Researchers:** Hannah Bullock, OTS, Chad Conroy, OTS, Lauren Vetter, OTS. Committee Chair: Dr. Jeanine Beasley, EdD, OTR, CHT.

3. **Purpose of Study:** One purpose of this study is to determine if the design of an ultrasound transducer affects the amount of pressure exerted by sonographers to achieve a quality scan. An additional purpose of this study would be examining the possibility of repetitive strain injuries resulting from awkward posture, repetitive movement, and griping force. The study will also examine if the amount of pressure exerted by the sonographer correlates with any possible subjective level pain as reported by the sonographer. This is not a medical procedure. This is not intended diagnose or treat any medical problem.

4. **How Participants Were Selected**: You were selected due to personal relationships between the researchers and members of the advisory committee, and a public notice advisory (flyer).

5. **Procedure Of Study:**
   - The study will take place in Cook-DeVos Center for Health Sciences, 4th Floor Sonography Room in Grand Rapids, MI.
   - You will be weighed using a scale, and your height will be measured using a tape measure. Your body mass index will be calculated using these numbers.
   - You will be asked to lie on a sonography bed and expose the skin on your back near your kidneys for scanning. An experienced sonographer will obtain a quality image of each of your kidneys. Your kidneys will be scanned a total of 42 times. They will do this using two different transducers, and they will use their right and left hands.
   - Each scan should not exceed 5-10 minutes. The entire data collection process should not exceed 3 hours.
   - There are no out of pocket costs to you for participation in this study.

6. **Risks and Benefits:**
   - There is no direct benefit of your participation in this study. However, the information obtained may benefit sonographers in the future.
   - We feel this study involves minimal risk. You may experience back pain from scanning, anxiety from providing your weight and height, and fatigue from lying down.

7. **Compensation for Harm:** If you are harmed from participating in this research emergency first aid will be provided to you and you will be referred to an appropriate medical care center. **Any costs for additional medical care that may be required are your responsibility and that of your medical insurance company.**

8. **Voluntary Participation:** Your participation in this research study is completely voluntary. You do not have to participate. You may quit at any time without any penalty to you.

9. **Privacy and Confidentiality:** Your name will not be given to anyone other than the research team. All the information collected from you or about you will be kept confidential, and filed in a locked cabinet in the Occupational Therapy Department Research file.

10. **Research Study Results:** If you wish to learn about the results of this research study, or if you have any questions after the study, you may request that information by contacting Dr. Jeanine Beasley at beasleyj@gvsu.edu or 616-331-3117.

11. **Payment:** There will be no payment for participation in the research.

12. **Agreement To Participate:** By signing this consent form below you are stating the following:
    - The details of this research study have been explained to me including what I am being asked to do and the anticipated risks and benefits;
    - I have had an opportunity to have my questions answered;
    - I am voluntarily agreeing to participate in the research as described on this form;
    - I may ask more questions or quit participating at any time without penalty.

_____ (Initial here) I have been given a copy of this document for my records.

Print Name: _____

Sign Name in ink: _____

Date Signed: _____

If you have any questions about your rights as a research participant, please contact the **Research Protections Office** at Grand Valley State University, Grand Rapids, MI

Phone: 616-331-3197 e-mail: HRRC@GVSU.EDU

10.5. Occupational Therapy Survey and Questionnaire

Pre – Scan Questionnaire

Sonographer Number: _____

Years of Sonography Work Experience: _____

Male/Female: _____

Location of Sonography Practice: _____

Area of Sonography Specialty: _____

Date of Birth: _____

Race/Ethnicity: _____

Hand Preference: _____

Weight: _____

Height: _____

BMI (Weight (kg) ÷ height² (m)):_____

Functional Pain Scale (Goth, et al.)

Rating	Description
0	No pain
1	Tolerable (and does not prevent any activities)
2	Tolerable (but does prevent some activities)
3	Intolerable (but can use telephone, watch TV, or read)
4	Intolerable (but cannot use telephone, watch TV, or read)
5	Intolerable (and unable to verbally communicate because of pain)

Using the scale above, please answer the following questions:

1. Are you currently experiencing any pain? 0 1 2 3 4 5
2. Have you experienced any pain while performing scans? 0 1 2 3 4 5
   If so, where is your pain localized?

   _____

   _____

Please place an **X** on the area(s) where you experience pain while performing scans.

Right Side

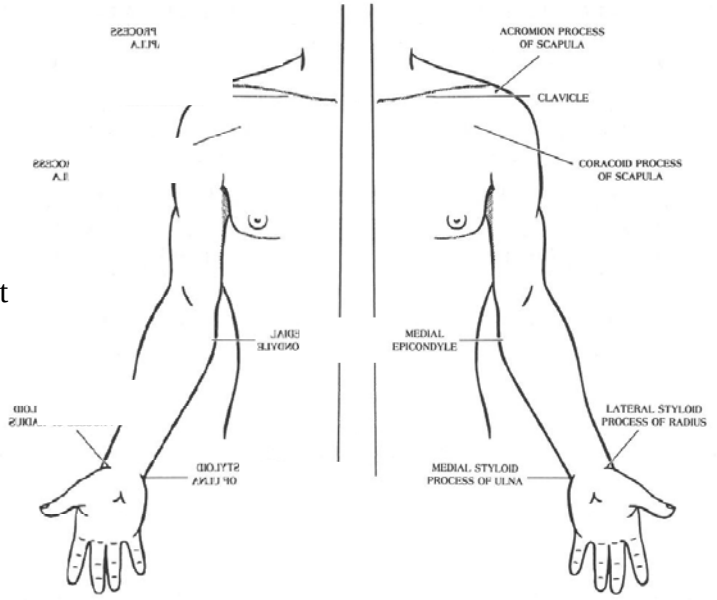

Left Side

3. Have you experienced any pain while performing activities of daily living (such as bathing, dressing, or cooking)? Please specify.

_____

_____

If so, what level would you classify your pain as? 0 1 2 3 4 5

Where is your pain localized?

_____

_____

Please place an **X** on the area(s) where you experience pain during activities of daily living.

Right Side

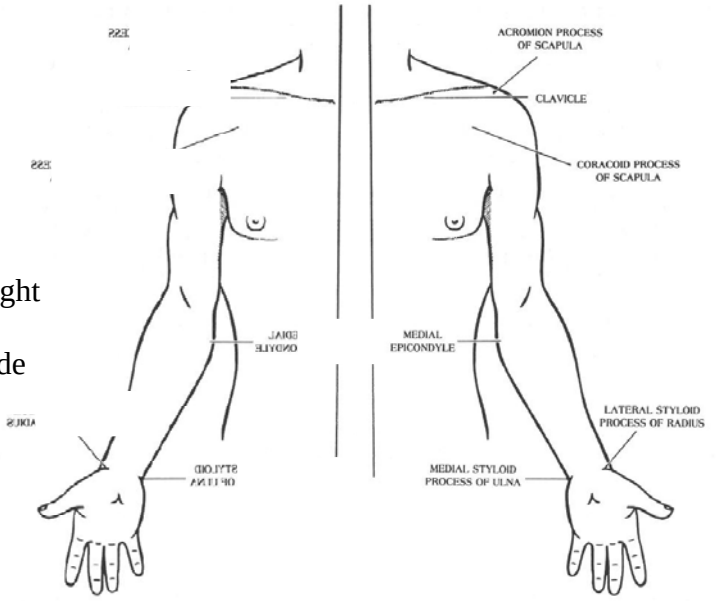

Left Side

4. Have you experienced any pain while performing leisure activities (such as card games, hiking, or gardening)? Please specify.

_____

_____

If so, what level would you classify your pain as? 0 1 2 3 4 5

Where is your pain localized?

_____

_____

Please place an **X** on the area(s) where you experience pain during leisure activities.

Right Side

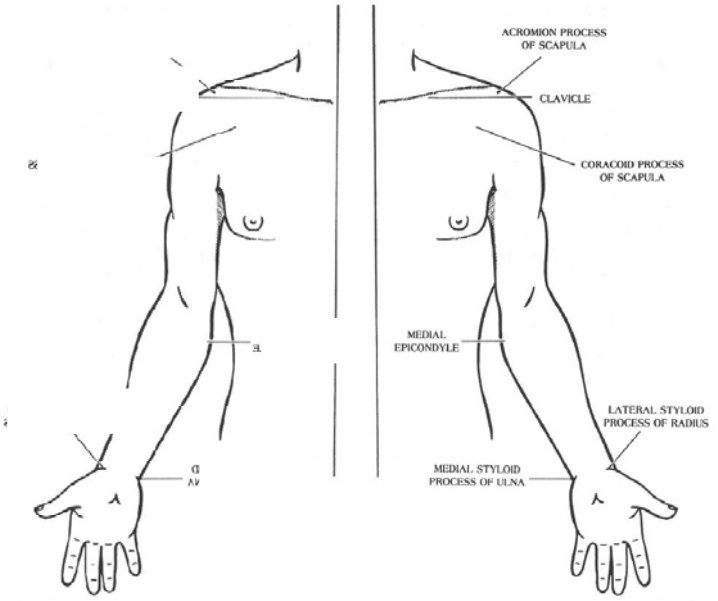

Left Side

Gloth, F. M., Scheve, A. A., Stober, C. V., Chow, S., & Prosser, J. (2001). The functional pain scale: Reliability, validity, and responsiveness in an elderly population. *Journal of American Medical Directors Association, 2*(3), 110-11.

Sonographer Number: _____

Volunteer Number Scanned: _____

Post – Scan Questionnaire

Rating	Description
0	No pain
1	Tolerable (and does not prevent any activities)
2	Tolerable (but does prevent some activities)
3	Intolerable (but can use telephone, watch TV, or read)
4	Intolerable (but cannot use telephone, watch TV, or read)
5	Intolerable (and unable to verbally communicate because of pain)

1. Did you experience any pain while scanning?

   If so, what level would you classify your pain as? 0 1 2 3 4 5

   Where is your pain localized?

   _____

   _____

Please place an **X** on the area(s) where you experienced pain while scanning.

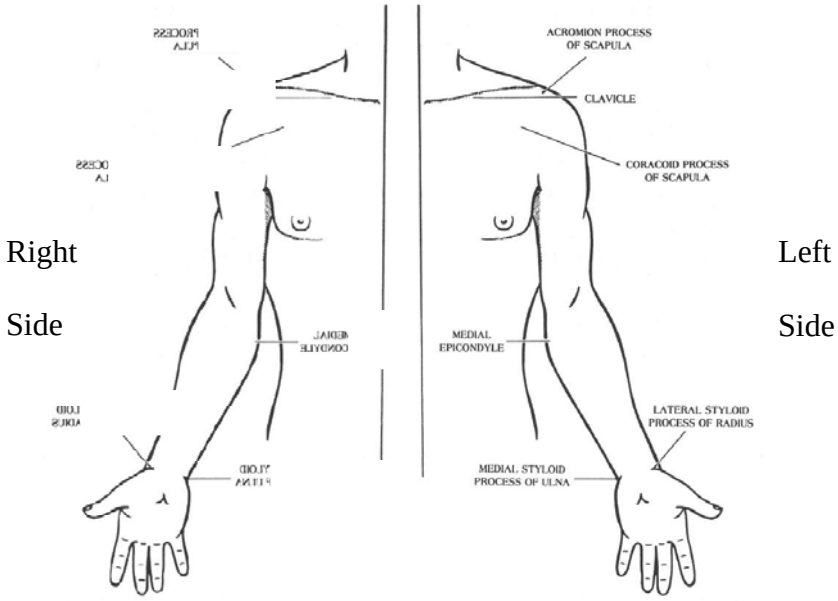

Right Side

Left Side

1. Did you have preference of A or B transducer handle design? _____

   If so, which design do you prefer? Why?

   _____

   _____

2. Do you prefer scanning with your right or left hand? Why?

   _____

   _____

   _____

   _____

Gloth, F. M., Scheve, A. A., Stober, C. V., Chow, S., & Prosser, J. (2001). The functional pain scale: Reliability, validity, and responsiveness in an elderly population. *Journal of American Medical Directors Association, 2*(3), 110-11.

10.6. Volunteer Flyer

Date of Study:
To be Determined

Location of Study:
Cook-DeVos Center for Health Sciences
4th Floor
Sonography Laboratory

Researchers: Hannah Bullock OTS, Chad Conroy OTS, Lauren Vetter OTS.

Committee Chair: Dr. Jeanine Beasley, EdD, OTR, CHT

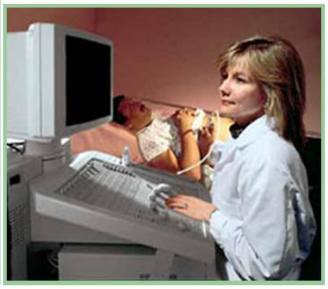

Research Volunteers Needed for Occupational Therapy Study!

Sonography uses sound waves to obtain images of internal organs. Radiation is not used making this a save and low-risk procedure!

Did you know that many sonographers experience pain in the hand and wrist due to obtaining ultrasound images? Students in the Occupational Therapy Master's program at GVSU, along with the Sonography Department, are performing a master's thesis in attempt to combat this problem.

If you choose to participate, you will be asked to expose your lower torso only, Three experienced sonographers will take images of your kidneys. The entire process is quick, performed in one day!

Please Email the Researchers If you are Interested in Participating!

- Participation in this study is voluntary and safe!
- Snacks will be provided!

Contact Information:

Hannah Bullock:
bullockh@mail.gvsu.edu

Chad Conroy:
conroyc@mail.gvsu.edu

Lauren Vetter:
duchemil@mail.gvsu.edu

GRAND VALLEY STATE UNIVERSITY
www.gvsu.edu

11. Bibliography

American Society for Hand Therapists (ASHT): clinical assessment recommendations. (1981). *Indianapolis: American Society of Hand Therapists*.

Berkowitz, J., Pike, I., Russo, A., Lessoway, V., & Baker, J. (1997). The prevalence of musculoskeletal disorders among diagnostic medical sonographers. *Journal of Diagnostic Medical Sonography,* 219-227.

Brown, G., & Baker, J. (2004). Work-related musculoskeletal disorders in sonographers. *Journal of Diagnostic Medical Sonography*, 85-93.

Bullock, H., Conroy, C., & Vetter, L. (2011). *Variation of pinch and grip force between different size transducers and the related perception of pain experienced by sonographers.* Grand Valley State University Occupational Therapy Master's Thesis, Grand Rapids.

Burnett, D., & Campbell-Kyureghyan, N. (2010). Quantification of scan-specific ergonomic risk-factors in medical sonography. *International Journal of Industrial Ergonomics*, 306-314.

Cram, J., Kasman, G., & Holtz, J. (1998). *Introduction to Surface Electromyography.* Gaithersburg: Aspen Publishers.

Garg, A., Hegmann, K., & Kapellusch, J. (2006). Short-cycle overhead work and shoulder girdle muscle fatigue. *International Journal of Industrical Ergonomics*, 581-597.

Go Further with Vicon MX T-Series. (2011). Retrieved 12 2011, 11, from Vicon: http://vicon.com/support/downloads_view.php?id=0858b2e0e0fb895f5a7236644c60edcd

Hedge, A. (1998). Design of hand-operated devices. In *Human Factors in Consumer Products* (pp. 203-222). London: Taylor & Francis.

Hutmire, C., Baker, J., Evans, K., & Roll, S. (2010). Factors that contribute to wrist-hand-finger discomfort in diagnostic medical sonographers and vascular technologists. *Journal of Diagnostic Medical Sonography*, 121-129.

Jakes, C. (2001). Sonographers and occupational overuse syndrome: Cause, effect, and solutions. *Journal of Diagnostic Medical Sonography*, 312-320.

JAMAR Hydrolic Hand Dynamometer User Instructions. (2004). Lafayette: Lafayette Instruments.

Malmivaara, A., van Tulder, M., & Koes, B. (2007). Repetitive strain injury. *The Lancet*, 1815-1822.

McCulloch, M., Xie, T., & Adams, D. (2002). Cardiovascular sonography: the painful art of scanning. *Cardiac Ultrasound Today*, 69-96.

Mesker, C., van der Helm, F., Rozendaal, L., & Rozing, P. (1998). In vivo estimation of the glenohumeral joint center from scapular bony landmarks by linear regression. *Journal of Biomechanics*, 93-96.

Milkowski, A., & Murphey, S. L. (2006). Surface EMG evaluation of sonographer scanning postures. *Journal of Diagnostic Medical Sonography*, 298-305.

Motion Lab Systems User Manual. (2007, November 19). Retrieved February 7, 2012, from Motion Lab Systems: http://www.udel.edu/PT/Research/MLS_MA300_EMG_manual.pdf

Murphy, C., & Russo, A. (2000). *An Update on Ergonomic Issues in Sonography.* Employee Health and Safety Services.

Pliance-X System Manual. (2011, February). Retrieved 5 19, 2011, from http://www.novelusa.com/assets/pdf/manuals/plianceX_v20_final.pdf

Quanbury, A., Friesen, M., Friesen, R., & Arpin, S. (2006). Musculoskeletal injuries among ultrasound sonographers in rural Manitoba: A study of workplace ergonomics. *AAOHN Journal : Official Journal of the American Association of Occupational Health Nurses*, 32.

Roll, S., Baker, J., & Evans, K. (2009). Work-related musculoskeletal disorders (WRMSD) among registered diagnostic medical sonographers and vascular technologists: A representative sample. *Journal of Diagnostic Medical Sonography*, 287-299.

Russo, A., Murphy, C., Lessoway, V., & Berkowitz, J. (2002). The prevalence of musculoskeletal symptoms among british columbia sonographers. *Applied Ergonomics*, 385-393.

Schoenfeld, A., Goverman, J., Weiss, D., & Meizner, I. (1999). Transducer user syndrome: an occupational hazard of the ultrasonographer. *European Journal of Ultrasound*, 41-45.

Sommer III, H. (1992). Determination of first and second order instant screw parameters from landmark trajectories. *ASME Journal of Mechanical Design*, 274-282.

Stokdijk, M., Nagels, J., & Rozing, P. (2000). The glenohumeral joint centre in vivo. *Journal of Biomechanics*, 1629-1636.

Swinker, M., & Randall, S. (2003). Musculoskeletal disorders. *Professional Safety*, 40-44.

Vanderpool, H., Friis, E., Smith, B., & Harms, K. (1993). Prevalence of carpal tunnel syndrome and other work-related musculoskeletal problems in cardiac sonographers. *Journal of Diagnostic Medical Sonography*, 604-610.

Veeger, H. (2000). The position of the rotation center of the glenohumeral joint. *Journal of Biomechanics*, 1171-1715.

Vicon MX Hardware System Reference. (2007). Retrieved 11 12, 2011, from Vicon: http://vicon.com/support/downloads_view.php?id=899b745c6d075163538ed23d60a43db1

Village, J., & Trask, C. (2007). Ergonomic analysis of postural and muscular loads to diagnostic sonographers. *International Journal of Industrial Ergonomics*, 781-789.

Wihlidal, L., & Kumar, S. (1997). An injury profile of practicing diagnostic medical sonographers in Alberta. *International Journal of Industrial Ergonomics*, 205-216.

Winter, D. (2009). *Biomechanics and Motor Control of Human Movement.* Hoboken: John Wiley and Sons.

Woltring, H. (1990). Model and measurement error influences in data processing. In A. B. Cappozzo, *Biomechanics of human movement : applications in rehabilitation, sports and ergonomics* (pp. 203-237). Worthington.

World Health Organization. (2012, 4 15). Retrieved 4 15, 2012, from http://apps.who.int/bmi/index.jsp?introPage=intro_3.html

Wu, G., van der Helm, F., Veeger, H., Makhsous, M., Van Roy, P., Anglin, C., . . . Buchholz, B. (2005). ISB recommendation on definitions of joint coordinate

systems of various joints for the reporting of human joint motion- Part II: shoulder, elbow, wrist and hand. *Journal of Biomechanics*, 981-992.

Yassi, A. (1997). Repetitive strain injuries. *The Lancet*, 943-947.